INFORMATION TO USERS

This manuscript has been reproduced from the microfilm master. UMI films the text directly from the original or copy submitted. Thus, some thesis and dissertation copies are in typewriter face, while others may be from any type of computer printer.

The quality of this reproduction is dependent upon the quality of the copy submitted. Broken or indistinct print, colored or poor quality illustrations and photographs, print bleedthrough, substandard margins, and improper alignment can adversely affect reproduction.

In the unlikely event that the author did not send UMI a complete manuscript and there are missing pages, these will be noted. Also, if unauthorized copyright material had to be removed, a note will indicate the deletion.

Oversize materials (e.g., maps, drawings, charts) are reproduced by sectioning the original, beginning at the upper left-hand corner and continuing from left to right in equal sections with small overlaps. Each original is also photographed in one exposure and is included in reduced form at the back of the book.

Photographs included in the original manuscript have been reproduced xerographically in this copy. Higher quality 6" x 9" black and white photographic prints are available for any photographs or illustrations appearing in this copy for an additional charge. Contact UMI directly to order.

UMI

A Bell & Howell Information Company
300 North Zeeb Road, Ann Arbor MI 48106-1346 USA
313/761-4700 800/521-0600

University of Alberta

Spatial Analysis Tools for Hazardous Materials Transportation Logistics

By

Jianjun Zhang 

A thesis submitted to the Faculty of Graduate Studies and Research in partial fulfillment of the requirements for the degree of Doctor of Philosophy

Department of Earth and Atmospheric Sciences

Edmonton, Alberta

Fall 1998

University of Alberta

Library Release Form

Name of Author: Jianjun Zhang

Title of Thesis: Spatial Analysis Tools for Hazardous Materials Transportation Logistics

Degree: Doctor of Philosophy

Year this Degree Granted: 1998

311 – 1580 Olive Diefenbaker Drive
Prince Albert, SK S6V 7M6
Canada

Date 10/1/1998

University of Alberta

Faculty of Graduate Studies and Research

The undersigned certify that they have read, and recommend to the Faculty of Graduate Studies and Research for acceptance, a thesis entitled *Spatial Analysis Tools for Hazardous Materials Transportation Logistics* submitted by Jianjun Zhang in partial fulfillment of the requirements for the degree of Doctor of Philosophy.

M. John Hodgson (Co-Supervisor)

Erhan Erkut (Co-Supervisor)

for Nigel Waters

Armann Ingolfsson

Arturo Sanchez-Azofeifa

for Said Salhi (External Examiner)

Date 25/9/98

ABSTRACT

Very large and ever-increasing amounts of hazardous materials (Hazmats) are transported daily on transport networks. Accidental release of Hazmat can have very undesirable environmental and economic consequences. Some measures to reduce the risk resulting from Hazmat transport are selecting safer roads, limiting Hazmat trucks to designated routes and making sure that government regulations and specifications on Hazmat shipment are strictly followed. This thesis mainly deals with four issues:

The first issue is to evaluate the capabilities of Geographic Information Systems (GIS) for hazardous materials transport decision support. Because most data needed for Hazmat transport decision making have a spatial dimension and GIS is an essential tool for the effective use of spatial data, I will evaluate the potential of using the state-of-the-art GIS technology as a framework for Hazmat transport decision support systems.

The second issue is to develop a methodology to incorporate dispersion models in network risk assessment since risks resulting from Hazmat transportation are often affected by wind conditions. Incorporating dispersion models that consider wind conditions in network risk assessment is very difficult and the existing methods for doing it are either not practical in computing time or can only deal with certain special cases. This research overcame the limitations of previous methods and developed a raster GIS approach that can compute the network risks efficiently and without making limiting assumptions to the dispersion models.

The third issue is to develop an approach for designing Hazmat networks for municipalities. Previous methods for designing Hazmat routes do not explicitly involve quantitative risk analysis, nor do they consider the multi-party, multi-objective nature of the problem. The procedure developed in this study addresses these factors.

The fourth issue is to develop a robust algorithm for the inspection station location model, which can be used to locate facilities that inspect Hazmat trucks.

The thesis emphasizes methodological developments and their practical uses. All methods developed in this study have been tested on a real network to ensure their applicability in real-world decision support.

Dedication

This dissertation is dedicated to my wife Qing Gu, my daughter Kaileen and my parents, Zhang Huisheng and Huang Aifeng.

ACKNOWLEDGEMENTS

I would like to extend my sincere appreciation to those who contributed to the completion of this thesis.

I am sincerely grateful to Dr. M. J. Hodgson, my primary supervisor, and Dr. E. Erkut, my co-supervisor, for their guidance, inputs and encouragement throughout this project. I would like to take this opportunity to thank both professors for being my friend throughout my Ph.D. study.

I owe special thanks to Drs. N. Waters and A. Ingolfsson for their criticisms and revisions. Both professors provided prompt feedback and constructive suggestions to my drafts, despite their busy schedule. My thanks also go to Dr. A. Sanchez-Azofeifa for his suggestions.

I also would like to thank Dr. E. Jackson, Ms. J. Enarson and other faculty and staff members in the Department of Earth and Atmospheric Sciences for making the department a nice place to study.

Most of all, I thank my wife Qing Gu for her constant patience, encouragement and for tolerating me spending extended hours in the lab. Without her support, this project would have taken much longer. I thank my daughter Kaileen and my parents for their unique contributions.

Finally, I would like to thank Drs. Hodgson and Erkut for their financial support in the last two years.

TABLE OF CONTENTS

LIST OF TABLES

LIST OF FIGURES

Chapter 1

INTRODUCTION

Hazardous materials (Hazmats) include explosives, flammables, oxidizing substances, poisonous gases, radioactive materials, and hazardous wastes. They can be such common substances as gasoline as well as such rare but more dangerous ones as radioactive materials. Virtually all modern economies rely heavily on the use, and therefore also the transportation, of many Hazmats. In industrial countries, significant amounts of Hazmats are shipped across the transportation network. According to the US Department of Commerce (DOC 1994), the US transportation network carries about 250,000 Hazmat shipments every day, totaling four billion tons or 200 billion ton-miles a year. In Canada, the amount of Hazmat is estimated to be increasing by five percent every year (Stewart 1990). Hazmats can be extremely harmful to the environment and to human health, since exposure to their toxic ingredients may lead to injury or death of plants, animals, and humans. Hazmat transportation is an important part of the Hazmat treatment process. Accidental releases of Hazmat during transit can have very undesirable consequences. For example, the 1979 train derailment in Mississauga, Ontario caused the evacuation of 200,000 people since chlorine was leaking from damaged tank cars (Grange 1980). This single incident cost about $65 million. Between 1971 and 1980, more than 111,000 accidents involving Hazmat were reported in the United States, resulting in a total of 248 fatalities, 6,873 injuries and approximately $120 million in property damages (Rowe 1983). In Canada, 8,308 Hazmat accidents were reported between 1987 and 1995, of which 82 accidents resulted in 133 fatalities, and 145 resulted in 857 injuries (Statistics Canada 1998). Hazmat accidents cost about one billion dollars a year in Canada (Transport Canada 1997b). Hazmat accidents always get a lot of attention from the media and the public is very sensitive to the risks associated with hazardous material shipments.

Hazmat transportation involves several stakeholders, each having a different set of objectives. It can be viewed from three perspectives: that of government regulators, that of the public and that of shippers. Government regulators must maintain throughput and

ensure that necessary safety measures are taken to minimize the shipping risk. The public, often represented by local authorities, is primarily concerned about the negative effects of, and risks resulting from, the Hazmat traffic. When accidents occur, it is the local authorities that have the primary responsibility for mitigating the incidents and taking emergency measures. Because eliminating the shipping risk completely is impossible in a modern society, distributing risks relatively equitably among different segments of society will make the risks more acceptable to the public. Shippers are primarily interested in minimizing shipping costs. They also have a secondary interest in safety because accidents related with Hazmat are costly. But shippers cannot be totally relied on to ensure safety. Therefore, Hazmat transportation is a multi-stakeholder, multi-objective problem. The primary objectives of Hazmat transportation are minimizing risk, minimizing the shipping cost, and maintaining equity among different segments of society.

There are several ways of reducing the shipping risks from the management perspective (as opposed to the engineering perspective): selecting safer paths, designating roads for Hazmat trucks and making sure that safety standards set by the government are followed strictly. Selecting paths for Hazmat shipments is usually a decision made by shippers. Hazmat routing is a multi-objective decision process that needs to use large amounts of data and compare different alternatives. This process can be facilitated by a decision support system (DSS) that brings data and routing algorithms together, and that has flexible reporting capabilities (Keen 1981, Sprague and Carlson 1982). Since much of the data needed in Hazmat transportation analysis are spatial data, geographic information systems (GIS), which are computerized systems for capturing, storing, processing, analyzing and displaying spatial data (Maguire 1991), can be used as a framework for Hazmat transport spatial decision support systems (SDSS). A GIS-based system will not only benefit from the existing GIS databases available in many private organizations and public agencies, but it can also be a cost-effective way of building a decision support system customized to satisfy the particular requirements of each organization.

Because of the possible severe consequences of Hazmat accidents, transportation of Hazmat is heavily regulated by the government. In Canada, The Transportation of Dangerous Goods Act 1992 is the latest version of federal regulations governing all matters

related to the transport of Hazmat via air, railway, highway and waterways within the legislative authority of Parliament. At the local level, municipalities often designate a network for Hazmat trucks and impose curfews (time of day restrictions) on Hazmat trucks. Previous methods for designing municipal Hazmat networks do not consider risks analytically, and they do not take account of the fact that the total transportation risk and its distribution are not only affected by the network design decision, but also affected by the routing decisions of shippers/drivers. A two-tiered analytical approach was developed to take these factors into consideration in this research.

Government regulations must be enforced. An important part of enforcement is inspecting the vehicles on the transportation network. The inspection station location model locates facilities to detect and remove hazardous vehicles as early in their trips as possible. I examined the inspection station location model (Hodgson *et al.* 1996) and implemented a tabu search algorithm (Glover and Laguna 1993) for it.

In order to take risk into account in Hazmat transport management, it is necessary to compute the amount of risk associated with road links. Risk is typically measured by the product of incident probability and expected consequences. Current risk assessment methods simply use the number of people living within a certain distance from the road to measure consequences, assuming that all people living within this band incur the same level of negative impact and people living outside the band are not affected at all. This method is not adequate for assessing the consequences of air-borne substances. The effect of Hazmat on human health is related to the concentration levels of contaminants to which the person is exposed. Wind speed and direction play an important role in the distribution of air-borne contaminants, which will have more serious effects on people in the downwind direction than on those in the upwind direction. When wind conditions change, the link risk resulting from the shipments of air-borne Hazmat on this link will also change. Therefore, we need to incorporate wind conditions in risk assessment models to estimate the consequences of such substances accurately. Considering air-dispersion in network risk analysis is conceptually simple yet is very difficult to implement because we need to apply the dispersion models that are framed for point sources to network links.

The objectives of this dissertation are to set up a framework for a Hazmat transport decision support system and to further the methodological developments for the three issues mentioned in the previous paragraphs. The objectives can be summarized as:

1) To evaluate the current status of GIS technology in the context of Hazmat transportation decision support. To identify the missing components in existing GIS technology and to explore the methods for enhancing the analytical capabilities of GIS;

2) To develop a method for incorporating dispersion models into network risk analysis;

3) To develop a procedure for designing municipal Hazmat routes;

4) To develop a robust algorithm for the inspection station model.

The dissertation is organized as follows. The second chapter discusses the capabilities of GIS for Hazmat transport decision support and the methods for building a GIS-based SDSS. The third chapter deals with incorporating dispersion models in network risk assessment. The fourth chapter describes a procedure for designing municipal Hazmat networks. The fifth chapter proposes a tabu search algorithm for the inspection station location problem. The last chapter summarizes the entire research.

Chapter 2

GIS TOOLS FOR HAZMAT TRANSPORT DECISION MAKING

2.1 Introduction

Geographic Information Systems (GIS) technology has developed so rapidly in the last two decades that it is now accepted as an essential tool for the effective use of geographic information. The majority of the data used for Hazmat transport logistics studies are spatially referenced. Therefore, GIS can play an important role in this field. In addition to the traditional geographic data processing and visualizing capabilities, GIS is incorporating more and more analytical and optimization tools to accommodate the demands for spatial decision support. In this chapter the application potential of GIS tools for Hazmat transport logistics research is explored. These tools include the traditional GIS functions such as spatial data management, buffer and intersection analysis, as well as the optimization tools that are becoming widely available in GIS software. The potential applications of GIS in Hazmat transportation are numerous. This study focuses on three aspects: a) Risk analysis; b) Routing; and c) Linking to external models. Risk analysis and routing may be the most popular research topics in Hazmat transportation. The analytical components of GIS have typically been restricted in both their scope and capabilities. Therefore, linking GIS with external models is necessary to enhance their analytical support to decision-makers (Densham 1996).

This chapter is organized as follows. The second section gives a brief introduction to spatial data and GIS capabilities. The third section demonstrates how GIS can improve risk analysis. The fourth section demonstrates the use of GIS in Hazmat routing. The fifth section explores methods for extending GIS's optimization capabilities. The last section contains a summary and concluding remarks.

2.2 Spatial Data, Spatial Data Models and GIS

2.2.1 Spatial data

Spatial data are commonly characterized as having two fundamental components: the spatial location of the phenomenon and the attribute data of the phenomenon. The location is usually specified with reference to a common coordinate system such as latitude and longitude. Attribute data describe the objects on the ground. Spatial data can be represented on a map as points, lines or areas.

2.2.2 Spatial data models

There are two fundamental approaches to the representation of the spatial component of geographic information: the vector model and the raster model. In the vector model, locational information about points, lines, and polygons is encoded and stored as a collection of x, y coordinates. The location of a point feature, such as a gas station, can be described by a single x, y coordinate. Linear features, such as roads and rivers, can be stored as a collection of point coordinates. Polygonal features, such as sales territories and census districts, can be stored as a closed loop of coordinates.

The vector model is extremely useful for describing discrete features, but less useful for describing continuously varying features such as elevation or temperature. The raster model has evolved to model such continuous features. In the raster model, space is divided into discrete, regularly spaced cells (usually square in shape), each of which can have a different value. A raster image is similar to a scanned map or picture. The location of each cell is defined by the row and column numbers. The area each cell represents defines the spatial resolution available. The value stored for each cell indicates the type or condition of the object it represents. Entities on the ground, points, lines and areas, are represented as one cell, a chain of cells or a block of cells. Cells representing the same entity (such as the same road segment) have the same cell value. Each cell is treated as an independent entity even if it represents the same geographic entity as other cells.

Each of the spatial data models has advantages and disadvantages (the major trade-offs are summarized in Table 1). Each data model tends to work best in situations where the spatial information is to be treated in a manner that closely matches the data model. Where the geographic information of interest is the spatial variability of a phenomenon, the raster

representation is generally more suitable. Where the information of interest is the distribution of objects in an area or the relationship between spatial objects, the vector approach is better suited.

GIS usually organize geographic data as a collection of map layers that can be linked together by geography. Each map layer represents one type of spatial objects. The attribute data of the objects are stored in a table consisting of rows and columns. The attribute table is inherently linked to its corresponding map layer. Each row in the table represents one object on the map. Each column represents an attribute describing the features. A geographic object can have multiple attributes (columns) describing it. Depending on the data model they use, GIS are usually classified into raster GIS and vector GIS. Raster GIS and vector GIS use different data storage and processing methods, which suit different applications.

Raster model	**Vector model**
Advantages: 1. It is a simple data structure 2. Overlay operations are easy and efficient 3. High spatial variability is efficiently represented 4. The raster format is more or less required for digital image manipulation and enhancement Disadvantages: 1. The raster data structure is less compact 2. Topological relations are more difficult to represent 3. The output of graphics may have a blocky boundary	Advantages: 1. It provides a more compact data structure than the raster model 2. It provides efficient encoding for topology, and as a result, more efficient implementation of operations that require topological information, such as network analysis 3. The vector model is better suited to supporting graphics that closely approximate hand-drawn maps Disadvantages: 1. It is a more complex data structure 2. Overlay operations are more difficult to implement 3. The representation of high spatial variability is inefficient 4. It is not effective for manipulation and enhancement of digital images

Table 1 Comparison of raster and vector data models
(Burrough 1986)

2.2.3 Capabilities of Raster and Vector GIS

2.2.3.1 Raster GIS

A map layer in raster GIS is called a grid. A grid is composed of cells. The raster data model is particularly suitable for representing a continuous surface. A continuous surface, like elevation or temperature, is a geographic feature or phenomenon that lacks definite boundaries and tends to change gradually. Because of this characteristic, raster GIS usually provide 3-D analysis and visualization capabilities (e.g., slope and aspect calculation, perspective view generation). Because a grid is essentially rows and columns of numbers as in a spreadsheet, it allows a wide range of mathematical operations on cells. Some of the functions that can be carried out very efficiently in a raster GIS include:

- Creating a distance grid from a source - for example, calculating the distance from each cell to an accident site can be finished quickly in a raster GIS.
- Defining areas nearest to points (Thiessen Polygons) - this function can be used to define service area boundaries of a facility.
- Spatial interpolation - this function is often used to estimate the value of cells based on neighboring cells.

In addition to the above functions, the most important advantage of a raster GIS over a vector GIS is the availability of map algebra functions. Map algebra operates on the values of individual cells in one or more grids returning one or more new grids (Tomlin 1990). The common map algebra functions available are addition, subtraction, multiplication, division, power functions, logarithms, arithmetic and trigonometric functions. When an algebraic function is applied to an individual grid, this function is applied to every cell in the grid. For example, when we calculate the logarithm of a grid, the value of each cell in the output grid is the logarithm of the same cell in the input grid. When the operation involves two or more grids, the operation is applied to the same cells from all input grids. For example, calculating the product of two grids means that the value of each cell in one input grid is multiplied by the value of the same cell in another grid to produce the corresponding cell in the output grid.

2.2.3.2 Vector GIS

The vector model can represent geographic objects more precisely and realistically than the raster model. It is a traditional method for representing geographic objects and phenomena in cartography. Most socio-economic data are in tabular format, often linked to spatial objects in vector representation. Therefore, vector GIS are more commonly used in socio-economic studies than raster GIS. The most important characteristic of vector GIS is that it stores data topology – the relationship between points, lines and polygons. Node-link topology is often required for network analysis, which is why network analysis routines are usually implemented in vector GIS.

2.2.3.3 GIS for Data Management

A GIS can maintain the same sort of attribute data as do other computerized database management systems (DBMS), but it also stores location information. GIS are usually designed to interface closely with conventional relational database management systems (RDBMS) and can perform complex Structured Query Language (SQL) queries and calculations. Their ability to integrate both spatial and attribute data is the unique strength of GIS.

Transportation analysis often requires that data be attached to either links or nodes. Transferring data among spatial features can be prohibitively time-consuming without GIS. For example, calculating link population, which is required to find minimum population exposure paths, will take a long time if done manually. However, it can be accomplished easily with buffer and intersection operations in GIS. GIS also allow us to analyze the data at finer scales.

An important feature of GIS is the ability to generate new information by integrating data from different sources using a geographical referencing system (Goodchild 1993). Typical GIS functions for generating new information are buffer and overlay operations. The buffer operation draws bands of specified width around certain points, lines or polygons, the bands can then be used to highlight and extract information from other map layers. Overlay is the process of comparing and intersecting features on different map layers. When buffer and overlay operations are combined, analysis such as point-in-polygon (e.g., find all points that are located in certain polygons), line-in-polygon (e.g., highlight all lines

or line segments that are located in certain polygons), point-near-line (e.g., allocate the points to a line that is the closest to them), and polygon-in-polygon (e.g., aggregate the values of a polygonal layer based on another polygonal layer) can be undertaken to transfer data between different spatial objects.

2.3 Risk Assessment

Risk assessment is a fundamental part of many Hazmat transport logistics studies. Many factors affect the consequences of a Hazmat release. The risk measurement commonly used for Hazmat transportation is the product of probability of release incidents and total potential consequence from such incidents. GIS can facilitate the calculation of consequences in both traditional and advanced methods.

2.3.1 GIS for traditional risk assessment

The traditional method for estimating the consequence of accidents is to draw a band around each link and count the number of people living within this band. This method is conceptually simple and can be done manually (with some perseverance). In a GIS framework, it can be carried out using buffer and intersection operations that are available in many commercial software packages. GIS will accomplish the process with great accuracy by using detailed demographic and network data. Although buffer and intersection operations are computationally intensive processes, they can usually be finished within a reasonable amount of time. For applications that need quick results, such as real-time spatial decision support systems (SDSS), this process can be finished beforehand. The calculated link population can be stored in the attribute table of network links and retrieved when needed.

The traditional method for estimating the consequences has been criticized by many researchers (McMaster 1988, ReVelle *et al.* 1991, Boffey and Karkazis 1995). It uses one band width for all links and is a one-size-fits-all approach, ignoring all other factors affecting the interaction between pollutant release and impact on humans. However, it is still a widely used method.

Many factors will affect the impact of Hazmat release on the nearby population. One important factor is the wind condition. Many hazardous materials become air-borne when released, and will have a much greater impact in the down-wind direction than in the up-wind direction. Different wind conditions put different people in danger. Therefore, it is important for SDSS to be able to incorporate wind conditions in analyzing network risks.

2.3.2 Incorporating wind conditions in risk analysis

The impact of Hazmat pollutants on the human body is related to the concentration level a person is exposed to. The concentration level of air-borne pollutants is usually predicted by dispersion models, which are designed to calculate the concentration at individual points from a point source. It becomes difficult to manage the data and results if we want to calculate the concentration at all points affected. It becomes much worse when we must analyze the risk from each link in the entire network.

By integrating the raster and vector GIS approaches, it is possible to evaluate the risks posed by the Hazmat traffic in the network. The raster GIS discretizes the space, manages data for individual layers and cells, and provides tools for carrying out computations among cells and layers. In the raster framework, the impact area is divided into discrete cells, each treated as an independent receptor point. Links are divided into chains of cells, each treated as a source point. Thus, dispersion models can be used to calculate cell by cell concentration from each source cell in the network grid. Once the concentration level at each cell is computed, it can be overlayed with the population layer to calculate the number of people under different impact levels. The risk analysis results are then sent back to the vector GIS and can be used in subsequent network analyses. Chapter 3 describes the procedure for analyzing network risks in detail.

2.4 Hazmat Routing

2.4.1 Single and multi-objective routing

Hazmat routing is the most popular topic in the Hazmat transport literature (List *et al.* 1991). Barber and Hilderbrand (1980) developed the methodology recommended by the

Treating Hazmat routing problems as SP problems does not explicitly consider the trade-off between different objectives such as risk, cost and equity. Shobrys (1981) and Robbins (1981) present the earliest efforts to deal explicitly with multiple objectives in Hazmat routing problems. Robbins considers two objectives: (1) minimize the population affected by the path, and (2) minimize the length of the path. By using a sample of 105 OD pairs connected by the Interstate Highway System, he determined that the number of people potentially affected by hazardous materials releases is quite sensitive to the selection of routing criteria. Shobrys points out that it is desirable to limit decisions to the Pareto-optimal solution set. Pareto optimality is named after Italian economist Vilfredo Pareto who was prominent in the 1890s. A Pareto-optimal solution is a solution that is superior to any other solution in at least one objective. By using various weights for ton-miles and population-tons, Shobrys was able to use a hybrid distance-population cost for each link, and hence, use a shortest path algorithm to obtain several Pareto-optimal solutions. Saccamanno and Chan (1985) examine three strategies for Hazmat routing: 1) minimize risk exposure; 2) minimize accident likelihood; and 3) minimize operating costs. Zografos and Davis (1989) develop a multi-criteria Hazmat routing model that considers the equity objective. Their model incorporates equitable distribution of risk by imposing capacity constraints on the network links. An alternative approach to the risk equity problem has been taken by Gopalan *et al.* (1990), who focus on a formulation specifying that the maximum difference in risk between any pair of zones must be below a given bound. Cox (1984) and Cox and Turnquist (1986) develop a model to schedule departure times for any given route that minimizes curfew delay en route where public authorities have enacted curfews. The multi-objective models discussed above are based on identifying some weighting scheme to make the multiple objectives commensurable. For a Hazmat risk problem, a commensurable objective (such as dollar value) is hard to find, although the methodology does provide an environment in which decision-makers can choose from different alternatives.

2.4.2 GIS tools for Hazmat routing

GIS have been criticized for lacking analytical capabilities (Openshaw 1996). It is true that the analytical capabilities of GIS are often limited in both scope and sophistication,

although much has been done in recent years in this regard. The most significant improvement can be seen in the customizability of major commercial software (see next section). Some simple optimization models have become widely available in many mainstream GIS software packages. To evaluate the routing tools in GIS for Hazmat transportation, the functions of a GIS are compared with a popular specialized Hazmat routing SDSS. The GIS tools used for evaluation are ArcView GIS for Windows and Network Analyst Extension for ArcView from Environment Systems Research Institute (ESRI) in Redlands, California. The software is selected with the following considerations: 1) it must be a popular GIS software because one of my primary interests is to see what can be done with an organization's existing GIS; 2) it should be a general purpose GIS rather than a specialized GIS; 3) it should run on the Windows platform. Several GIS software packages including MapInfo from MapInfo Corporation in Troy, New York and Maptitude from Caliper Corporation in Newton, Massachusetts meet the above requirements. A combination of ArcView and its Network Analyst extension was selected because ArcView is one of the most popular GIS software running on Windows and because it is available in the lab in which I work. However, my evaluation procedure is not limited to a certain product and the conclusions drawn can be applied to other products as well. Specialized software such as TransCAD (Caliper 1997) from Caliper Corporation is not selected as an evaluation platform because it specializes in transportation applications, so conclusions based on TransCAD may not be applicable to general GIS. On the other hand, conclusions based on a general GIS are usually applicable to TransCAD. For benchmark comparisons, I use PC*HAZROUTE, a specialized Hazmat routing package from ALK Associates Inc. in Princeton, New Jersey. ALK Associates Inc. is one of the largest software companies developing logistics software. PC*HAZROUTE is a popular Hazmat routing software used by many highway and railway carriers.

> PC*HAZROUTE is a decision support system that provides an objective, scientific analysis of the cost and risk factors involved in shipping hazardous materials over any highway or rail route in the United States. It assists in choosing the best route for a shipment based on given routing criteria (ALK Associates 1996).

Figure 1 shows the interface of PC*HAZROUTE. The three windows displayed are the main windows users interact with while using the software. The window at the upper right corner accepts user input of origin and destination points. The window below it allows the

user to specify routing criteria. The map window shows the geographic data and routing results. Figure 2 shows some sample runs of the Hazmat routing tools implemented in ArcView. The small window at the upper-right corner is a floating toolbar containing the tools created for this exercise. The window below it is the Find Best Route dialogue box. It lets users select the origin-destination points and the routing criteria. The next window is the attribute table of the network. Each row corresponds to a link, and each column corresponds to an attribute of the links. The map window shows a sample session of a routing exercise. The map layers displayed are Edmonton's arterial network, the barrier points with one-mile buffer zones, and the paths for different routing criteria. The buffer zones around points on the map are the restricted areas that Hazmat trucks are not allowed to pass. The window below the map window is the report table of one of the paths. In the floating toolbar, the two diamond buttons are there just to reserve the space. The functions of each button in Figure 3 (from left to right, then from up to down) are:

- Buffer Tool  . Create buffer area around each link. Users are prompted for buffer width.

- Intersect Tool  . Intersect two polygonal layers. This tool is mainly used to calculate the population within the buffer area.

- Diamond Tool (1)  . No function implemented for it yet, reserves space for future development.

- Circle Restriction Tool  . Specify the area Hazmat trucks should avoid around certain points.

- Path Tool  . Find the shortest path between user specified origin and destination points.

- Add Location Tool  . Let user specify the origin and destination points.

- Clear Path Tool  . Clear selected paths.

- Weighted Combination Tool  . Calculate weighted combination of selected criteria (fields), with weights chosen to correct for different scales of measurement for different criteria.

- Diamond Tool (2)  . No function implemented for it yet, reserves space for future development.

Interface customization is very easy in ArcView as menus, button bars and toolbars are fully customizable in a graphical environment without writing a single line of code. Although the procedure for customizing interfaces is different from one system to another, it is generally true that the procedure is easy for mainstream Windows GIS software packages. As for functionality, I am only interested in the capabilities that come with ArcView and Network Analyst or that can be implemented with very modest programming.

2.4.3 Hazmat routing experiments using GIS tools

The GIS tools described above were tested on a real world network. The experiments carried out were single objective routing, multi-objective routing and routing with mandatory restrictions. The network used was the arterial road network of Edmonton, Canada, a city with a 1996 population of 626,423 (Statistics Canada 1996). The Edmonton arterial road network is extracted from the digital geographic database maintained by the Planning Department of City of Edmonton and has 1,238 links and 736 nodes. The attribute data for part of the arterial network are listed in Table 2. Each column in the table corresponds to a field. We can add as many fields to the GIS attribute table as we want. Each row corresponds to a link object except for the first two rows. The first row is the field name and the second row is the alias of the field. Aliases are optional for all fields. However, ArcView Network Analyst only allows users to select the fields that are named (or have an alias of) COST, UNITS, HOURS, MINUTES, METERS and a few others as impedance fields. Therefore, I have assigned an (perhaps meaningless) alias to some of the

fields so that they can be used as impedances in the subsequent routing analysis. This restriction does not affect the capability of the software. However, in a decision support system, this is not acceptable; users should be allowed to name the fields in their own (meaningful) way. In Table 2, LINK_ID stores a unique ID for each link. This ID links the attribute data in the table with the link objects in the map. The FNODE and TNODE fields contain the ID numbers for the beginning and ending nodes of each link. The LENGTH field contains the link length. The RISK8DIR field represents the link risks calculated using the Gaussian plume model considering the annual average wind distribution. RISK90 and RISK315 represent the link risks when the wind is blowing from the east and northwest respectively. The procedure for calculating the link risks considering wind conditions is detailed in Chapter 3. The data in the POP1600 field are the number of people living within 1600 meters of the link. Link population is calculated using the Buffer and Intersection tools introduced in the previous section. The steps for calculating the population of a link are:

Step 1. Use the Buffer tool to create a 1600m buffer zone for a link in the network. Figure 4 shows the network and the buffer zone for one link.

Step 2. Use the Intersection tool to intersect the buffer zone with the population layer (Figure 5). The population layer is shaded with population density by 1996 census enumeration area (EA). In this operation, the buffer layer is used as a "cookie cutter" to cut out the buffer area from the population map.

Step 3. Calculate link population by summing the population in the EAs and portions of EAs that are contained in the buffer. Calculating link population is based on the unrealistic assumption that the population is distributed evenly in each enumeration area. However, the EA is the lowest level of aggregation for the census data in Canada, although GIS have the capability to handle much more detailed data.

Step 4. Repeat steps 1 to 3 for every link in the network to calculate the link population for the entire network (Figure 6). Line widths in Figure 6 are proportional to the link population.

It should be noted that the population near a link intersection is counted for all links that intersect at that point. Therefore, when the resulting link population is used for routing, the population near intersection points on the path is double counted.

LINK_ID	FNODE	TNODE	LENGTH	RISK8DIR	RISK90	RISK315	POP1600
			Meters	Hours	Seconds	Minutes	Units
1	4	5	1623.5	2692.8	1.3	132.6	39
2	2	3	1622.0	2559.8	0.6	364.0	28
3	1	2	843.4	1432.9	0.0	143.4	12
4	8	2	3239.5	9544.2	0.0	549.1	45
5	98	94	152.0	0.0	0.0	0.0	20204
...	...	...	...	...	...	...	...
1234	397	385	437.4	119409.4	3822.3	10388.7	17460
1235	342	284	1005.7	214309.0	6052.0	20049.1	19181
1236	328	321	230.4	87062.9	2051.8	12306.1	17082
1237	450	442	717.9	132281.3	2045.3	26772.7	26284
1238	536	616	2942.4	63749.8	1697.4	0.0	2458

Table 2 Attribute data for the Edmonton arterial network

2.4.3.1 Single objective routing

In this exercise, I want to calculate the shortest path and the minimum risk path between two points in ArcView. First I click on the Path tool in Figure 3. ArcView displays the Find Best Route dialogue box (the second right window in Figure 2) allowing users to specify origin and destination (OD) points, and the routing criterion – the column to be used as impedance. I specify the OD points by clicking on two points on the map. To select the routing criterion, I click on the Properties button in the Find Best Route dialogue window and select the field as routing criterion in the Properties window (Figure 7). For the shortest path problem, the METERS (LENGTH) field is selected for impedance. With inputs of OD points and routing criterion, Network Analyst solves the problem and displays the shortest path on the map. Then I open the Properties window again and this time the

HOURS (RISK8DIR) field is selected for impedance and the problem is solved again. Figure 8 shows the two paths calculated. The risk and distance values are shown in Figure 9. The entire procedure is similar to working with PC*HAZROUTE. The advantage of the GIS-based system is that the user can enter OD points either graphically or by specifying an OD table, whereas in PC*HAZROUTE, the user can only enter origins and destinations by typing in their names.

2.4.3.2 Multiple objective routing

In PC*HAZROUTE, multiple objective routing problems are converted to single-objective problems with the weighting method, which normalizes selected criteria and combines them into one criterion. This can be easily accomplished using the Weighted Combination tool implemented in ArcView. The combined field is calculated by specifying the fields and their weights in the Field Combination dialogue window. This tool is implemented for combining up to three fields. The dialogue can be easily modified to allow more fields to be combined. The path minimizing the combination of fields specified in Figure 10 is displayed in Figure 11.

2.4.3.3 Avoiding certain links

Avoiding the links that meet certain criteria is a difficult and time-consuming task in PC*HAZROUTE, whereas in GIS it can be accomplished easily using spatial query and database query functions. Spatial query allows the user to select features based on their relative location to other features (e.g., selecting all links that are within two kilometers of a school). Database query allows the user to select features based on their attributes (e.g., selecting all links that have a traffic density greater than 2000 cars per hour). Therefore, it only takes two straightforward steps to select a path that avoids certain roads in GIS: first select the links using spatial or database query, then run the routing algorithm. The shortest path algorithm in Network Analyst ignores the selected links automatically. Figure 12 shows the shortest path that avoids all the links that have a per kilometer population greater than 18000 (1000*POP1600/LENGTH). The light lines are the links to be avoided. Figure 13 shows the shortest path that is at least two kilometers away from the specified points. Black crosses represent the points specified. Light circles are the areas within two kilometers of the crosses.

2.5 Linking External Models with GIS

GIS are inadequate for many applications in terms of functionality. Even with software specialized in transportation GIS such as TransCAD GIS (Caliper 1997), users will need to implement customized functions and interfaces for their special needs. For Hazmat routing decision-making, interfaces need to be customized to simplify input of problem parameters and to facilitate the interpretation of analysis results. Some special functions may need to be implemented. For example, Hazmat network design procedure and inspection station location models are not typical functions of GIS. If we want to take advantage of the spatial data processing capability of GIS, we need to link these models with GIS. Customization is facilitated by macro languages that come with the software, such as Avenue for ArcView GIS, GDK (Geographic Development Kit) for TransCAD and MapBasic for MapInfo Professional. Customizability and ease of using their macro languages are becoming key competition factors for GIS software companies.

There are three main approaches to enhancing the analytical capabilities in GIS: 1) implementing analytical functions inside the GIS software; 2) developing add-in modules for GIS; and 3) linking GIS with stand-alone software (such as a mathematical program solver).

2.5.1 Implementing analytical functions internally

With the rapid expansion of the application areas of GIS, even general-purpose GIS software packages are incorporating more and more application specific functions. For example, early versions of ARC/INFO, a popular GIS package, included some hydrological models since the product was used in many environmental management applications. After the business community started to use the software, some location-allocation and routing functions were built into versions 7 and up. Other examples are the customized versions these companies build for their customers (ESRI 1997).

More extensive modeling capabilities can be found in specialized GIS, such as TransCAD, a GIS software package for transportation. In addition to special data models for transportation, such as dynamic segmentation, it also has a network builder, which builds a network structure from linear map layers as input data for operations research models. The

operations research procedures include shortest path, traffic assignment, routing and scheduling, flow problems, spatial interaction, and location-allocation models.

2.5.2 Developing add-in modules for GIS

Researchers have been working on extending the analytical capabilities of GIS for at least a decade. Bosque and Moreno (1990), for example, developed a set of location-allocation programs for IDRISI GIS (Eastman 1992). A better known research tool is LADSS (Locational Analysis Decision Support System) that includes a suite of location-allocation algorithms, a menu user interface and an interface to GIS software (Willer 1990). LADSS has been linked to several GIS and mapping software including PC ARC/INFO, TransCAD, Atlas Graphics and MapViewer (Densham 1996). These pioneering efforts showed the benefit of incorporating analytical functions with the graphics capabilities of GIS to the decision making process. They were typically implemented on the DOS PC platform, which provides limited inter-connectivity among different software programs. Today, Windows-based software is much easier to customize than its DOS predecessors. Developing add-in modules for commercial GIS software has become a task every programmer can do, regardless of whether he/she is connected to the original GIS software company. This is facilitated by two trends. The first trend is the architectural improvement at the operating system (OS) level and the adoption of an object oriented programming (OOP) standard. For example, software designed for the Microsoft Windows platform can call and link DLL (Dynamic Link Library) functions during runtime (most other OS have a similar capability, but use different terminology), which means that programs can be compiled into DLL functions and interfaced to other Windows-based software. AvRoute, a set of DLL routing functions developed by RT-Soft, can be called from ArcView GIS. These functions can be used in the same way as other macro language functions of the GIS software. The following is quoted from AvRoute documents:

> AvRoute is designed to allow ArcView GIS users and developers to incorporate routing and transportation models directly into their applications. AvRoute consists of a set of 32 bit dynamic link libraries (DLLs) that, when attached by ArcView, seamlessly extend the functionality of ArcView to include a set of routing and transportation methods. AvRoute is fully integrated into the ArcView 2.1 or 3.0 environment. AvRoute allows users to develop routing applications and store the results in ArcView route systems which can be used with the dynamic segmentation

(DynSeg) data model to analyze and display a wide variety of transportation related data (RT-Soft 1996).

The second trend that facilitates the development of specialized applications by third parties is the "open structure" approach taken by GIS companies. ArcView may be the best example of the latest development in this trend. Starting from version 3.0, ESRI introduced the extension concept for ArcView. The base module provides core functions of a GIS including database management, graphic display and query. More specialized functions or applications are delivered in optional extensions. ArcView extensions work much the same way as Netscape plug-ins. Netscape itself provides the framework and basic tools for exploring the Internet. When it encounters an audio file, it loads the audio reader plug-in from the third-party developer and plays the sound files. The main difference between extensions and DLLs is that the user does not need to program for extensions. Once the desired extension is loaded (through the menu), all the functions included in the extension become available just like the standard functions of ArcView. An extension can be as simple as drawing a circle around a selected point, or as complex as providing a whole suite of raster processing capabilities to ArcView. Extensions are easy to build with the tools provided by ESRI. There are dozens of ArcView extensions available in the market and more are coming out. It is a very exciting trend for GIS users and may be a cost-effective way to develop SDSS for Hazmat transportation.

2.5.3 Linking GIS with a professional solver

Professional solvers refer to the types of software packages that solve mathematical models. Solver products can also be distributed as dynamic link library functions and called by GIS software as discussed in the previous section. In this section I deal with linking a stand-alone mathematical program solver with GIS. Linking GIS with a stand-alone solver is an important way to extend the analytical functions of GIS, especially when the problem faced needs extensive modeling capabilities. By using professional solvers, we can access sophisticated algorithms implemented by highly specialized programmers. By interfacing GIS with solvers, we are taking advantage of the strengths of both fields.

I tested this approach with a small exercise. The problem I solved is a balanced transportation problem that is formulated as follows (Hillier and Lieberman 1990):

Minimize: $Z = \sum_{i=1}^{m}\sum_{j=1}^{n} c_{ij} x_{ij}$

Subject to: $\sum_{j=1}^{n} x_{ij} = s_i$ for $i = 1, 2, \ldots, m$

$$\sum_{i=1}^{m} x_{ij} = d_j \quad \text{for } j = 1, 2, \ldots, n$$

$$x_{ij} \geq 0 \quad \text{for all } i \text{ and } j$$

Where:

Z is the total transportation cost

x_{ij} ($i = 1, 2, \ldots, m; j = 1, 2, \ldots, n$) is the number of units to be shipped from source i to destination j

c_{ij} is the cost for shipping one unit of product from source i to destination j

s_i is the number of units available at source i

d_j is the number of units needed at destination j

The objective of the model is to minimize the total shipping cost. The first constraint set ensures the total number of units shipped from i is equal to the number of units available at i. The second constraint set states the number of units shipped to j is equal to the demand at j. The third constraint states the number of units shipped cannot be a negative number.

The software used for this test were ArcView GIS, Network Analyst and GAMS (General Algebraic Modeling System). ArcView was used to store the network data and supply-demand point data. Network Analyst was used to calculate the shipping costs between the supply-demand pairs. GAMS is a professional solver designed to solve mathematical programming models (Brooke *et al.* 1988). With the input of the cost matrix calculated in Network Analyst and the supply-demand data, GAMS solves the problem and outputs the

result in its own format. The user interface is a single menu item "Transportation" added to the standard ArcView graphical user interface (Figure 14). The menu item is associated with an Avenue program that carries out the following sequence of actions:

- Run shortest path array routine to find the cost between each supply and each demand point;
- Run a C++ program that reads the cost matrix and supply-demand data and writes a text file in the GAMS modeling language describing the transportation problem;
- Start GAMS to solve the problem;

The test problem used the Alberta primary highway network, and has two supply points (Edmonton and Calgary) and two demand points (Swan Hills and Lloydminster). This is a trivial problem in terms of solution methods, but it is sufficient to demonstrate the procedure for solving optimization models using a combination of GIS and solver packages. The supply and demand data are stored in the attribute table linked to the demand and supply point map in ArcView (Table 3). Negative supply values denote demand points. I assume all shipments take the shortest path and the cost is proportional to the distance. After the "Transportation" menu is clicked, the Avenue program calculates the shortest paths between all source and destination points and displays the paths on the map (Figure 14). The resulting distance matrix is stored in ArcView as a table (Table 4). The demand-supply data and the cost matrix are all the data needed to solve the transportation problem in GAMS. ArcView stores data tables in standard dBase format. Since GAMS requires input files in the GAMS modeling language, I wrote a C++ program to read the ArcView data tables and to write a GAMS input file automatically. The GAMS input file for the transportation problem is listed in Appendix 2. After the C++ program finishes operation, GAMS starts to work. It reads the input file, solves the problem and writes the result in an output file in text format (Appendix 2). GAMS output files are lengthy. The first part lists the input file with each line numbered, the second part shows how GAMS interprets the problem (pages 2-5), the third part is the Solve Summary (pages 6-8) which includes the solution status, objective function value, decision variable values and sensitivity analysis. The objective function value (the total cost) for the test problem is 11860. The values of decision variables (optimal shipping pattern) are listed in Table 5. The first two

parts are for debugging and error checking. Sensitivity analysis is an important part of decision analysis, but it is usually not implemented in optimization tools within GIS. This is an advantage of using professional solvers.

	Supply
Calgary	18
Edmonton	12
Lloydminster	-14
Swan Hills	-16

Table 3 Supply and demand data for the transportation problem

	Lloydminster	Swan Hills
Calgary	518	504
Edmonton	246	216

Table 4 Distance matrix between all source and destination points (km)

	Lloydminster	Swan Hills
Calgary	14	4
Edmonton	0	12

Table 5 Optimal shipping pattern for the test problem

This whole process works very smoothly and the programming requirements for it are modest. Writing the C++ program for reading the ArcView table and writing the GAMS input file may be the most challenging part. However, this program is not necessary because the input data can be simply typed (or copied and pasted) into the GAMS input

file. The new versions of GAMS or other solvers will probably be able to read ArcView tables, which are in dBase format, directly. This will make it easier to pass the data back and forth between GIS and solver. Linking a professional solver with GIS is particularly suitable for people who need access to extensive modeling capabilities.

The level of integration between GIS and spatial analysis capabilities can be classified into four levels: 1) stand-alone spatial analysis software; 2) loose coupling of existing GIS software with spatial analysis software; 3) close coupling of GIS with spatial analysis software; and 4) full integration of spatial analysis with GIS (Goodchild 1992). There are no clear-cut boundaries between these methods. The implementation of spatial analysis functions in TransCAD GIS is an example of full integration. The Network Analyst module for ArcView can be considered an example of close integration or full integration. Our exercise with GAMS and ArcView is an example of standalone to loose coupling.

2.6 Summary and Conclusions

In this chapter I briefly introduced some GIS concepts and evaluated the tools available in GIS for Hazmat transport decision making. I focused on the application of GIS in spatial data management, risk analysis and routing. I also explored methods for expanding the analytical capability of GIS. I worked on some exercises to compare the GIS tools with a specialized Hazmat routing decision support system. I also worked on a small project using GIS and a professional solver together for decision support. Based on the experiments, I make the following observations:

- Hazmat transport decision-making will benefit from the spatial data management and processing capabilities in GIS. These benefits can be seen in more efficient and cheaper data processing, allowing analysis on finer scales and creating new information by integrating data from different sources.

- Network risk analysis is simplistic in traditional methods. By utilizing raster GIS data structure and raster analysis functions, I am able to incorporate wind conditions into risk analysis for the entire network. Other researchers are only able to apply the dispersion models for point sources risk analysis (McMaster 1990) or have to simplify the dispersion model for network risk analysis. I believe the application potential of

GIS in this regard can go farther. With the help of GIS, we may be able to incorporate any risk factors we want realistically in network risk analysis.

- The routing tools available in GIS are as good as specialized Hazmat decision support systems and are enough for common demands. With modest programming, I am able to develop an interface that is comparable to PC*HAZROUTE. In fact, I built a simple Hazmat routing package using the tools available in GIS in a very short time. For organizations that already have a GIS, it is more cost-effective and flexible to build Hazmat routing procedures in GIS than to purchase a specialized decision support system. However, this does not mean that everybody should buy and build a GIS rather than buying a specialized Hazmat routing decision support system such as PC*HAZROUTE. A specialized SDSS usually includes data as well as software. A major part of the price paid for SDSS is for the data that are very expensive to collect and clean for individual organizations. Therefore, if the organization does not have a GIS database that can be used for Hazmat decision support, it may be less expensive to buy an off-the-shelf SDSS.

- Expanding the analytical capabilities is not restricted to the original GIS company and does not require extensive programming skills. Several methods are available for extending GIS capabilities. This further strengthens my argument that GIS is an ideal framework for Hazmat transport decision support systems.

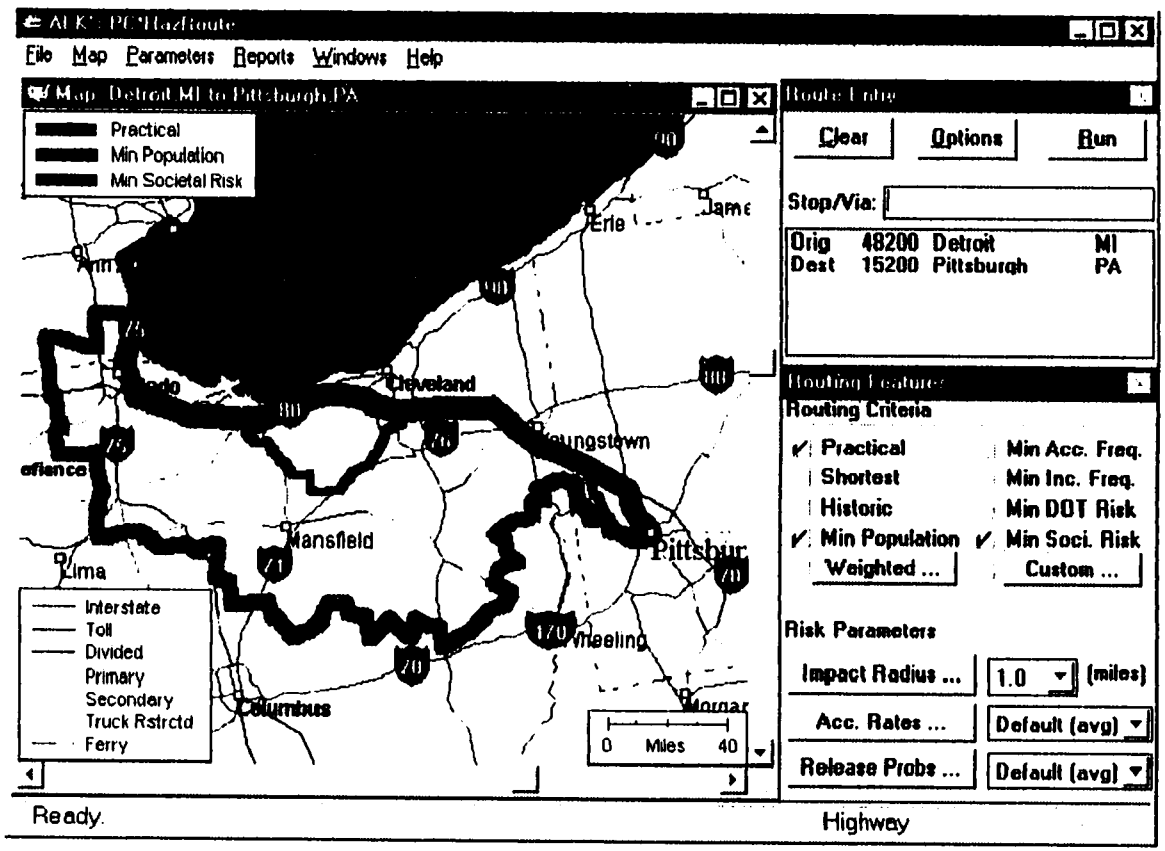

Figure 1 The main interface of PC*HAZROUTE

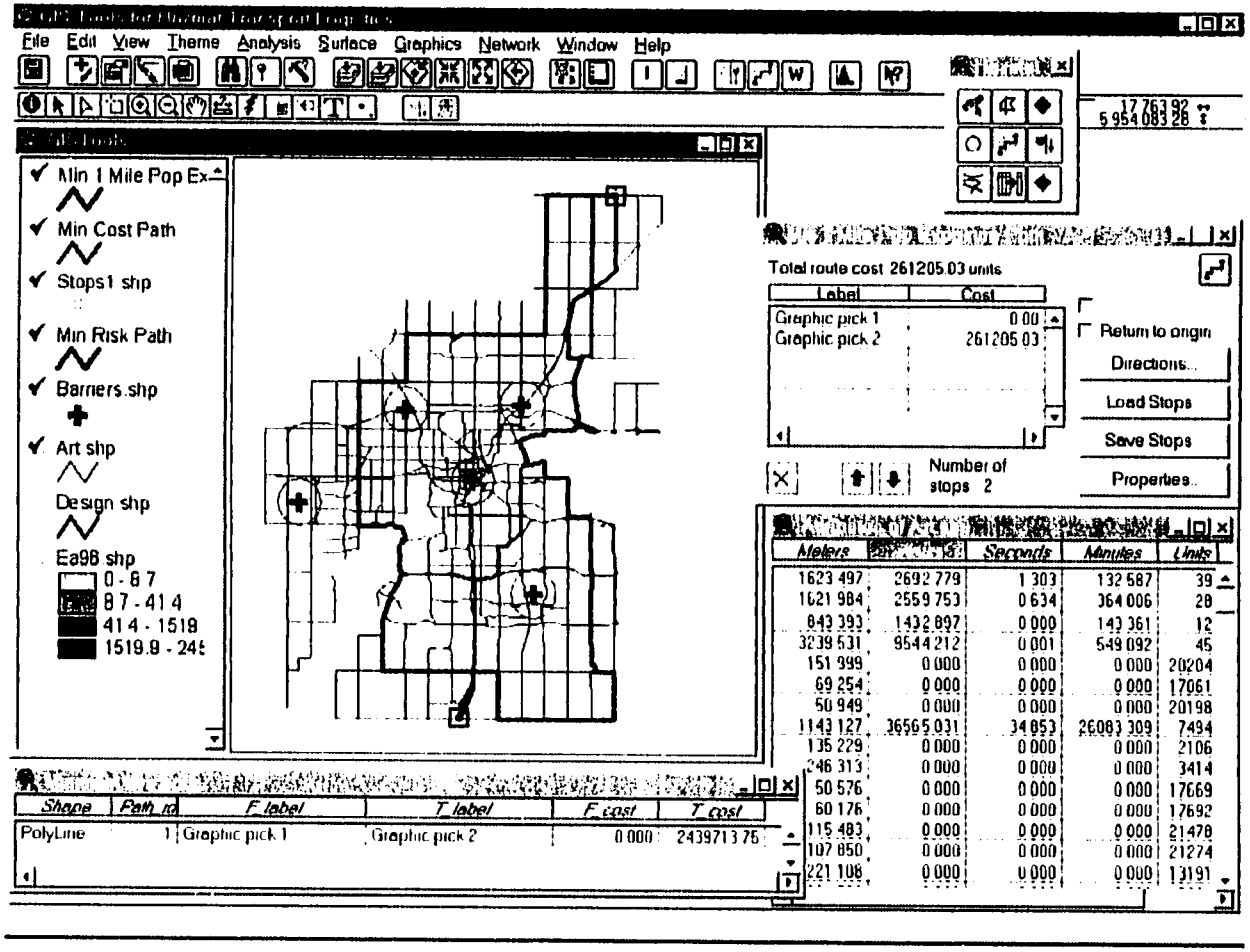

Figure 2 Customized routing tools for ArcView GIS

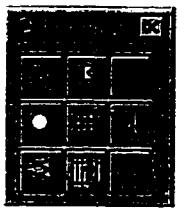

Figure 3 Hazmat routing tools implemented in ArcView GIS

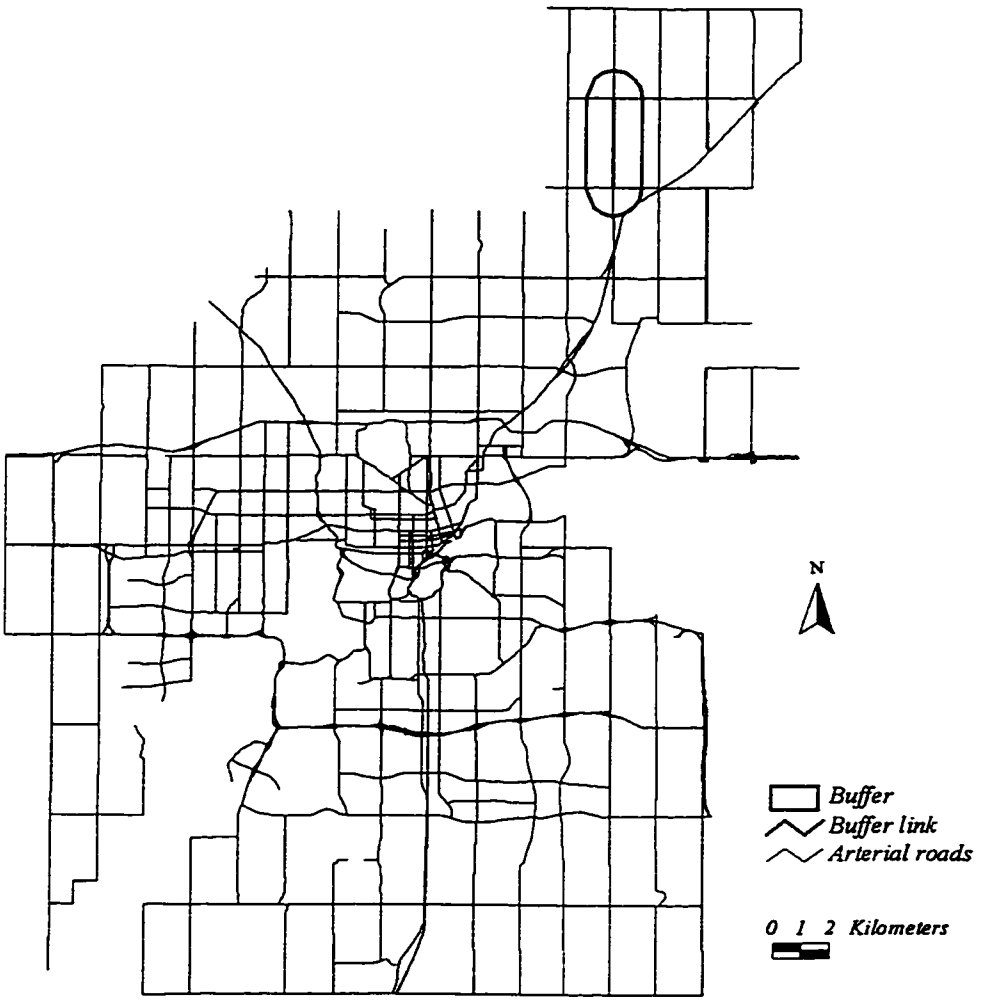

Figure 4 Buffer analysis for the Edmonton arterial network

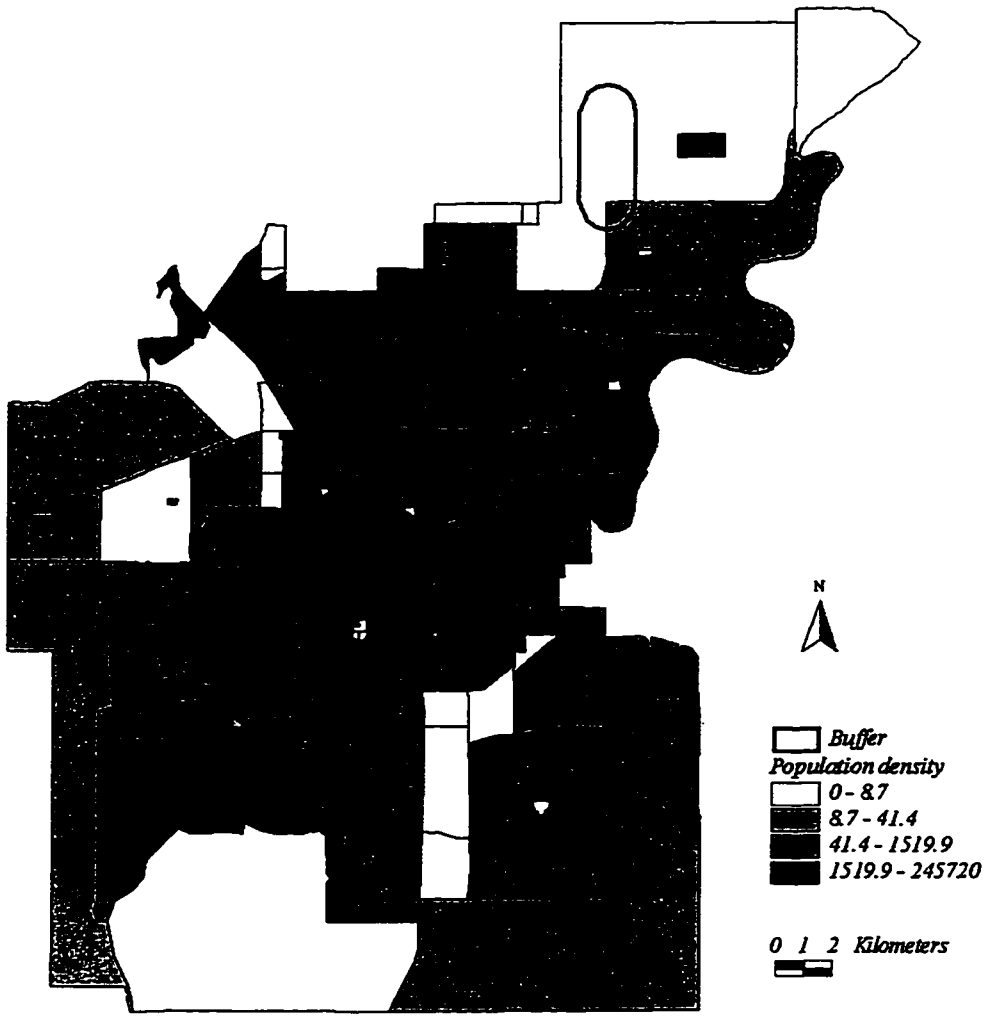

Figure 5 Intersect of buffer zone layer with population layer

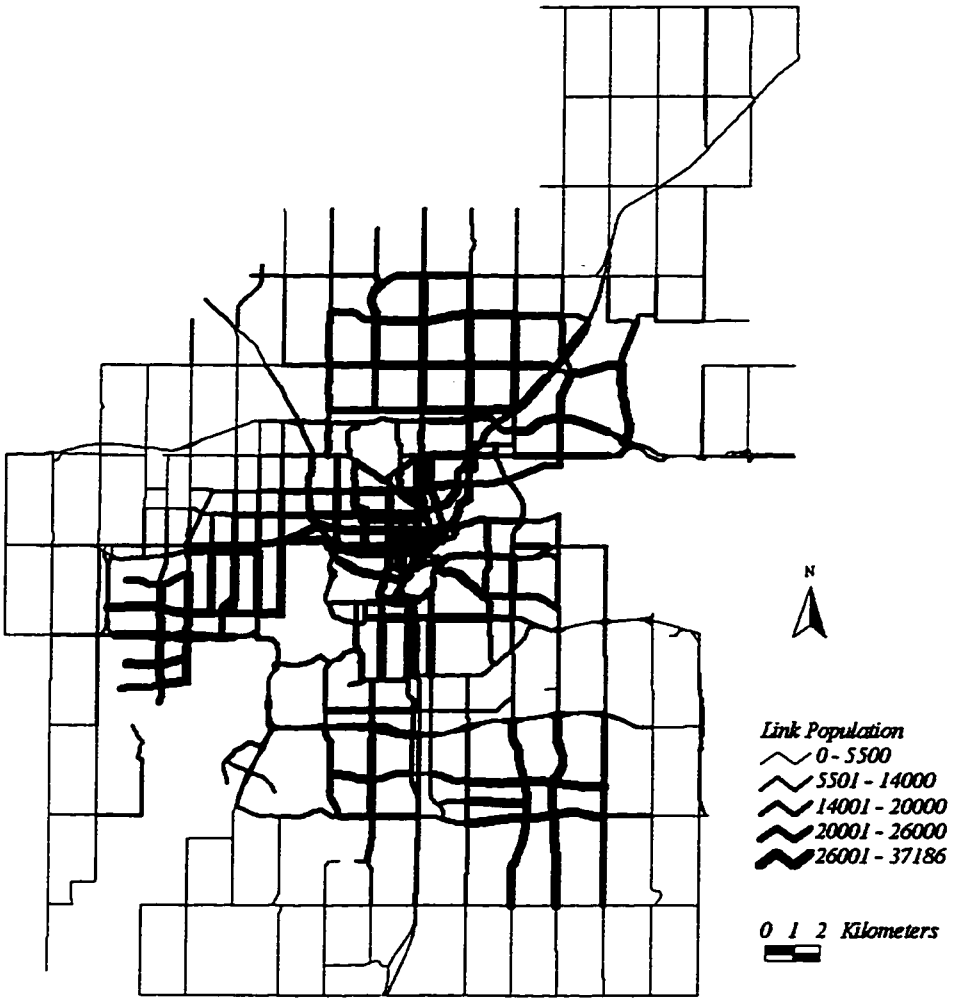

Figure 6 Number of people living within 1600m of each link

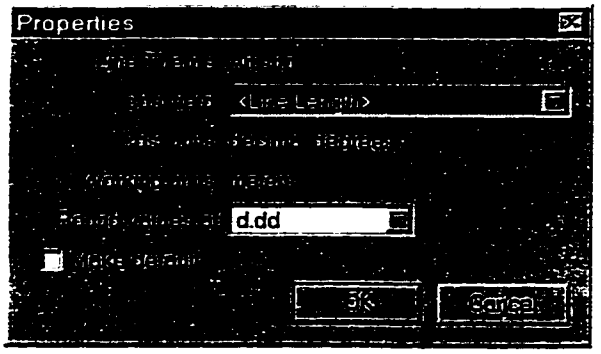

Figure 7 Properties (routing criteria selection) dialogue box

Note: Cost units is decimal degrees (in latitude and longitude) for Line Length because the data is stored in GIS using the Geographic Coordinate System. Output values will be in working units (meters)

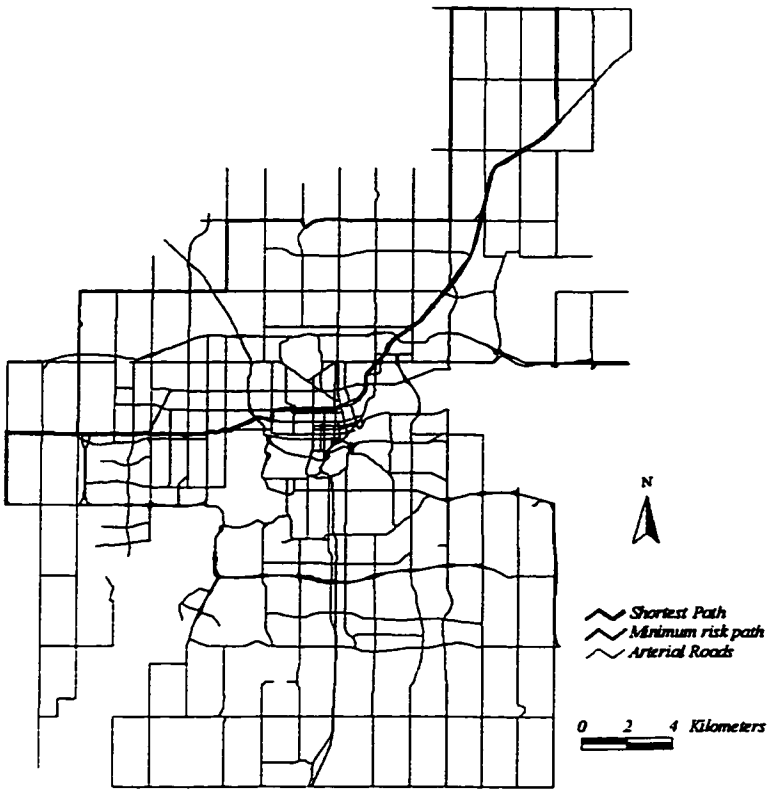

Figure 8 The shortest and the minimum risk paths

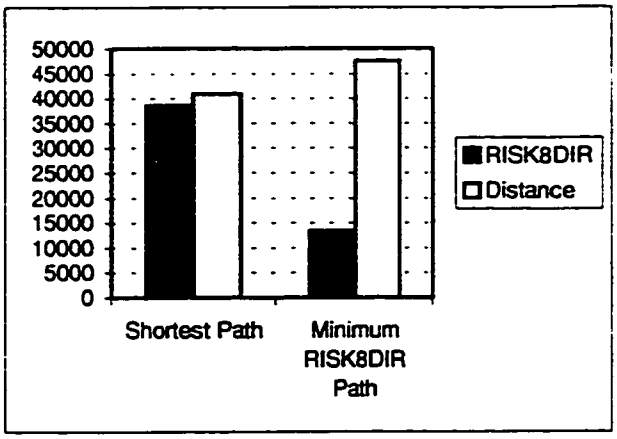

Figure 9 Trade-off between the two objectives in single objective paths

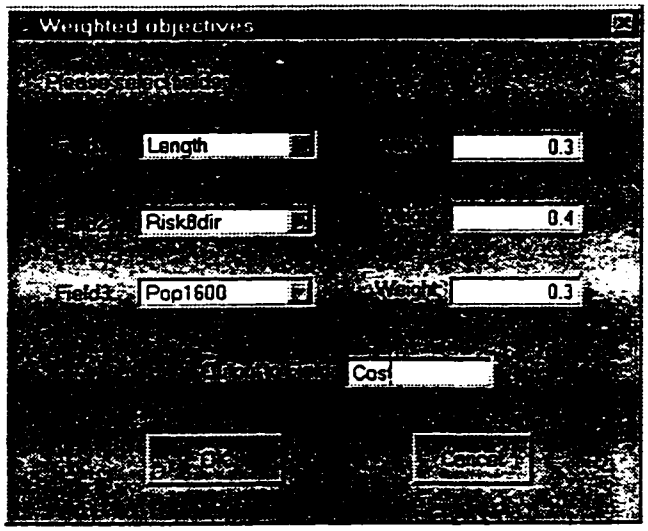

Figure 10 Field combination dialogue window

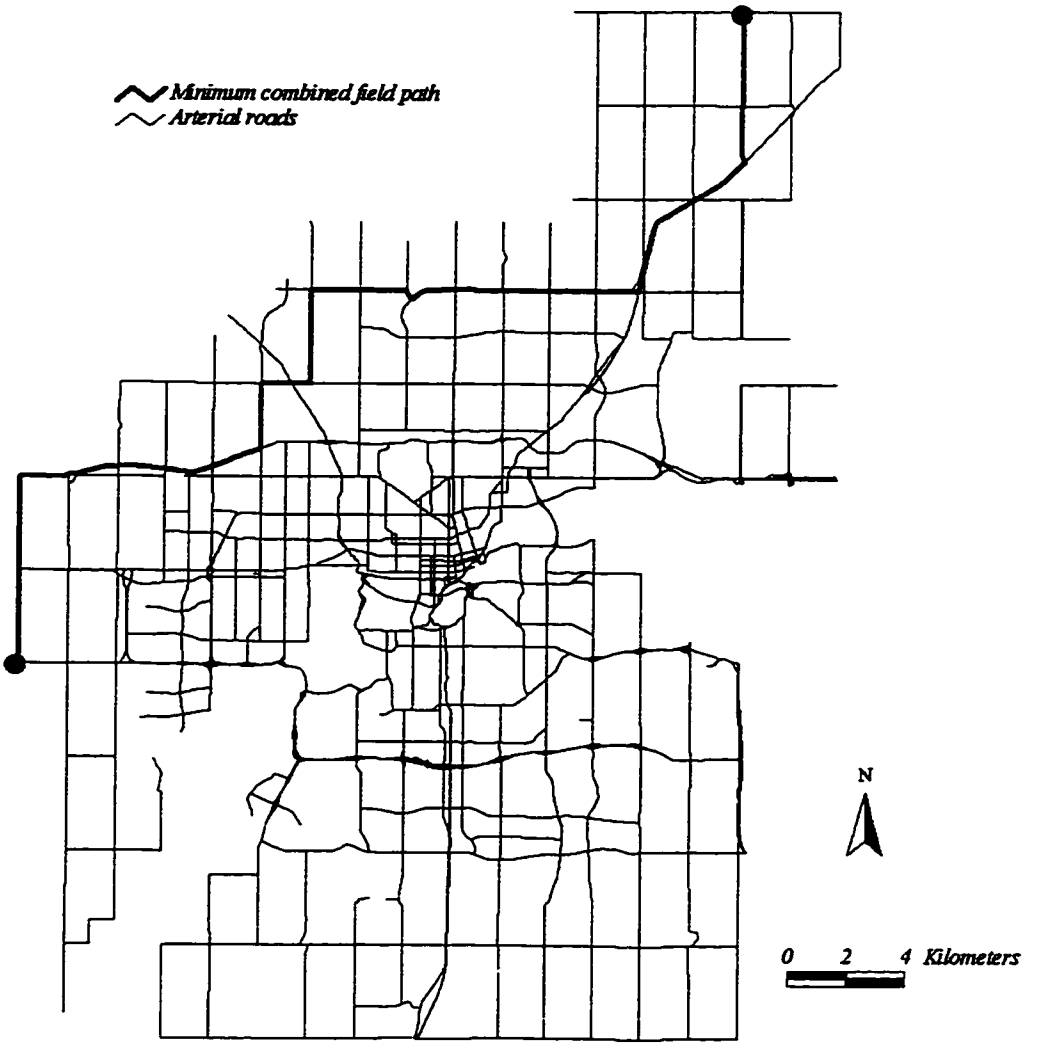

Figure 11 The path minimizing the combined field

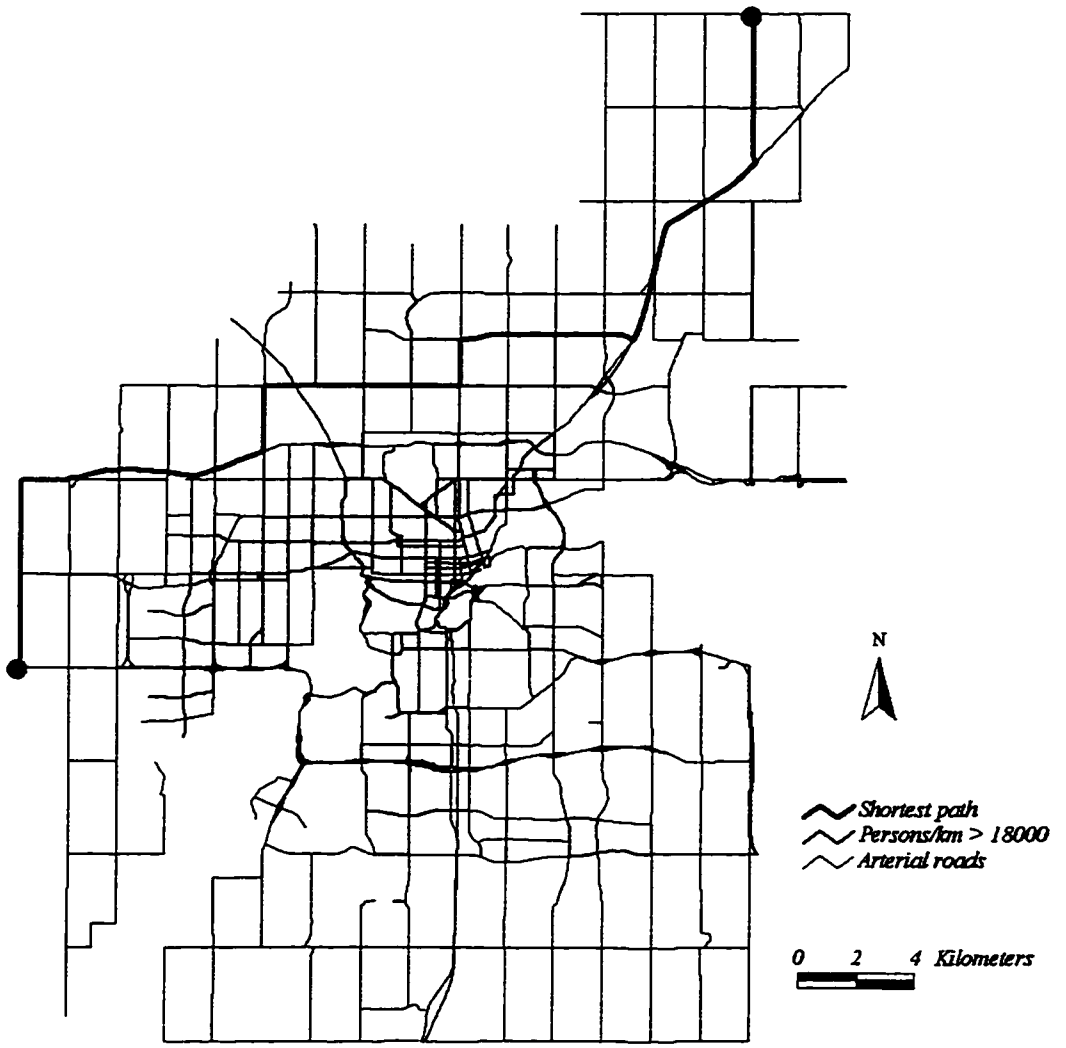

Figure 12 The shortest path avoiding links with population density > 18000 persons/km

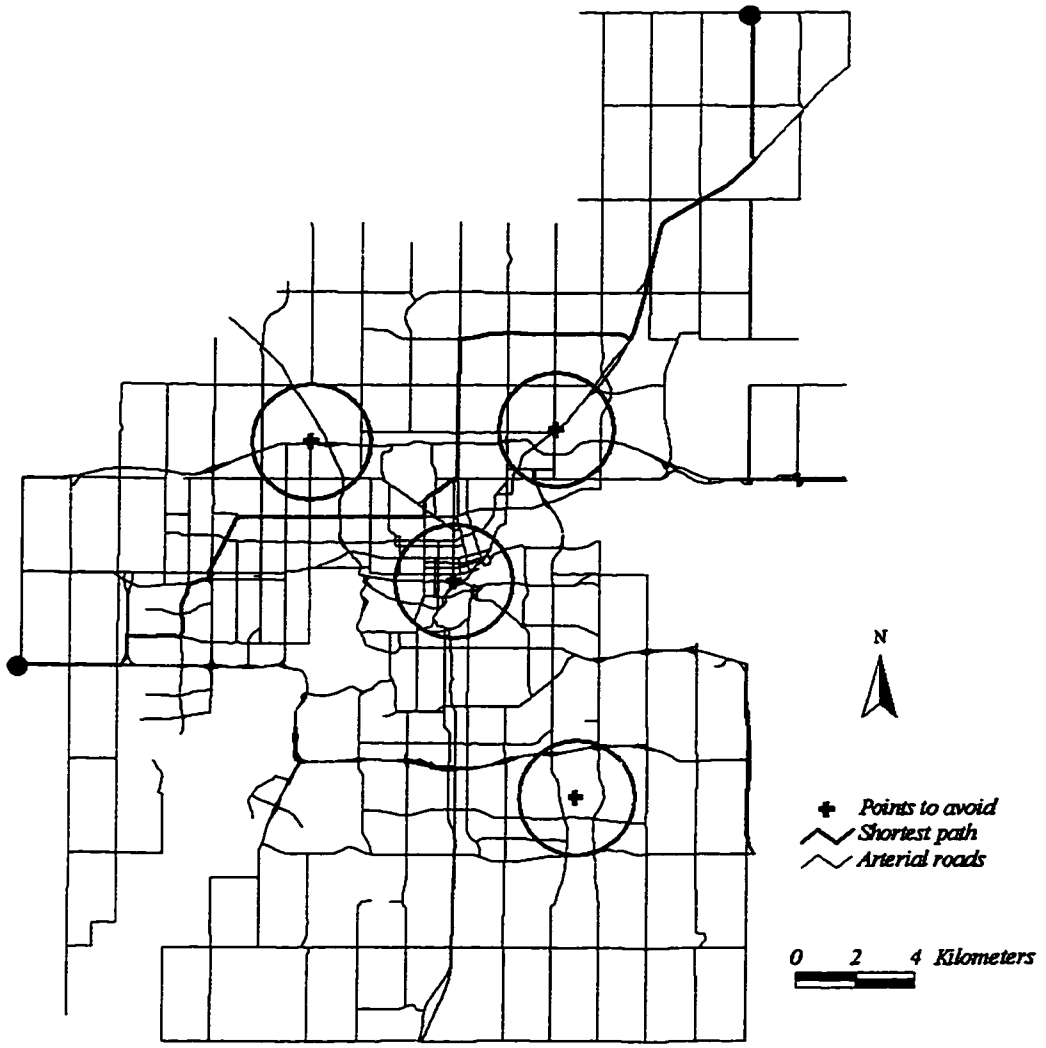

Figure 13 The shortest path at least 2km away from the specified points

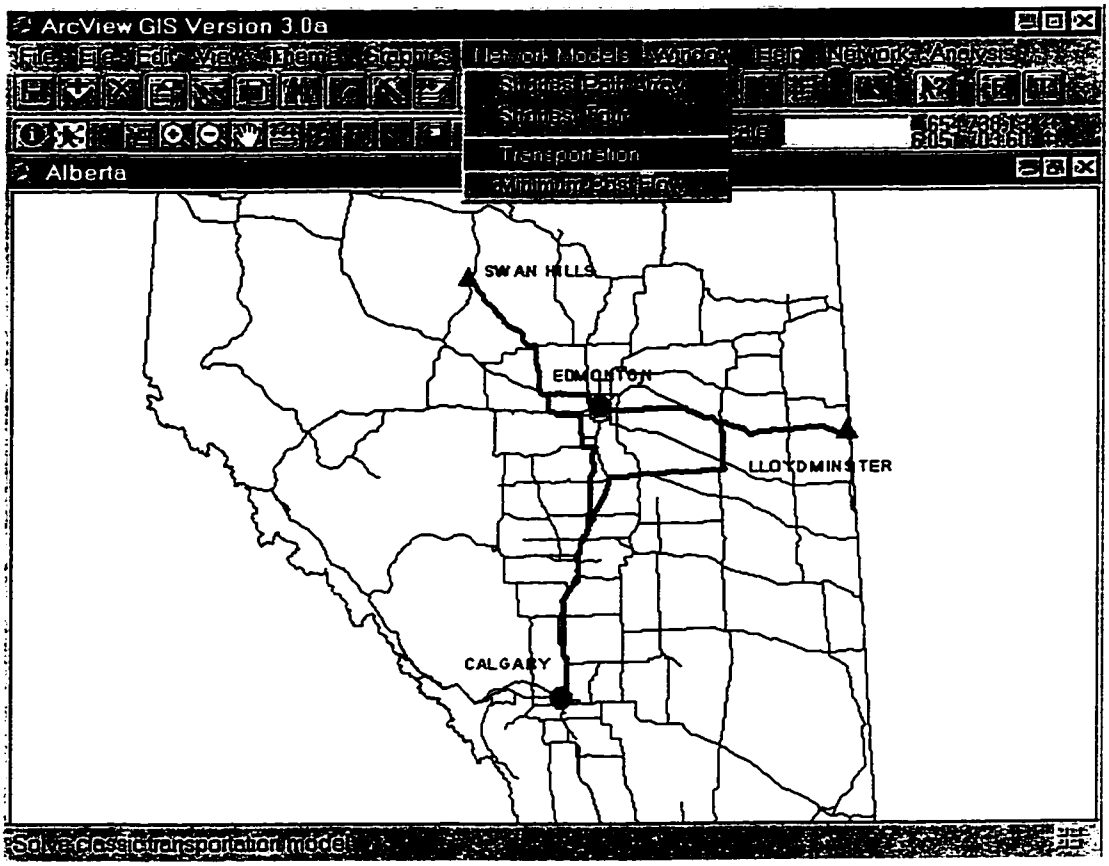

Figure 14 Solving the transportation problem in ArcView

Chapter 3

RISK ANALYSIS

3.1 Introduction

Risk analysis is fundamental to many Hazmat transportation studies. The primary objective of Hazmat routing, Hazmat network design and inspection station location models is to minimize the risk imposed on society. Therefore, it is necessary to assess the link risk associated with shipments traversing each link in a network. Hazmat transport risk is commonly defined as the product of probability of release accidents and the potential consequences of the accidents (Erkut and Verter 1994). We assume that the probability of release accidents is available. Determining the potential consequence of Hazmat releases is very complex. The traditional method for estimating consequences assumes that all people living within a certain distance of the accident receive the same level of impact. This method is simplistic and has been criticized by several researchers (e.g., ReVelle *et al.* 1991). However, it is still a widely used method because differentiating impact levels will increase computational complexity immensely.

It is obvious that the impact of pollutants on human health is affected by many factors. One of the most important factors is the concentration level of pollutants. Generally the concentration level at locations close to the source is higher than that at locations far away from the source. Spatial variation of concentration levels is even greater for airborne pollutants. When the wind is blowing, air-borne substances can have a more significant impact in the downwind direction than in the upwind direction. Therefore, it is important to consider wind conditions in assessing the risks from airborne pollutants. Dispersion models, commonly used for calculating the concentration levels at different distances from the pollution source, have been used to analyze the risk from point based sources (e.g., Chakraborty and Armstrong 1995). To incorporate dispersion models in link risk analysis, the models will need to be integrated over the link. Because dispersion models are usually very complex, it is very difficult, if possible, to derive closed-form solutions to the integral. Numerical methods can be used to solve the integration approximately. In this chapter, I

use GIS map algebra techniques to implement a numerical method to estimate the risk associated with each link in the network.

The focus of this study is restricted to the risks posed to people by air-borne contaminants. The rest of the chapter is organized as follows. The second section describes the risk assessment method currently used by most researchers and practitioners. The third section introduces the Gaussian plume model (GPM), the dispersion model we use to calculate the concentration levels of contaminants. The fourth section demonstrates the GIS method for incorporating dispersion models in calculating the risk from a point source. The fifth section extends the method to calculate the risk from linear sources. The last section is the summary and concluding remarks.

3.2 Traditional Methods of Hazmat Transport Risk Assessment

As early as 1971, the US National Transportation Safety Board was urging a risk-based approach to developing regulations for transporting hazardous materials. Ang *et al.* (1989) suggested a general framework for risk analysis in transportation. The key idea in this approach is to decompose the problem into three separate stages:

1) Determine the probability of an undesirable event (e.g., an accident involving release of hazardous material);

2) Determine the level of potential exposure, given the nature of the event; and

3) Estimate the magnitude of the consequences (i.e., fatalities, injuries and property damage) given the level of exposure.

Each stage of the process produces one or more probability distributions, with the second and third stages involving conditional distributions. In practice, the process is seldom carried out all the way through. A frequent shortcut is to bypass the conditional distributions and use the product of probability of an incident and the extreme consequence of the incident to estimate the risk. The potential impact population is often used as the extreme consequence. Therefore, the traditional risk evaluation can be formulated as:

$$R_i = S_i * P_i * N_i \tag{3.1}$$

where:

R_i is the total risk from Hazmat shipments on link i

S_i is the number of shipments on link i

P_i is the probability of release from a single shipment on link i

N_i is the total number of people who will be affected by the accident on link i

The rarity of Hazmat accidents makes it difficult to calculate Hazmat accident probabilities for each link empirically; truck accident rates are sometimes used to estimate these rates (Chakraborty and Armstrong 1995). Estimating the number of persons impacted is a two-step process:

1) Estimate the potential impact area of Hazmat accidents;

2) Calculate the number of people within the impact area.

Estimating, *a priori*, the impact area of a potential accident is difficult. It is possible to perform a detailed risk assessment for any particular accident location, but for routing purposes, risks must be estimated for the infinite number of points on a transportation network. Hence, a common shortcut is to draw a band of fixed width around each link and to use the number of people living within this band as the link consequence. This approach assumes that all people within the band will get the same negative impact from the accident, whereas the people outside of the band are not affected at all. For emergency evacuation in response to an actual accident, this approach is direct, and may be safe if the evacuation area is sufficiently large. It is, however, inappropriate to use this approach to calculate the risks associated with airborne Hazmat accidents. In the first place, it does not consider the very important effects of wind direction and velocity on dispersion. Neither does it consider the effects of distance on the level of impact. The width of bands is often determined arbitrarily. Determining the size of the evacuation area is easier in the

emergency response setting for a particular accident, but is hardly possible to determine a generally applicable band width for risk analysis. These drawbacks are especially obvious for assessing the impact of accidents where the substances become airborne when released.

Substances that become airborne when released, such as chlorine and radioactive particles, can be very dangerous to the people living in the downwind direction. Air-borne substances impose a much greater threat in the downwind direction than in the upwind direction. Therefore, consequence estimates made by drawing a single band around the road may be quite erroneous, because the probability of a consequence depends on the concentration of contaminants. Since people exposed to a higher concentration of hazardous gases suffer greater consequences, it is important to differentiate between the probabilities of a consequence at different locations and to apply these levels to the number of persons exposed at each location.

This approach addresses the usually shortcutted second and third stages in Ang *et al.*'s (1989) framework. To implement this approach, we must estimate the concentration level at every location impacted by the pollution source. We can do this using dispersion models. The Gaussian plume model (GPM) is the most popular dispersion model used by micro-meteorologists and air pollution analysts (Angle and Sakiyama 1991). Therefore, we use GPM for this analysis.

3.3 The Gaussian Plume Model (GPM)

3.3.1 The model

The Gaussian plume model is formulated as (Stern *et al.* 1976):

$$C(x,y,z)=\frac{Q}{2\pi u\sigma_y\sigma_z}e^{-\frac{1}{2}\left(\frac{y}{\sigma_y}\right)^2}\left[e^{-\frac{1}{2}\left(\frac{z-h_e}{\sigma_z}\right)^2}+e^{-\frac{1}{2}\left(\frac{z+h_e}{\sigma_z}\right)^2}\right] \tag{3.2}$$

where:

C is the concentration level

x is the distance downwind from the source

y is the distance from a line through the source parallel to the wind direction

z is the elevation of the point

h_e is the elevation of the source

Q is the release rate of the pollutant

u is the average wind speed

σ_y and σ_z are diffusion parameters in the y and z directions

The term $\frac{Q}{2\pi u\sigma_y\sigma_z}$ is the centerline concentration; $e^{-\frac{1}{2}\left(\frac{y}{\sigma_y}\right)^2}$ accounts for an off-axis location; $e^{-\frac{1}{2}\left(\frac{z-h_e}{\sigma_z}\right)^2}$ accounts for the elevation of the source above the ground surface; and $e^{-\frac{1}{2}\left(\frac{z+h_e}{\sigma_z}\right)^2}$ treats the ground surface as a perfect reflector, absorbing none of the pollutant. Any consistent set of units may be used. It is customary to employ the SI system: $x, y, z, \sigma_y, \sigma_z$ are in meters and u is in meters per second. Source strength Q can be expressed as a mass emission rate (g/s) which yields a concentration as a mass per unit volume ($\mu g/m^3$) or as a volumetric flow rate (m^3/s) which yields a concentration as a ratio (fraction or ppm). In Hazmat dispersion resulting from traffic accidents, we assume the source to be near the ground and we usually consider the concentration level on the ground. For a ground source, concentration on the ground level ($h_e = 0$, $z = 0$) is:

$$C(x,y,z) = \frac{Q}{\pi\sigma_y\sigma_z u} e^{-\frac{1}{2}\left(\frac{y}{\sigma_y}\right)^2} \tag{3.3}$$

The concentration on the plume's center line ($y = 0$) is:

$$C(x,y,z) = \frac{Q}{\pi\sigma_y\sigma_z u} \tag{3.4}$$

3.3.2 Dispersion parameters

The dispersion parameters, σ_y and σ_z, are affected by atmospheric stability, which is in turn affected by the time of day, solar radiation strength, wind velocity and cloudiness. They are determined empirically according to several systems. A widely used system in North America is a graphical summary of experimental data originally used by The British Meteorological Office (Angle and Sakiyama 1991). This system classifies atmospheric stability into six categories: very unstable (A), moderately unstable (B), slightly unstable (C), neutral (D), slightly stable (E) and moderately stable (F). The graphics, known as Pasquill-Gifford curves, consist of log-log plots of σ_y and σ_z as a function of downwind distance and stability category (Figure 15 and Figure 16).

In dispersion formulae it is convenient to have analytical expressions for σ_y and σ_z. Many of the empirically determined forms can be represented as power-law expressions,

$$\sigma_z = a * x^b \tag{3.5}$$

$$\sigma_y = c * x^d \tag{3.6}$$

where:

a, *b*, *c* and *d* are constants corresponding to different atmospheric stability categories.

Because the vertical Pasquill-Gifford curve is nonlinear, no single power law function can fit the vertical spread data over all distances. Consequently most workers have used two or three different sets of power law constants for different distance ranges. Each power law function will fit one segment of the line with a different slope. Single power law approximations for the Pasquill-Gifford parameters are given in Table 6 (Turner 1970). Selection of stability categories for a given application is facilitated with Table 7 taken from Slade (1968). Atmospheric variables are wind velocity and thermal conditions classified by day and night with subdivisions shown in the table. Night is taken as the period from one hour before sunset to one hour after sunrise. Solar radiation strength depends on solar

altitude and amount of cloudiness. Cloudiness is that fraction of the sky above the horizon covered with clouds. Additional details are given in Turner (1970).

Stability	a	b	c	d
Very unstable (A)	0.00022	2.10	0.59	0.85
Moderately unstable (B)	0.056	1.10	0.41	0.86
Slightly unstable (C)	0.12	0.91	0.24	0.88
Neutral (D)	0.73	0.55	0.14	0.89
Slightly stable (E)	0.82	0.48	0.11	0.89
Moderately stable (F)	0.63	0.45	0.075	0.89

Table 6 Coefficients in single power-law approximations to the Pasquill-Gifford curves

Wind velocity, u (m/s)	Day, incoming solar radiation			Night, cloudiness	
	Strong	Moderate	Slight	Thin overcast or >=4/8 cloudiness	<=3/8 cloudiness
<2	A	A-B	B		
2-3	A-B	B	C	E	F
3-5	B	B-C	C	D	D
5-6	C	C-D	D	D	D
>6	C	D	D	D	D

Table 7 Guide for selection of stability categories Pasquill-Gifford data

Under different atmospheric stability conditions, the concentration on the centerline as a function of downwind distance is shown in Figure 17. The concentration across the centerline is shown in Figure 18. Figure 17 and Figure 18 show that when atmospheric conditions are stable, the pollutants are concentrated along a narrow area along the plume line. Under unstable atmospheric conditions, the pollutants spread across a much wider area.

3.3.3 Discussion of the Gaussian Plume Model

The dispersion of air-borne materials by the wind is a very complex phenomenon. Even under the idealized conditions of a laboratory, the dynamics of turbulence and turbulent diffusion are generally regarded as intractable problems. In the real world, the problems are complicated by the irregular nature of the earth's surface. Therefore, there is no general complete formula to express the physical relationship between ambient concentrations of air pollution and the causative meteorological factors and processes. However, a large body of empirical data on atmospheric dispersion has been accumulated. Practical and/or semi-theoretical expressions and working equations derived from field studies have proven useful in estimating the dispersion of pollutants in the air (R. P. Angle and S. K. Sakiyama 1991).

The Gaussian plume model is a popular model for air pollution dispersion. It is simple, yet flexible enough to incorporate a host of special phenomena. The Gaussian plume model has been checked against numerous field data. It agrees reasonably well with the bulk of experimental data, although non-systematic deviations from a Gaussian distribution are common.

> The important point is that the Gaussian formula, properly used, is peerless as a practical diffusion modeling tool. It is mathematically simple and flexible, it is in accord with much though not all of working diffusion theory, and it provides a reliable framework for the correlation of field diffusion trials as well as the results of both mathematical and physical diffusion modeling studies. (Gifford 1975)

In a major Alberta study, the Energy Resource Conservation Board reported that a large portion of their 846 test plumes were reasonably approximated by Gaussian profiles, many were virtually indistinguishable, and a few were skewed or bi-modal. Skewness coefficients were normally distributed about zero, indicating that departures from Gaussian shape are random. Kurtosis coefficients showed that many observed profiles were slightly less peaked than the Gaussian shape, but that on average, there was good agreement with the Gaussian shape (Angle and Sakiyama 1991).

The Gaussian plume model is based on several limiting assumptions:

1) The gas does not change its chemical properties during dispersion.

2) The rate of emission is continuous and steady.

3) Atmospheric conditions are homogeneous in the study area and constant over the period of dispersion.

4) The terrain is gentle or flat and the ground surface does not absorb the gas.

Assumptions 1 and 2 limit the applicability of the Gaussian plume model to stable chemicals and to accidents that do not result in explosion. Assumptions 3 is realistic for many situations, but in some cases, wind conditions change very quickly and vary within a small geographic area. Because of the complexity of atmospheric dispersion processes, a dispersion model that is general enough to remove all the restrictions has not yet been developed. Therefore, several dispersion models should be implemented in a decision support system so that an appropriate model can be chosen to deal with a particular situation. The limitations of the dispersion models do not limit the applicability of the methodology developed in this chapter, however, which can be used to incorporate other dispersion models in network risk analysis. It is even possible to remove some of the assumptions of the Gaussian plume model with the raster GIS tools used in this chapter. Further discussion of this can be found in later sections.

Accidental release of Hazmat during transportation can be continuous or instantaneous. The nature of release depends on both the severity of the accident and the properties of the substance carried. No single dispersion model can accommodate all release scenarios. To estimate risk for long-term planning needs, all possible scenarios must be considered. A possible solution to this problem is to calculate the risks for each scenario using a suitable model, then to calculate the weighted summation of the risk values using the frequency of incident scenarios as weights.

For specific release accidents during shipments, the rate of release is not known instantly. Therefore, for immediate emergency response, computation speed should be fast enough so that the model can be solved immediately after accurate field data are obtained.

3.4 Calculating Expected Consequences from a Point Source

Dispersion models have been used for emergency response for many years (Chakraborty and Armstrong 1995). Published research papers on the use of dispersion models in Hazmat risk analysis include Hillsman and Coleman (1989), Glickman and Raj (1993), and Chakraborty and Armstrong (1995). The calculation of expected consequences from a point pollution source is a four- step process:

Step 1. Calculate the concentration level at each receptor point

The concentration level at each receptor point from a point source can be calculated efficiently using the Gaussian plume model (3.3). In Figure 19, the concentration at point k from source s is (when z=0):

$$C(x, y, z = 0, h_e = 0) = \frac{Q}{\pi \sigma_y \sigma_z u} e^{-\frac{1}{2}(\frac{\Delta y}{\sigma_y})^2} \tag{3.7}$$

$$\sigma_z = a^*(\Delta x)^b \tag{3.7a}$$

$$\sigma_y = c^*(\Delta x)^d \tag{3.7b}$$

(3.7) is the same as (3.3) except that we denote downwind and crosswind distance from the source as Δx and Δy instead of x and y, because eventually we want to apply the model to a linear source. If only the concentration levels from a point source need to be calculated, we can set the origin of the coordinate system at the source point with the x axis pointing in the downwind direction. In this case, the downwind and crosswind distances between a receptor point and the source point are equal to x and y coordinates of the receptor point. However, if we want to calculate the concentration from all cells of a linear source, a uniform coordinate system for all source points will make calculation and aggregation easier. Therefore, we use x and y to represent the coordinates of a point and use Δx and Δy to represent the distances from the source point in the down-wind and cross-wind directions.

Since the Gaussian plume model, as well as other dispersion models, is framed for continuous space, I adopt a raster approach to transform the continuous space into a discrete one by modeling the space as a grid. Raster is a standard data format for modelling continuous surfaces in GIS. One main advantage of raster format is computational efficiency. One main disadvantage is it introduces inaccuracy when representing a continuous surface with cells of equal size; this inaccuracy can be reduced by carefully determining the cell size (resolution) according to the requirements of the analysis. In raster GIS, each cell is referenced by its row and column number. The upper-left corner cell is the origin of the reference system and has a row and column number of 0. If we set the upper-left corner of the grid as the origin of the coordinate system and the x and y axes point to the right and down respectively, the coordinates of the lower-left corner of each cell can be easily converted from and to its grid reference (x=column*cellsize, y=row*cellsize).

Before going on to derive the relationship between cell coordinates and Δx, Δy, let's define the reference system for wind directions. Conventionally, wind directions are measured by azimuths in clockwise degrees or radians from the north and have a range of (0, 360°) or (0, 2π) in radians. Thus, an east wind is 90° or 1.57 in radians, a southeast wind is 135° or 2.36 in radians, and a west wind is 270° or 4.71 in radians. I use a similar method to describe the location of a target cell relative to a source cell. For example, in Figure 19 the true location of k is (x_k, y_k), its location relative to s is (α, l), where α is the azimuth degree of line sk and l is the Euclidean distance between k and s:

$$l = \sqrt{(x_k - x_s)^2 + (y_k - y_s)^2} \tag{3.8}$$

The formulas for calculating α, Δx and Δy of all cells on the downwind side of the source ($|\theta - \alpha| < 90°$) are:

If $x_k > x_s$ and $y_k > y_s$, then $\alpha = \arcsin(\frac{x_k - x_s}{l})$

If $x_k > x_s$ and $y_k < y_s$, then $\alpha = \pi - \arcsin(\frac{x_k - x_s}{l})$

If $x_k<x_s$ and $y_k>y_s$, then $\alpha = \pi + \arcsin(\frac{|x_k - x_s|}{l})$

If $x_k<x_s$ and $y_k<y_s$, then $\alpha = 2\pi - \arcsin(\frac{|x_k - x_s|}{l})$

$\Delta x = l * \cos |(\theta - \alpha)|$

$\Delta y = l * \sin |(\theta - \alpha)|$

Now let us use a numerical example to illustrate the procedure for calculating the concentration level at each receptor cell from a point source in the raster GIS framework. Suppose a traffic accident happened during the day in the City of Edmonton. The coordinates of the accident are (15700m, 9420m) or (column=100, row=60). The gaseous Hazmat is leaking from the tank at a rate of Q=80 l/s (liters per second). The wind is blowing from the south-west direction (θ=3.93) at a speed of 20 km/h. The incoming solar radiation is moderate at the time. Based on the time of the day, solar radiation strength, and wind speed, the atmospheric stability is determined to be neutral (category D) according to Table 7. Therefore, the dispersion parameters are $\sigma_z=0.73(\Delta x)^{0.55}$ and $\sigma_y=0.14(\Delta x)^{0.89}$ (see Table 6). Thus, for a receptor cell at (column=130, row=70) or (20410m, 10900m):

$$l = \sqrt{(20410-15700)^2 + (10900-9420)^2} = 4937m$$

$$\alpha = \arcsin(\frac{20410-15700}{l}) = 1.266 radians$$

$$\Delta x = l * \cos|\theta - \alpha| = 4931.6m$$

$$\Delta y = l * \sin|\theta - \alpha| = 229.5m$$

Now substitute the values for Δx and Δy into (3.7a) and (3.7b) with numbers:

$$\sigma_z = 0.73 * \Delta x^{0.55} = 78.4m$$

$$\sigma_y = 0.14 * \Delta x^{0.89} = 270.9m$$

Then substituting the values of σ_y, σ_z Q, u and Δy into (3.7), the concentration at this cell is:

$$C(x,y,z=0,h_e=0)=\frac{Q}{\pi\sigma_y\sigma_z u}e^{-\frac{1}{2}(\frac{\Delta y}{\sigma_y})^2}=37.7ppm$$

Repeating this process for all cells on the downwind side of the accident results in a matrix of numbers, each of which represents the concentration at the corresponding cell. If we had approximated σ_y and σ_z to be linear functions of Δx like Patel and Horowitz (1994), the concentrations at this cell would be 0.44 ppm. Table 8 shows the concentrations in this cell calculated with the original Pasquill-Gifford parameters and approximated parameters under six atmospheric condition categories. We can see that the approximation greatly affects the computational results.

	Original Parameters	Approximated Parameters
A	0.11	362.05
B	2.69	2.04
C	8.45	1.61
D	37.69	0.44
E	62.00	0.48
F	78.26	0.82

Table 8 Concentrations calculated with original parameters and approximated parameters

The grid data model is simple. A grid is a matrix of numbers, each number representing the attribute value at that cell. Therefore, it is straightforward to bring the plume result into a raster GIS. Figure 20 is the concentration grid displayed in ArcView. Shades of color represent the levels of concentration. Because the grid is spatially registered in GIS (that is, the image covers the same area as other data layers), it can be overlayed with other data layers for further analysis.

Step 2. Calculate consequence probabilities

The probability that an individual at location *j* will experience an undesirable consequence (such as evacuation, injury, or fatality) as a result of a Hazmat release at *i*, is a function of the concentration C_{ij}. The function is clearly substance-dependent, and the exact form is only known for a few Hazmats. The procedure described here does not depend on the shape or the parameters of this function. For demonstration purposes, we employ a very simple consequence probability function here:

$$p_{ij} = C_{ij} / MAX \tag{3.9}$$

where MAX is the maximum concentration computed by the Gaussian plume model. This implies that the consequence probability is a linear function of concentration level. (In reality, this function is likely to be S-shaped.)

Step 3. Calculate expected consequences

Combine the probability of consequence at each destination location with its population to produce the expected consequence at that location.

[Expected Consequence map] =

[Prob. of Consequence map]*[Density map]*[Area of cell] (3.10)

In the formula, [Density map]*[Area of cell] produces a map showing the number of people in each cell. Then the number of people in each cell is multiplied by the cell value in the consequence probability map to produce the expected consequence map. Figure 21 displays the consequence map

Step 4. Calculate the total expected consequence from the point source

The summation of expected consequence at all impacted cells is the total expected consequence resulting from this source.

3.5 Calculating the Risk from a Linear Source

3.5.1 Calculate link risk for specific wind direction

Boffey and Karkazis (1995) suggest incorporating dispersion models into Hazmat route selection. Incorporating dispersion in transport route selection is a natural evolution from accident (point) consequence analysis. This is simple conceptually but it is also very computationally intensive. To find a minimal risk path on a network, we must be able to calculate the risk associated with individual links in the network. As stated above, the risk imposed on a point from a point source is given by (3.3):

$$C(x, y, z = 0, h_e = 0) = \frac{Q}{\pi \sigma_y \sigma_z u} e^{-\frac{1}{2}(\frac{y}{\sigma_y})^2}$$

This formula includes two power functions σ_y and σ_z. To calculate the consequence at the receptor point from a link, it is necessary to integrate (3.3) over the whole link. Patel and Horowitz (1994) tried to solve the problem analytically. In order to integrate, they had to make some simplifying assumptions about the dispersion parameters in the Gaussian plume model: the vertical and horizontal dispersion parameters are approximated as linear functions of downwind distance ($\sigma_z = ax$ and $\sigma_y = cx$), assuming b and d to equal 1.0. After the simplification, they analyzed three cases: the first case is to calculate the risk when all wind directions are equally likely with a given wind velocity; the second case is to calculate the maximum risk at receptor points; the third case is to calculate the risk for a given wind direction. They were able to find a closed-form solution for the first and second case. They were not able to find a closed-form solution for the particular wind direction case. In this case, they had to use some numerical integration method.

Risk calculation for all three cases by Patel and Horowitz were based on the assumption that the vertical and horizontal dispersion parameters are linear functions of downwind distance. This is a damaging assumption for the Gaussian plume model. Because b and d differ by atmospheric stability category, assuming them to be 1.0 entirely ignores the matter of atmospheric stability. In the Pasquill stability categories, the range of b is (0.45, 2.1) and the range of d is (0.85, 0.89) (See Table 6). More detailed discussion about the effect of dispersion parameters on the resulting plume can be found in Section 3.3.2. Assuming σ_y

and σ_z to be linear functions of x not only introduces error, but also loses one major advantage of the Gaussian plume model: its flexibility for adopting localized parameters based on field experiments. Furthermore, even if the assumption about the dispersion parameters is realistic, a closed-form solution cannot be found for probably the most important case: when wind is blowing from a particular direction. Therefore, we turn to numerical methods to compute the risks associated with links.

In the previous section, we converted the impact area into a grid to calculate the expected consequence at each receptor cell from a point source. Since we cannot integrate the Gaussian plume model over a link, we also transform the network links into strings of pixels and treat each pixel as a point source. The concentration from a link is the summation of the concentrations resulting from all pixels representing this link. The consequence from a link is the product of consequence probability map (which is a function of concentration level) and population distribution map. By representing continuous objects (links and regions) using discrete cells, we are actually replacing integration with simple summation.

Figure 22 displays the concentration from a test link. The probability of consequence at each cell can be calculated using (3.9). The expected consequence is the product of total population at each cell and the probability of consequence at this cell. Figure 23 is the expected consequence map produced by using (3.10). Repeating the whole process for every link produces link by link potential consequence. Figure 24 shows the expected link consequence for the entire network, where the thickness of a link is proportional to the link consequence.

Link consequence can then be modified with the number of shipments on this link.

3.5.2 Calculating risk for strategic planning

The previous section considers a specific wind direction. For long-term planning such as Hazmat network planning, we must get average wind conditions, which requires data on wind speed and direction distribution. The wind data in Canada are recorded on an hourly basis for each weather station. Since the wind can come from any direction from azimuth

0° to 360°, the data are aggregated to a smaller number of directions, each direction having an attribute of frequency of occurrence and the average wind speed during a given time period. Traditionally, the wind data is aggregated to eight or sixteen directions and is displayed in a spider diagram called a "wind rose". Although the average wind speed and frequency in Edmonton is available for every 10° (36 directions), the eight direction wind rose data is used for our demonstration. Table 9 is the mean wind speed by direction for every month in 1993 recorded by the Edmonton International Airport Weather Station. The Overall row in the table is the mean speed for all directions in that month or year. Table 10 is the frequency distribution by direction. Figure 25 is the wind rose for the Full Year column in Table 9. The length from the origin to each intersection point is proportional to the frequency. Figure 26 is a similar diagram for the wind speed. Notice that the %calm (no wind) row is not represented in Figure 25 and was not mentioned in the previous sections. Because the wind speed is in the denominator of the Gaussian plume model, the model does not work when the wind speed is zero. Unfortunately, when wind speed approaches zero, Hazmat release can be very dangerous if there are people nearby (Glickman and Raj 1993). This is relatively easy to handle in the real world, however. When the wind speed is close to zero, the impact area is a circular area surrounding the accident site. The size of the area can be determined by factors such as the physical and chemical property of the gas, the nature of the accident and the amount of the gas. To calculate the link risk, we can simply draw a narrow band along the roads, counting the number of people within the band and assigning a severe concentration level to the area. We do not include the no-wind scenario in our analysis.

Incorporating the annual or monthly wind rose to calculate the average risk is easy. First we can calculate the risk for each link for each wind direction as in the previous section, then use the percent frequency to calculate the weighted average for all directions. The result is the average monthly or annual link risk, depending on which wind rose is being used. Figure 27 is the link risk for the Edmonton arterial network calculated using annual wind distribution data.

	Jan	Feb	Mar	Apr	May	Jun	Jul	Aug	Sep	Oct	Nov	Dec	Full year
#observations	744	672	744	720	744	720	744	744	720	744	720	744	8760
Overall	10	10	12	11	13	13	11	11	12	11	11	11	11.3
N	11	14	15	14	13	14	12	12	15	17	16	14	13.9
NE	9	11	14	10	12	14	10	9	13	12	11	12	11.4
E	8	11	12	10	10	14	9	8	9	9	8	10	9.8
SE	10	13	15	13	15	14	11	11	10	9	10	13	12.0
S	11	9	13	9	14	12	10	10	9	10	10	10	10.6
SW	9	9	9	8	10	8	8	9	9	8	9	8	8.7
W	12	11	12	10	17	16	13	14	13	12	13	14	13.1
NW	11	14	15	15	19	16	14	14	16	18	18	17	15.6

Table 9 Mean hourly wind speed (knots) by direction
in Edmonton in 1993

	Jan	Feb	Mar	Apr	May	Jun	Jul	Aug	Sep	Oct	Nov	Dec	Full year
#observations	744	672	744	720	744	720	744	744	720	744	720	744	8760
%calm	5.6	4.6	6.3	7.2	3.1	4	7.8	7.3	5.8	6.6	3.1	4.7	5.52
N	7.7	9.6	6	10.5	8.1	9.4	13.6	11.5	13.3	6.4	4.9	5.8	8.89
NE	3.6	10.9	4.6	10.5	11.5	9.9	6.4	7.3	2.3	3.3	3.7	5.1	6.56
E	4.3	5.4	5.9	12.6	14.3	13.8	6.9	5.1	0.6	3.7	3.3	3.4	6.61
SE	4.7	6.2	13.6	15	22.7	17.5	8.3	7.9	3.1	6.2	4	4.1	9.46
S	25.9	15.5	22.7	12.4	15.6	14.2	5.5	10.8	14.3	18.4	19.5	21.3	16.36
SW	24.9	24.4	13.5	8	4.5	5.7	5	9.2	18.6	20.6	27.3	23.3	15.35
W	15.5	12.6	14	8.6	9.1	11.3	18.4	21.3	19.9	19.8	20.9	18.5	15.86
NW	7.8	10.8	13.4	15.2	11	14.3	28.1	19.5	22.1	15.1	13.4	13.8	15.40

Table 10 Percentage frequency of hourly wind
direction in Edmonton in 1993

The procedure described in the previous paragraphs specifies that the plume is calculated for each source cell. Repeating the plume calculation for each source cell can be time-consuming especially if the analysis is carried out at high resolutions. The procedure is described this way to make it easier to understand, but in practice, the plume model does not need to be calculated repeatedly. Because the wind condition is assumed to be the same in the entire network, all parameters for the plume model remain the same for all source cells. Thus, the plume only needs to be calculated once, and can then be shifted according to the relative locations of the current source cell and the previous source cell. For example, if the first source cell is (row = 20, column = 20), and the resulting concentration at cell (40, 40) is 120 ppm, then without recalculating the Gaussian plume model, we know that

the second source cell (20, 21) will result in a concentration of 120 ppm at (40, 41). Therefore, the amount of computation involved in calculating the network risk using the raster approach is limited.

Being able to incorporate wind conditions in network risk analysis contributes to real-time routing decision-making. Real time routing is very demanding in computing speed. Calculating the network risk considering wind conditions for real time routing may be too slow even if we use the method above. In this case, we can use a routing algorithm that does not require the link risks for the entire network be calculated (Zhan and Noon 1998).

3.5.3 Potential uses of raster GIS to improve the dispersion model

Concentration level of contaminants varies continuously in space. It is very difficult to analyze this kind of phenomenon in the traditional vector framework. Factors, such as wind conditions, that affect the concentration levels also vary continuously in space. However, if these factors are to be accounted for realistically, i.e., considering their spatial distribution, the modeling process will become too complicated in the vector framework. This is why some models need to assume that the influencing factors are homogeneous over space. For example, the Gaussian plume model is based, in part, on the assumptions that atmospheric conditions are homogeneous in the study area, that the terrain is gentle or flat, and that the ground surface is homogeneous. Since the raster data model is a powerful tool for describing and analyzing continuous surface data, it may help to relax some of the assumptions. In the raster data model, a continuous phenomenon is represented by a regular array of z values over a two-dimensional space. For example, topography is usually represented by digital elevation models (DEM), whose cell values are the average elevation of each cell. Continuously changing wind speed and direction can be represented by a wind speed grid and wind direction grid. With a DEM, cell-by-cell slope (change of elevation over distance) and aspect (the compass direction toward which a slope faces), both affecting the dispersion of pollutants (Venkatram 1988), can be calculated efficiently in raster GIS. With continuous wind data, each cell has its own wind speed and direction values. A molecule's path is affected by the wind condition in which it travels. It may be possible to model the dispersion process taking into account the variation of wind in a raster framework.

3.6 Conclusions

The traditional way of estimating the spatial consequences of Hazmat releases on networks involves producing all-or-nothing distance bands around links and counting the number of persons inside the bands. This approach lacks realism in that it does not consider the effects of wind conditions on the width and intensity of this band. For point-based leaks of air-borne Hazmat, concentration dispersion models that consider wind direction have been used. In this chapter, these models are extended to account for releases anywhere in a network.

The use of even a very simple such model, the Gaussian plume model, demands certain limiting assumptions about the model's stability parameters. I have demonstrated that by transforming continuous space to the discrete, gridded space of raster GIS, we can overcome this problem. Having produced more realistic (non-symmetric, probability-based) zones of influence, I use traditional raster GIS overlay techniques to predict the spatial consequences of potential releases of airborne Hazmat in a network. We can further assign risks to all links in a network.

More realistic ways of predicting Hazmat consequences can inform several important management procedures that rely on such risk predictions. Network routing will be more realistic. Practical development of models such as the one developed in this research will allow real-time routing decisions, reacting to the substance transported and weather conditions, to be made. Better estimates can aid in the design of evacuation guidelines. If such models are shown to be accurate, they might be used to make actual real-time evacuation procedures more expeditious, efficient, and safe. Better estimates of Hazmat transport risks can also aid Hazmat network design and locating network inspection stations (Hodgson *et al.* 1996). I hope that as more realistic estimates become available, researchers will pursue further management applications aggressively.

Because raster GIS approaches can make important contributions to calculating concentration levels and predicting consequences, it is appropriate to demonstrate them with the popular GPM. I have no illusions, however, that this model is the most suitable to airborne Hazmat releases. The GPM assumes a continuous point source of contaminant. For accidents involving trucks, models accommodating an instantaneous point source

might be more realistic. The Gaussian "puff" model (Stern 1976) tracks individual releases as they move along wind trajectories and diffuse in Gaussian fashion. These models present greater difficulties for network applications; for instance, spatial variability in meteorological parameters is difficult to incorporate. Raster techniques may also bring the solution of these models into our grasp.

Raster representation offers further advantages. It is an efficient format in which to capture, store, and manipulate other data which might reasonably be expected to enter into dispersion models as they become easier to work with. Such characteristics are location-specific wind velocity and direction and ground roughness and absorption characteristics. We continue to develop these extensions in the belief that GIS techniques will allow us to develop models that are both more realistic and efficient.

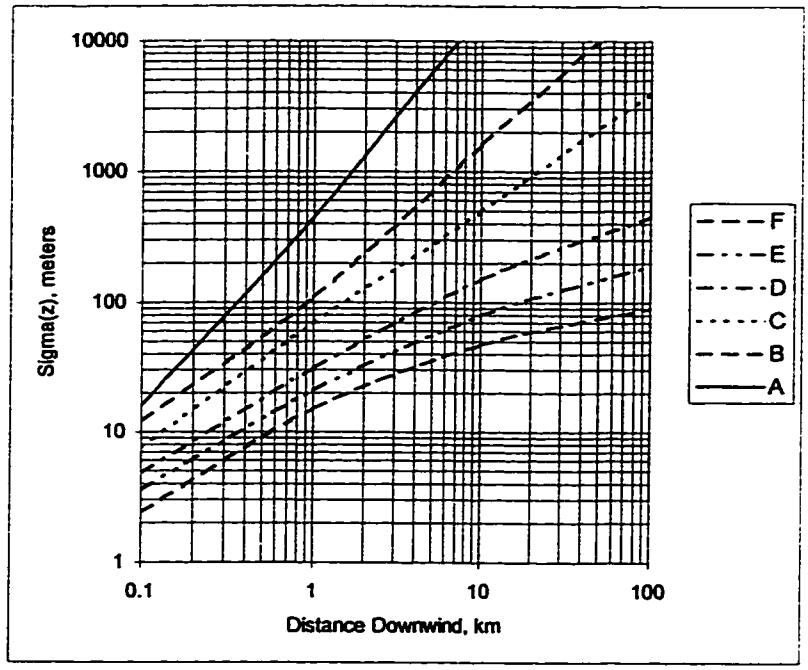

Figure 15 Vertical dispersion coefficient as a function of downwind distance from the source (Turner 1970)

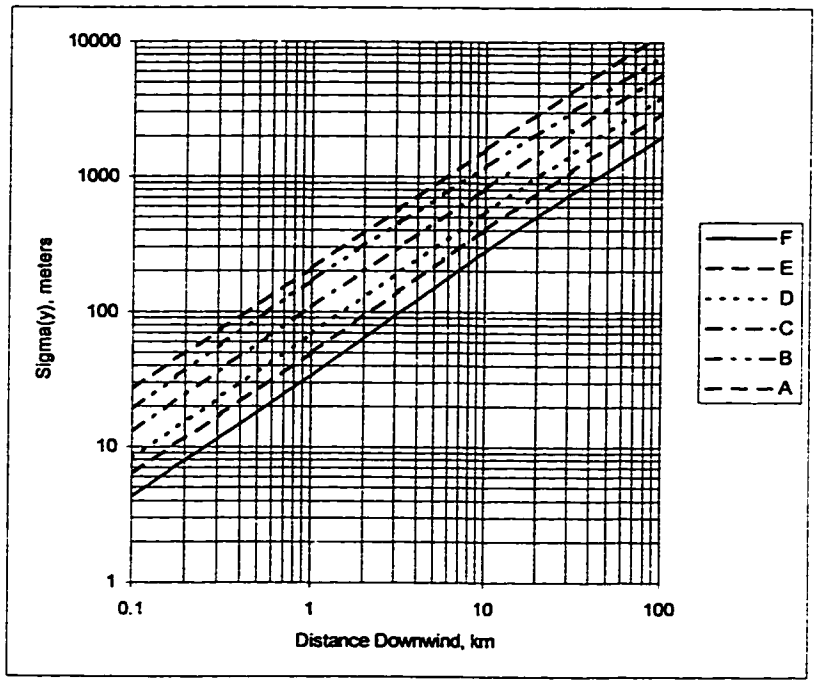

Figure 16 Horizontal dispersion coefficient as a function of downwind distance from the source (Turner 1970)

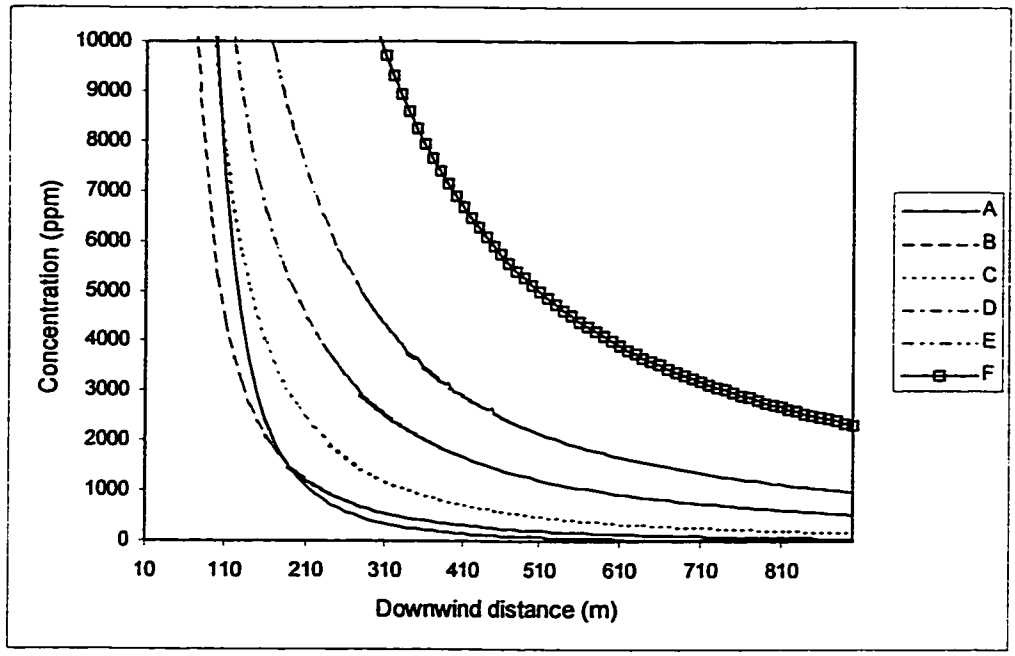

Figure 17 Concentration along center line as a function of downwind distance and atmospheric stability
(Q=3.14 m^3/s, u=1 m/s)

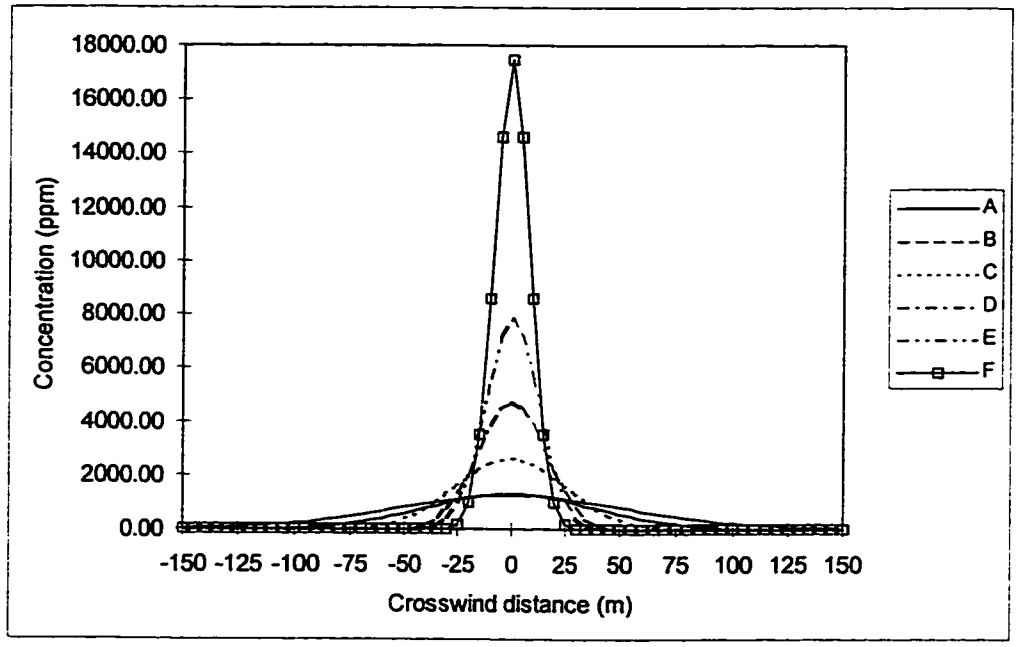

Figure 18 Concentration on crosswind direction as a function of crosswind distance and atmospheric stability
(Q=3.14 m^3/s, u=1 m/s, downwind distance from source is 500 m)

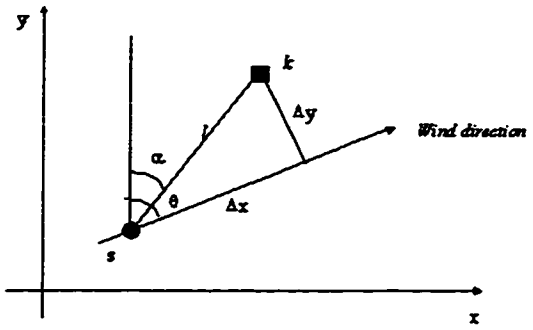

Figure 19 Point source dispersion model

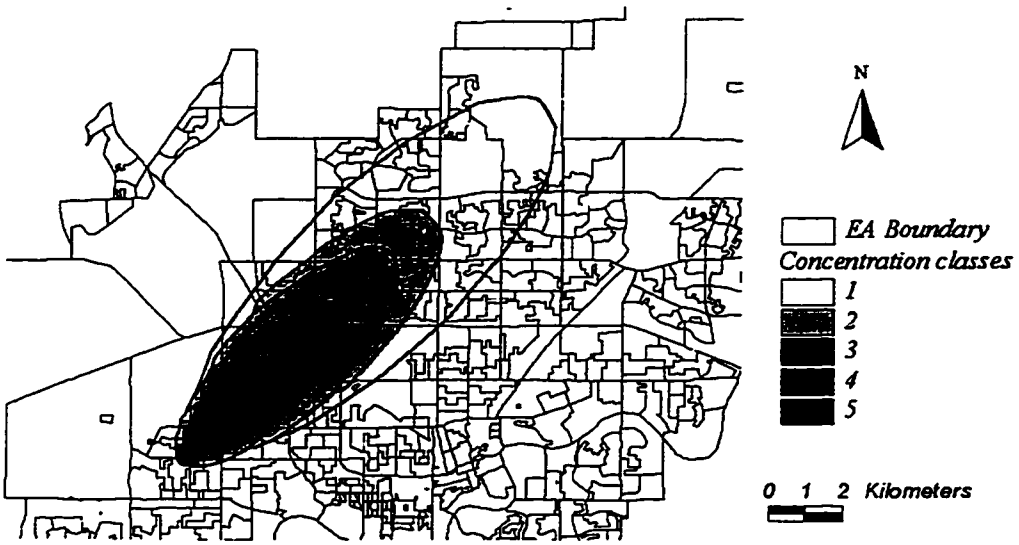

Figure 20 Concentration level at different distances
from the accident

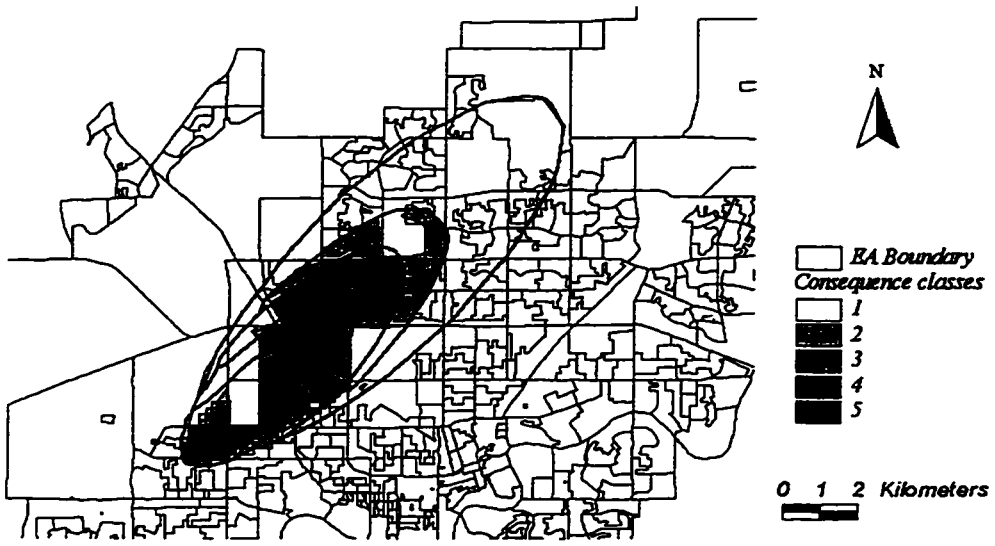

Figure 21 Consequences of an accident

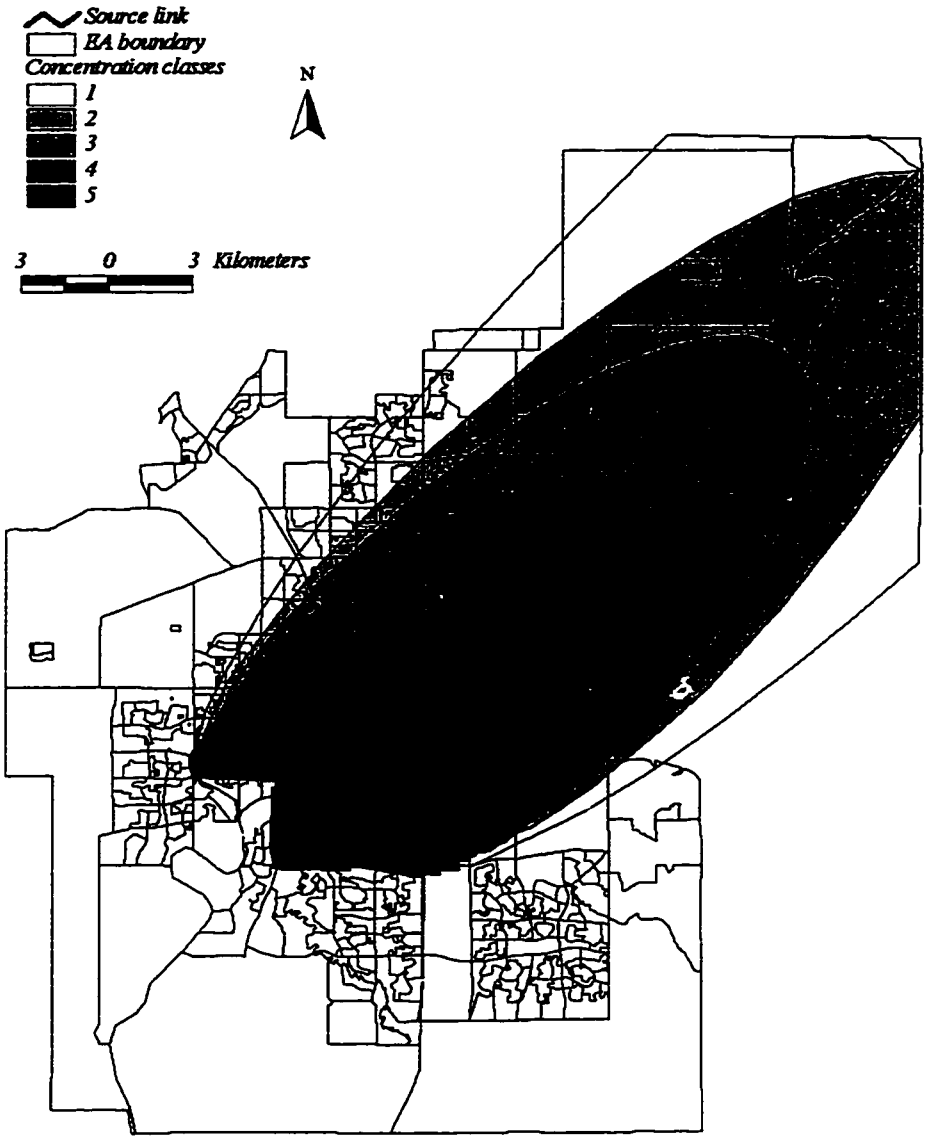

Figure 22 Concentration distribution from a linear source

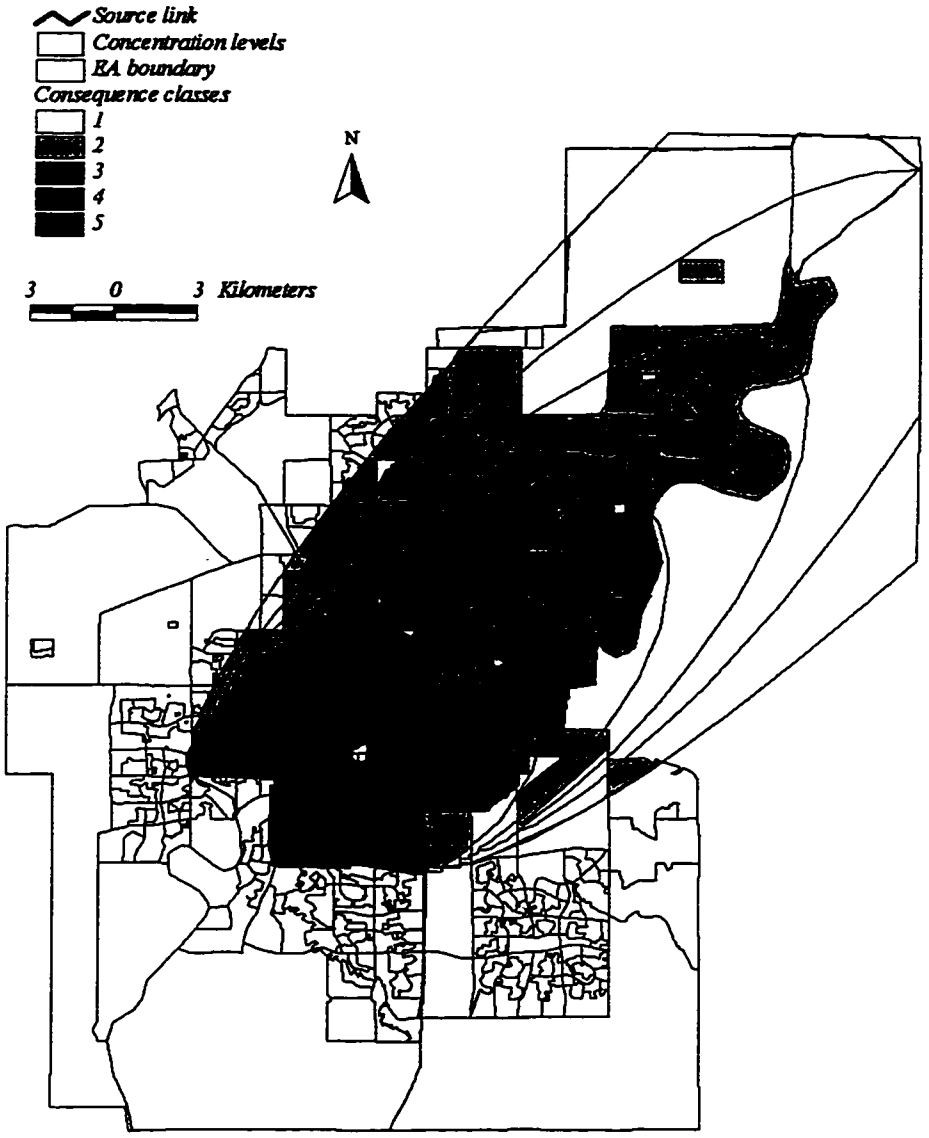

Figure 23 Concentration overlayed with population

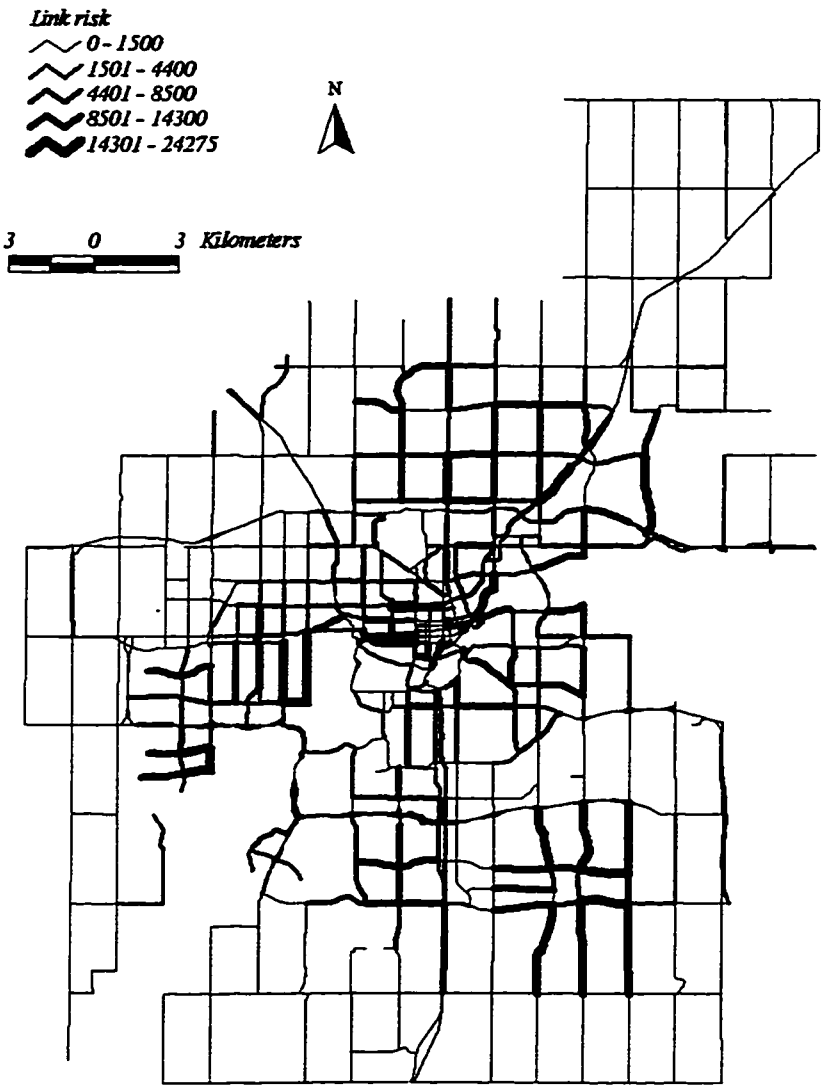

Figure 24 Link risk for a particular wind condition

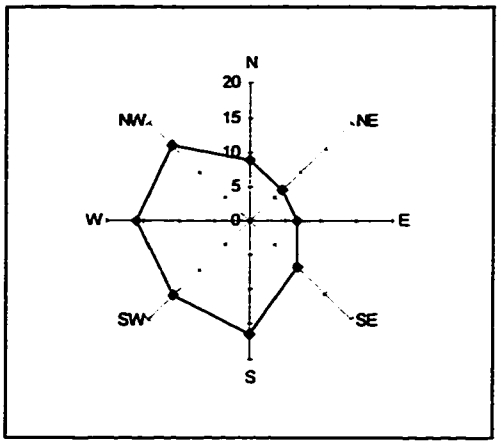

Figure 25 Wind rose for prevailing wind direction in Edmonton (1993)

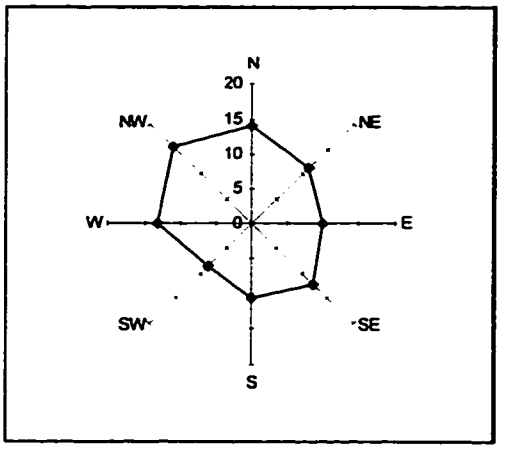

Figure 26 Average wind speed by direction (1993)

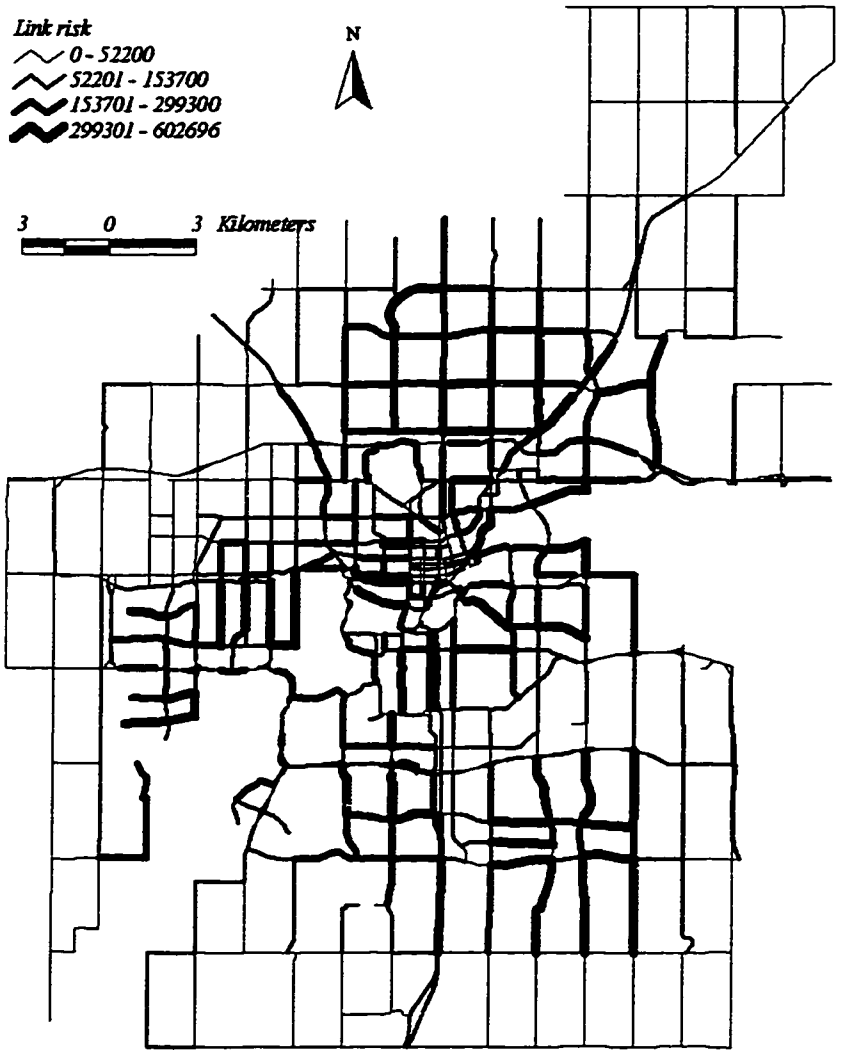

Figure 27 Link risk considering annual wind distributions

Chapter 4

HAZMAT NETWORK DESIGN

4.1 Introduction

Hazmat accidents can have serious environmental and economic consequences. To improve the safety of Hazmat transportation, many cities restrict the roads that may be used for Hazmat trucks. In Edmonton, the roads on which Hazmat trucks can travel are called Designated Dangerous Goods Routes, referred to as Hazmat routes in this thesis. Maps showing Hazmat routes are usually available in City Hall and in the information kiosks near the major entry and exit points of the city.

Network design deals with the selection of those arcs (i.e., roadways) to be included in, or added to, a transportation network, accounting for the effects that the design decision will have on the operating characteristics of the transportation system (Magnanti and Wong 1984). Hazmat network design focuses on the selection of arcs from the existing network for Hazmat routes and is a multi-objective problem in nature. The network design decision affects the Hazmat traffic pattern, which in turn affects the shipping cost, total amount of risk imposed on the city and the spatial distribution of risks (risk equity). There are mainly three parties concerned with Hazmat network design decisions: network designer, shippers and drivers, and local communities. Each party has different objectives. The primary concern of the network designer may be the total amount of risk resulting from the Hazmat traffic; the primary concern of shippers may be the travel time and distance; and the local communities may mainly be concerned about the risk and other negative impacts resulting from the Hazmat traffic at the local level. This research is confined to two parties: administrators whose objective is to minimize the total risk and drivers whose objective is to minimize the total shipping cost.

The Hazmat network design problem is modeled as a single-objective problem that involves two decision-making processes. The administrator has the authority for the network design decision; his objective is to minimize the total risk. The drivers decide

which path to take after the network is designed. The results of these two decision processes affect each other: the network design decision controls the roads available to the drivers, and the route drivers take affects the total risk resulting from the shipment of hazardous materials. The total risk is not only affected by the decision of the network designer, but also by routing decisions of drivers. Drivers make the routing decisions after the Hazmat network is designed. If the administrator and the drivers can behave in a seamlessly coordinated fashion, the problem can be modeled as a two-objective problem minimizing risk and cost, and can be solved with one of the multi-objective methods. One such example is the minimum-covering shortest path problem introduced by Current, ReVelle and Cohon (1988), where the objective is to minimize both the travel distance and the number of people who live within a certain distance of the path. However, for the administrator and driver to behave as one party, the administrator would have to tell each driver which path to take on every shipment. This option is not popular, nor is it feasible to enforce it. Therefore, unless drivers voluntarily take both objectives seriously (forced by insurance policy requirements, for example), the problem involves two parties whose decisions will have different effects on the total risk.

The United States Federal Highway Administration (FHWA) developed an approach for designing Hazmat truck networks based on a risk-assessment methodology, published in *Guidelines for Applying Criteria to Designate Routes for Transporting Hazardous Materials* (Barber and Hilderbrand 1980). This approach outlines the design process as a four-step procedure. The first step is to define issues, responsibilities and alternative routes. The second step is to select links based on legal and physical factors, risk analysis, and other subjective factors such as special population and properties. The third step is to compare alternatives. The last step is making the network design decision. Although this approach does have a risk analysis component in the second step, it fails to acknowledge that risk is also affected by the routing decisions of drivers. Therefore, this approach does not take routing decisions into consideration. One such example is the design of Hazmat truck routes for the Dallas-Fort Worth Area (Kessler 1986).

If there is only one origin and one destination, we only need to calculate the minimum risk path and designate this path as the Hazmat network. The Hazmat network consisting of the

minimum risk path is the optimal network in terms of the total risk. However, when there are many OD pairs, the union of the minimal risk paths can be quite large and well connected. The drivers will be able to choose which way to go, and sometimes their choices will sacrifice other objectives. Therefore, the administrator should consider the possible routing decisions of shippers during the network design process. The Hazmat network design problem has a game-playing component: the administrator wants the drivers to take the paths that will minimize the total risk, whereas the drivers will take the shortest paths whenever possible. This chapter develops a network design procedure that attempts to minimize the total of risk even if the drivers choose the shortest paths on the designated network.

The network design procedure consists of two stages. The first stage is a screening process, selecting a starting network from the entire network. The second stage removes some of the links from the starting network to minimize the total risk using a greedy-removal algorithm. I tested the procedure on random networks and then applied it to the real network of Edmonton, Canada.

The procedure developed here is purely one of selection, i.e., of selecting roads from the existing road network without considering the option of building new roads. In a real world situation, it is possible that building some new roads will reduce the total risk. However, road networks in cities are usually well connected and if we start from a network that is detailed enough, it will not be a problem if we do not consider adding new links to the network. Therefore, it is important that we use a detailed network as the starting network, even if some of the links do not meet the engineering requirements for Hazmat trucks. If some of the roads selected do not meet the engineering requirements, we can carry out cost-benefit analysis for each road to decide whether it should be upgraded. First, we calculate the cost for upgrading the road, then calculate the reduction in total risk if we upgrade it and use it for a Hazmat route. By analyzing the cost and risk reduction, we can decide whether or not to upgrade it.

The remainder of this chapter is organized as follows. The second section describes the network design procedure. The third section reports the computational experiments on random networks. The fourth section reports the results from the application of the

procedure in designing the Hazmat network for Edmonton. The last section consists of the concluding remarks.

4.2 The Hazmat Network Design Procedure

Hazmat network design is to select those roads to include in, or add to, a Hazmat route so that the total risk resulting from the Hazmat traffic is minimized. The problem can be described as follows. Let $N = (V, E)$ be an undirected network where $V = \{v_1, \ldots, v_n\}$ is the vertex set, and $E = \{(v_i, v_j): v_i, v_j \in V, i \neq j\}$ is the set of edges. Certain amounts of Hazmat must be shipped from a set of origin points $O_i \in V$ to a set of destination points $D_j \in V$. Assume the amount of Hazmat flow is much smaller than the link capacity and that the accident probability on each link per traversal of each Hazmat truck is not affected by the amount of Hazmat traffic on this link. Assume further the objective of the administrator is to minimize the total amount of risk posed to the community, and that the objective of the shippers is to minimize the travel distance for each shipment. We want to select the arcs that should be included in the Hazmat network so that the total risk is minimized.

The network design procedure is based on the following scenario. The administrator's job is to design a Hazmat network for his community. Once the network is designated, he does not have control over how the drivers travel. For the administrator, the ideal situation is that every driver takes the minimal risk path, so the total amount of risk is minimized. However, because the drivers may take different paths, the minimal risk path network (MRPN, the union of all minimal risk paths) does not necessarily ensure the total amount of risk is minimized. In some instances, the paths the drivers take happen to be the same paths the administrator would like them to take. But more often, the minimal cost paths the drivers take are different from the minimal risk paths because MRPN is a well-connected network in which the drivers are able to take shortcuts, thereby increasing the risk. Therefore, the administrator must remove some links that will break the shortcuts to reduce the total risk.

The procedure can be described as follows. First, select a starting network from the entire network. This phase can be viewed as a screening process. Second, based on the starting network, find out which links are on the union of all minimum cost paths. Then try every link and remove the ones that will reduce the total risk without breaking the network. The

procedure has two components: initial network selection and a greedy removal algorithm (Dionne and Florian 1979). To select a starting network, we can carry out a simple screening process on the entire network to exclude some of the links (e.g., based on physical constraints). Or we can use the union of minimal risk paths as the initial network. In the greedy algorithm, we use two methods for selecting the link to remove in each step: first improvement and maximum improvement. *First improvement greedy* removes the first link that improves the result and starts a new iteration until no improvement can be made. *Maximum improvement greedy* tries all links first and then removes the link that reduces the risk the most. Based on how the initial network is determined and the way the removal links are selected, I implemented four versions of the procedure (Table 11). The first implementation uses MRPN as the initial network and applies the first improvement greedy to it. The second version also uses MRPN as the starting network but applies the maximum improvement greedy to it. The third and fourth versions start with the entire network (EN) and take the first and maximum improvements respectively. I name these four versions of the procedure First_MRPN, Max_MRPN, First_EN and Max_EN respectively.

Starting Network	Selection Rule	
	First Improvement	Max Improvement
MRPN	**First_MRPN**	**Max_MRPN**
EN	**First_EN**	**Max_EN**

(MRPN – Minimum Risk Path Network, EN – Entire Network)

Table 11 Four implementations of the algorithm

The procedure can be detailed with the following pseudo-code:

1) Select the starting network. The starting network can be either MRPN or the entire network.

2) Calculate the Ideal Risk (*IR*). *IR* is the total amount of risk if all drivers take minimal risk paths in the starting network.

3) Based on the starting network, calculate the shortest paths and Real Risk (*RR*). *RR* is the total amount of risk associated with the shortest paths. Set $RR_{BEST} = RR$.

4) If $RR_{BEST} = IR$, optimal solution is found; stop. Otherwise, set remaining network (*RN*) = starting network, go to 5)

5) Repeat until no improvement is possible

   For each link i on the shortest paths

   Remove i from the remaining network (*RN*).

   Recalculate the shortest paths between OD pairs that use i

   (For First_MRPN and First_EN only) Compute the total risk associated with the shortest paths, RR_i. If $RR_i < RR_{BEST}$, then delete i, set $RR_{BEST} = RR_i$, remove link i from RN. otherwise replace i, next i.

   (For Max_MRPN and Max_EN only) Compute the total risk associated with the shortest paths, RR_i. If $RR_i < RR_{BEST}$, set $RR_{BEST} = RR_i$, $i^* = i$. If i is the last link, then remove i^* from *RN*, otherwise, replace i, next i. If $RR_i \geq RR_{BEST}$ and i is not the last link, then replace i, next i. If i is the last link, then remove i^* from *RN*.

4.3 Computational Experiments

The algorithms described in Section 2 were tested on randomly generated networks. For these networks, I first generated a square rectangular grid network with $m*m$ nodes. Each node was 50 units away from its closest neighbors. Therefore, the network had $|V| = m^2$ nodes and $|E| = 2*m*(m - 1)$ edges. Then I perturbed the x-coordinate of each node by a uniform random number less than 25 and repeated the process for the y-coordinate to introduce some irregularity into the network (See Figure 28 for an example network with $m = 12$). For link lengths, I used the Euclidean distance between end points. Because in urban areas population density is usually higher in the center (downtown) and lower in the periphery, node risk was assigned in such a way that the farther a node is from the center, the smaller its risk was. Define MAXDIST to be the distance between the network center and the node farthest away from the center after perturbation. Then compute a risk number for each node, which was equal to MAXDIST minus the distance between the

node and the network center. The risk for each link was calculated by averaging the risk of its two end nodes. The travel speed was assumed to be uniform in the whole network. Thus, link travel time was proportional to link length. The Hazmat origin and destination points were selected randomly from the nodes. The amount of flow between each origin and each destination is one unit.

The size of the Hazmat network design problem is mainly determined by the size of the network and the number of OD pairs. I tested each algorithm with three problem settings. In each setting, I generated 20 problems (instances). The first problem configuration had ten origin points and three destination points (10x3 OD pairs) on a 64-node network. The second configuration had 15x6 OD pairs on the same 64-node network. The third configuration had 10x3 OD pairs on a 144-node network. Figure 28 shows a 10x3 OD problem on a 12x12(144)-node network. The circles are origin points. The triangles are destination points. The thickness of the lines is proportional to the amount of risk resulting from one shipment on this link.

The solutions (distance and risk) were recorded for the starting network (MRPN and the entire network) and the solution network. For comparison purposes, the objective function values were calculated based on two routing approaches. The first approach is called centralized routing (C) in which the administrator selects all the paths, i.e., all drivers must travel on the (minimal risk) paths that are specified for them. Although this routing approach is not considered an option in this study, the risk value calculated from this approach in the entire network provides an important benchmark; it is the ideal minimum risk value for the administrator. It can be used for evaluating the performance of the network design procedure and for studying the trade-off between distance and risk. The associated cost value can also be used as a benchmark. If the cost in the solution network is greater than this cost value, it signals a lose-lose situation, which means that the drivers overall are travelling longer than the minimum risk paths. The second approach, decentralized routing (D) in which the drivers select their own paths, is more realistic. Figure 29 shows the mean cost and risk for all the test problems. Figure 30, Figure 31 and Figure 32 show the results from each problem setting. The solution values are listed in Table 12.

	10x3 OD, 8x8 Network		15x6 OD, 8x8 Network		10x3 OD, 12x12 Network		All Problems	
	Mean Cost	Mean Risk	Mean Cost	Mean Risk	Mean Cost	Mean Risk	Mean Cost	Mean Risk
EN(D)	**100.0**	**141.1**	**100.0**	**141.1**	**100.0**	**142.3**	**100.0**	**141.6**
EN(C)	127.9	100.0	128.0	100.0	131.1	100.0	128.8	100.0
MRPN(D)	**113.3**	**117.7**	**105.5**	**131.5**	**117.3**	**122.5**	**110.2**	**126.0**
First_MRPN(D)	**130.0**	**110.1**	**133.0**	**117.4**	**137.7**	**111.0**	**133.7**	**113.9**
Max_MRPN(D)	**127.6**	**108.4**	**121.1**	**116.1**	**132.1**	**110.1**	**125.4**	**112.6**
First_EN(D)	**122.5**	**114.4**	**124.1**	**119.0**	**112.7**	**117.4**	**120.6**	**117.7**
Max_EN(D)	**119.7**	**114.5**	**120.3**	**118.2**	**108.1**	**118.4**	**116.0**	**117.7**

Table 12 Solutions for the test problems

In the figures, the EN(D) category represents the cost and risk values resulting from decentralized routing in the entire network. The EN(C) category represents the cost and risk values resulting from centralized routing in the entire network. MRPN(D) represents the cost and risk values resulting from decentralized routing in the minimum risk path network. The remaining four categories represent the cost and risk values resulting from decentralized routing in the solution networks solved with four versions of the procedure. All values are relative values after the minimum cost and risk values are scaled to 100. Figure 29 tells us that if the drivers are allowed to travel anywhere in the entire network and if, according to our assumption, they all take the shortest path, the resulting mean travel cost is 100 units and the resulting mean risk is 141.6 units. The cost values associated with this scenario are the minimum travel cost. If the administrator can get all drivers to take the minimal risk paths, the risk will be reduced to 100 units, but the shipping cost will be increased to 128.8 units. The risk value associated with this scenario is the potential minimum value that may never be achieved in reality. The values resulting from the previous two scenarios provide some important benchmark values: the minimum cost, the minimum risk, and the risk and cost values associated with the minimum cost and the minimum risk. If the union of minimal risk paths is designated as the Hazmat network and the drivers are allowed to travel freely on this network, the mean cost will be 110.2 units and the mean risk will be 126.0 units. In the First_MRPN and Max_MRPN solution networks, the mean risks are 113.9 and 112.6 respectively and the mean costs are 133.7 and 125.4 respectively. In the First_EN and Max_EN solution networks, the mean risks are

both 117.7 units and the costs are 120.6 and 116.0 respectively. It should be noted that in the First_MRPN solution network, both the cost and risk values are greater than the values in EN(C), which means that the drivers as a group would be better off in terms of travel cost if they gave up the freedom of choosing their own travel paths. Although this lose-lose situation is not desirable for everybody, it is not uncommon in a non-cooperation situation.

The network design procedure is evaluated in two aspects. The first aspect is the effectiveness of the procedure in terms of risk reduction. The second aspect is the trade-off between risk and cost as a result of the network design process. The effectiveness of the network design procedure is evaluated using two risk reduction measurements. The first measurement is the percentage of risk reduction (benefit), which is the total risk reduction from the solution networks divided by the risks from the entire network (EN-D):

$$Benefit = \frac{Risk\_from\_EN(D) - Risk\_from\_solution\_network}{Risk\_from\_EN(D)} \times 100\%$$

Table 13 lists the benefits and cost increases for all 60 test problems. The percentage cost increase is calculated using the following formula:

$$Cost\_Increase = \frac{Cost\_from\_solution\_network - Cost\_from\_EN(D)}{Cost\_from\_EN(D)} \times 100\%$$

The largest benefit is 20.6% resulting from the Max_MRPN procedure. The risk reduction from the First_MRPN procedure is 19.6%. The increase in travel cost for these two implementations are 25.4% and 33.7% respectively.

The trade-off between cost and risk can be measured by the cost-benefit ratio between the cost increase and the benefit (the fourth column in Table 13). The cost-benefit ratio indicates the average percent travel cost increase incurred to achieve one percent of risk reduction. The results show that although First_MRPN achieved almost as much risk reduction as Max_MRPN, the cost-benefit ratio is much higher for First_MRPN than Max_MRPN. In the first stage of First_MRPN and Max_MRPN, the ratio is smaller than 1.0. But in the final solutions, the ratios are all greater than 1.0 except for Max_EN. However, the risk reductions from procedures starting from EN are about 20% less than

those starting from MRPN. In a real world decision-making situation, each criterion should be assigned a relative weight before the cost-benefit ratio is calculated.

The second measurement of the effectiveness of the procedure is the risk reduction in the greedy link removal stage, which is the difference between the benefit from MRPN and the benefit of the solution networks. This measurement is used to evaluate the value of the greedy link removal stage, which is usually not part of the design procedure used by others (e.g., Kessler 1986). The risk reduction and cost increase during both stages are listed in Table 13. The MRPN contributions in First_EN and Max_EN are zero because the greedy algorithm starts directly from the entire network. In First_MRPN and Max_MRPN, the greedy algorithm accounts for more than 43% of the total risk reduction. However, the results also show that for every unit of risk reduction in the second stage, the increase in travel costs is greater than in the first stage.

	Entire Procedure			MRPN Contribution		Greedy Stage Contribution	
	Benefit (1)	Cost Increase (2)	(2)/(1)	Benefit	Cost Increase	Benefit	Cost Increase
MRPN(D)	11.0%	10.2%	0.9				
First_MRPN(D)	19.6%	33.7%	1.7	56.3%	30.3%	43.7%	69.7%
Max_MPRN(D)	20.4%	25.4%	1.2	53.9%	40.3%	46.1%	59.7%
First_EN(D)	16.9%	20.6%	1.2	0.0%	0.0%	100.0%	100.0%
Max_EN(D)	16.9%	16.0%	1.0	0.0%	0.0%	100.0%	100.0%

Table 13 The risk reduction benefits and the cost increase from using MRPN and solution networks for all test problems

Among the four implementations of the design procedure tested, Max_MRPN produces the best results in terms of the average risk values in all three problem-settings. The maximum improvement greedy performs better than the first improvement greedy for the test problems when starting from both MRPN and the entire network. First_MRPN is quite close to Max_MRPN in terms of the risk values; however, it costs much more to achieve the same amount of risk reduction than Max_MRPN. First_EN and Max_EN are not as effective as the versions starting from MRPN in terms of risk reduction.

Figure 33 and Table 14 show the performance statistics of different implementations for all test problems. Figure 33 shows that the risks from Max_MRPN's solution networks are smaller than or equal to First_MRPN, First_EN and Max_EN in 80%, 85% and 75% of problem instances, respectively. Table 14 shows that Max_MRPN produces the lowest risk value in 57.8% of the problems solved.

	10x3 OD, 8x8 Network	15x6 OD, 8x8 Network	10x3 OD, 12x12 Network	Total	%
First_MRPN	4	6	6	16	25.0%
Max_MPRN	13	11	13	37	57.8%
First_EN	1	1	1	3	4.7%
Max_EN	4	2	2	8	12.5%
Sum	22	20	22	64	100.0%

Table 14 Number of times each algorithm produced the best solution in terms of risk

(Note: Sum for the first and third problem settings is greater than 20 due to ties)

4.4 Applying the Methodology in a Real Network

I applied the algorithms in the real network in Edmonton. The City of Edmonton divides the road network into four categories: arterial, collector, neighborhood and private roads. The arterial roads provide more direct connections between different parts of the city and have a higher engineering quality. Therefore, I chose the arterial roads as candidates for the Hazmat network. The arterial roads are extracted from the City of Edmonton's digital street network database. The arterial network consists of 736 nodes and 1,238 links. The link lengths were calculated using ArcView GIS. The link risks were calculated using the method detailed in Chapter 3 considering the average annual wind distribution (Figure 27).

Because the Edmonton network is much larger than the test networks used in the previous section, processing speed becomes an important issue. We can reduce the processing time significantly by dynamically adjusting the network structure. In the previous greedy algorithms, each link that was on the shortest path was tested to see whether it could be removed to reduce the total risk. Since the removal of some links will have the same effect on solution values, these links can be combined into one temporary link if they are

connected and only need to be tested once. For example, the thin lines in Figure 35 are the links that belong to the union of minimal risk paths. The thick lines are the links that are used by the shortest paths in MRPN. Among the numbered links, we can see that links 29 and 31 will have the same result if either of them is removed; therefore, 29 and 31 can be considered a single link in Figure 35 and only need to be tested once. The same is true for links 6, 8 and 10. This combines the eight numbered links into four temporary links: {29, 31}, {6, 8, 10}, {12} and {85, 87}. Please note that {29, 31} can not be further combined with {6, 8, 10} because they are separated by an intersection in MRPN. The removal of {29, 31} may or may not affect the amount of flow on {6, 8, 10}, and vice versa. {12} and {6, 8, 10} can not be combined either, because they are separated by a source node. The removal of {12} will definitely change the amount of flow on {6, 8, 10} and vise versa. The rule for redefining links and compressing the network is that the neighboring links that are not separated by an intersection in MRPN or an origin node or a destination node can be considered as one temporary link. The savings in processing time resulting from this restructuring are significant. They are even more significant in real world networks because real networks are usually very dense and the number of links between intersections can be quite large. Our tests in the Edmonton network showed that the number of trial links can be reduced seven folds by using this procedure.

I solved two problems in the Edmonton network. First, I used sixteen randomly generated points as OD points. Eight of them were used for origins, the other eight for destinations. Then I used eight realistic OD points, each point being a major entry and exit point to Edmonton (Figure 34). Because all the industrial areas were very close to these points, no extra points were added for industrial areas. The amount of flow was assumed to be one unit from every point to all other points. Since in the realistic problem, all points were treated as both origins and destinations, the number of paths was 8*7 = 56. In the random problem, the number of paths was 8*8 = 64. Both problems were solved with all four implementations. The results were listed in Table 15 and displayed in Figure 36 and Figure 37. As in the previous section, the cost values in EN(D) and the risk values in EN(C) were scaled to 100.

In the realistic problem, First_MRPN and Max_MRPN produced the same results (Figure 38). In the random problem, First_MRPN produced the best result in terms of risk. Because the original network is quite large, First_EN and Max_EN take a very long time to finish and the risk values are significantly worse than those from First_MRPN and Max_MRPN in terms of risk. This indicates that for real world applications, MRPN is a much better starting network for the greedy removal procedure than is the entire network.

	Realistic OD		Random OD		Average	
	Cost	Risk	Cost	Risk	Cost	Risk
EN(D)	**100.0**	**163.8**	**100.0**	**152.9**	**100.0**	**158.3**
EN(C)	**140.0**	**100.0**	**149.6**	**100.0**	**144.8**	**100.0**
MRPN(D)	**129.0**	**122.3**	**120.7**	**119.9**	**124.8**	**121.1**
First_MRPN(D)	**147.5**	**103.4**	**165.8**	**106.4**	**156.7**	**104.9**
Max_MRPN(D)	**147.5**	**103.4**	**158.6**	**110.7**	**153.1**	**107.0**
First_EN(D)	**110.5**	**129.9**	**113.1**	**121.6**	**111.8**	**125.7**
Max_EN(D)	**107.2**	**134.7**	**108.3**	**125.8**	**107.8**	**130.3**

Table 15 Solutions for the realistic and random problems in the Edmonton network

Figure 39 and Figure 40 show the minimum risk paths and least cost paths for realistic OD pairs in the original network respectively. As expected, the minimum risk paths tend to go by peripheral roads where the population density is lower. The least cost paths go straight to destinations even if they have to go through the downtown area. The cost and risk values for these two extreme scenarios are listed in EN(C) and EN(D) rows in Table 15. The risks resulting from the minimum risk paths are 100 units, the cost associated with this scenario is 140 units. If the drivers all take shortest paths, the total cost is 100 units, the total risk will be increased to 163.8 units, a 63.8% increase. The range of cost and risk values indicates that both administrators and drivers have a lot at stake in determining Hazmat routes.

For the realistic problem, the risk before the network design procedure was 163.8 units. In the solution networks from First_MRPN and Max_MRPN, the risk was reduced to 103.4

units, a 36.9% reduction. The total potential risk reduction—the risk associated with EN(D) (the risk before designing the network) minus the risk in EN(C) (the potential minimum risk)—was 63.8 units. Therefore, the entire network design procedure was able to achieve 94.7% potential risk reduction (Table 16). The greedy removal stage contributed 45.5% of the total risk reduction.

	Risk			Potential	Achieved	Achieved/ Potential
	EN(D) (1)	EN(C) (2)	Best Solution (3)	(1)-(2)	(1)-(3)	
Average	158.3	100.0	104.9	58.3	53.4	91.6%
Realistic	163.8	100.0	103.4	63.8	60.4	94.7%
Random	152.9	100.0	106.4	52.9	46.5	87.9%

Table 16 Potential and achieved risk reductions

For the two test problems, the greatest benefit from the network design procedure was 33.7%, which was defined as the total percentage risk reduction from EN(D). The associated cost increase was 56.7%. The cost-benefit ratio was 1.7. In the first stage of the procedure (MRPN), the cost-benefit ratio was 1.1 (Table 17). In the greedy link removal stage, the cost-benefit was 3.13, calculated with the following formula:

$$Cost\_benefit\_in\_greedy = \frac{Cost\_increase\_in\_solution - Cost\_increase\_in\_MRPN}{Benefit\_in\_solution - Benefit\_in\_MRPN}$$

Figure 41 shows the shortest paths in MRPN. Although the union of the shortest paths does not look much different from MRPN in the figure, the cost and risk values in EN(C), which is the same as MRPN, and MRPN(D) rows in Table 15 are quite different. Therefore, I looked into some individual paths under these two routing approaches (risk or cost minimization). The paths displayed in Figure 42 and Figure 43 are the paths from Point 1 to all other Points. Table 18 lists the cost and risk values of these paths in EN, MRPN and the solution network from Max_MPRN. Figure 42 and Figure 43 show that four out of seven OD pairs have a different path between centralized and decentralized routing decisions.

The maximum differences in cost and risk are 68.3% (Path 7) and 190.5% (Path 5) respectively. The average differences in cost and risk for all seven paths are 40.5% and 57.5% respectively.

	Entire Procedure			MRPN Contribution		Greedy Stage Contribution	
	Benefit (1)	Cost Increase (2)	(2)/(1)	Benefit	Cost Increase	Benefit	Cost Increase
MRPN(D)	23.5%	24.8%	1.1				
First_MRPN(D)	33.7%	56.7%	1.7	69.7%	43.8%	30.3%	56.2%
Max_MPRN(D)	32.4%	53.1%	1.6	72.6%	46.7%	27.4%	53.3%
First_EN(D)	20.6%	11.8%	0.6	0.0%	0.0%	100.0%	100.0%
Max_EN(D)	17.7%	7.8%	0.4	0.0%	0.0%	100.0%	100.0%

Table 17 Benefits and cost increases for two test problems in the Edmonton network

		Path1	Path2	Path3	Path4	Path5	Path6	Path7	Total
Cost	EN(D)	1.34	1.80	2.43	1.47	2.73	2.28	2.71	14.76
	EN(C)	2.09	2.54	3.48	1.75	3.83	2.48	4.56	20.74
	MRPN(D)	1.45	1.90	2.67	1.75	3.02	2.48	4.56	17.83
	Max_MRPN(D)	2.09	2.54	4.12	2.62	3.74	3.40	5.48	23.99
Risk	EN(D)	0.98	1.66	2.68	1.73	5.57	2.85	5.25	20.71
	EN(C)	0.93	1.61	1.85	1.39	1.92	2.56	2.90	13.15
	MRPN(D)	0.95	1.64	2.33	1.39	2.40	2.56	2.90	14.16
	Max_MRPN(D)	0.93	1.61	2.02	1.46	1.95	2.68	3.02	13.67

Table 18 Cost and risk for paths from node 1 to other nodes

In the solution network, the minimum risk paths originating at Point 1 happened to be the same as the shortest paths. In the greedy link removal process, we were able to reduce the total risk for all OD pairs. However, the risks for shipments between some OD pairs were increased due to the removal of some links. To visualize the trade-off of risk and cost in different stages of network design, I plot the risk and cost values for Paths 3, 4 and 5 in

Figure 44, Figure 45 and Figure 46. Among the three paths, the risk for Path 4 in the solution network is greater than that in MRPN, although it is still much smaller than that in the original network.

The link removal algorithm involves very intensive computation. The network design routine was programmed in Microsoft Visual C++ 5.0, running on a Pentium 166 PC with 64M RAM. Table 19 lists the solution times for the test problems in the Edmonton network and the random networks in the previous section.

Network	OD Pairs	Solution Time (Seconds)			
		First_MRPN	Max_MRPN	First_EN	Max_EN
8x8	10x3	225	421	1160	2227
	15x6	3048	6231	6621	12922
12x12	10x3	1367	2612	13610	24609
Edmonton	Realistic(8x7)	261	606	29918	50986
	Random(8x8)	2655	3874	55910	82853

Table 19 Solution times in seconds

4.5 Conclusions

In this chapter I developed a two-stage approach for designing a municipal Hazmat network to minimize transportation risk. The first stage is to calculate the minimum risk paths for all transport demands in the original network. The union of minimum risk paths is used as the initial network for the link removal algorithm in the second stage. The second stage involves a balance between drivers and administrator: the drivers always want to take the least cost paths, and the administrator then restricts the use of some links to reduce the total risk. I also tried using the entire network as the initial network for the second stage and found it was not satisfactory in both solution quality and computing speed. The main contribution of this chapter is that it proves that the union of minimal risk paths, which is used as Hazmat routes by some practitioners, is often not a good Hazmat network in terms of risk. Based on my computational experiments in both random and real-world networks, I draw the following conclusions:

- The total risk in the solution network is significantly smaller than that in the original network, which indicates that Hazmat network design should be an important part of the efforts in improving the safety of Hazmat transportation in cities.

- The game-like link removal process I added to the network design procedure contributes a significant part of the total risk reduction. I suggest that this stage become an integral part of the network design process and hope it will become a standard practice in the Hazmat network design process. Even a simple greedy link removal algorithm reduces the total risk significantly. For the test problems in the Edmonton network, the solution risk values are very close to the ideal minimum value. This is not true for all problems, however. For some problems in the test networks, a better algorithm may be able to bring the risk value closer to optimality.

The amount of Hazmat transported on national highways is increasing every year (DOC 1994). Cities are the main terminals of Hazmat traffic, hence, urban roads carry a large portion of the Hazmat traffic. Both the amount and the flow pattern of Hazmat traffic are changing in urban areas. The distribution of population and property are changing too. Therefore, municipal Hazmat networks should be updated regularly and the application potential of new methods is very large. The following are some interesting topics for further research:

- Developing a decision support system (DSS) that provides data (social, economic and environmental data), relevant models and algorithms (risk analysis, network design, etc.) and a user interface. A DSS will reduce the cost of the network design process, facilitate what-if analysis and enhance communication among all parties.

- Enhancing the network design procedure. Hazmat network design is a multi-objective problem in nature. This research modeled it as a single objective problem, although some what-if analysis involving several objectives can be carried out in the procedure developed. In addition to cost and risk, network design often must consider other factors such as risk equity, which deals with the spatial distribution of risk in relation to the distribution of population segments.

- Exploring the cost-benefit of seasonal Hazmat networks. Because wind conditions affect risk distribution in the city and prevailing wind conditions are quite different from season to season, it may be beneficial for some cities to change the Hazmat network on a seasonal basis. With a network design DSS, technical and financial barriers for updating Hazmat network design can be overcome rather easily. However, the true cost-benefit of seasonal Hazmat networks remains to be explored.

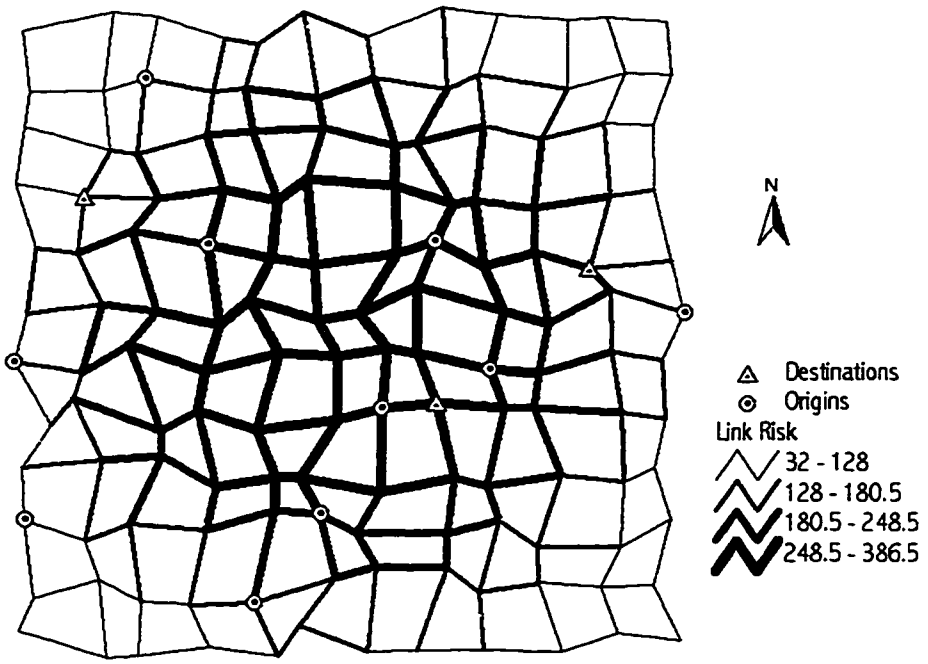

Figure 28 A test problem in the 144-node network

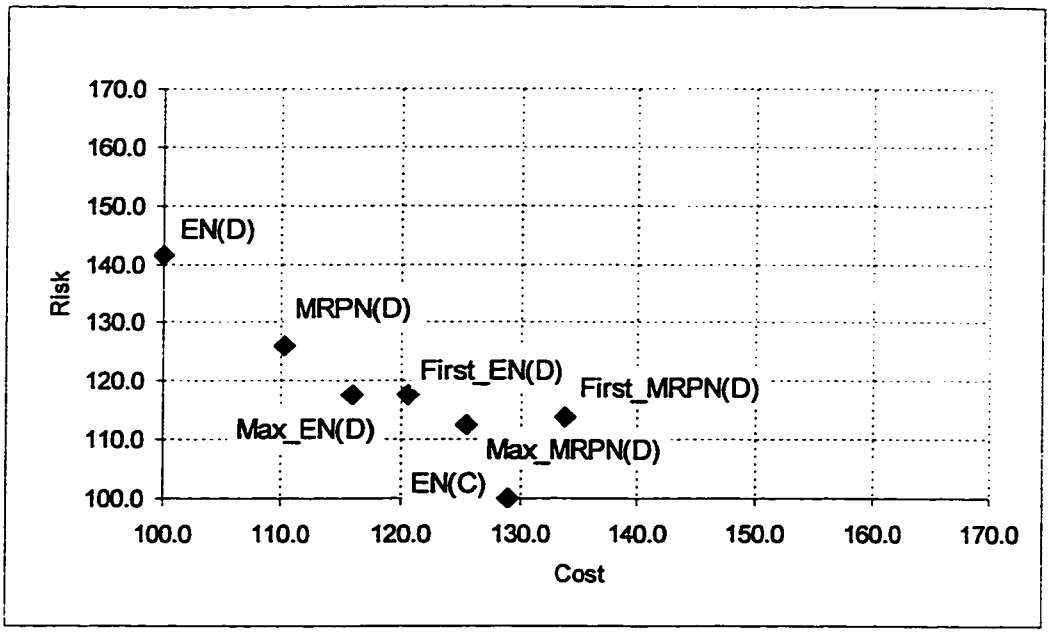

Figure 29 Cost-risk tradeoff for all test problems

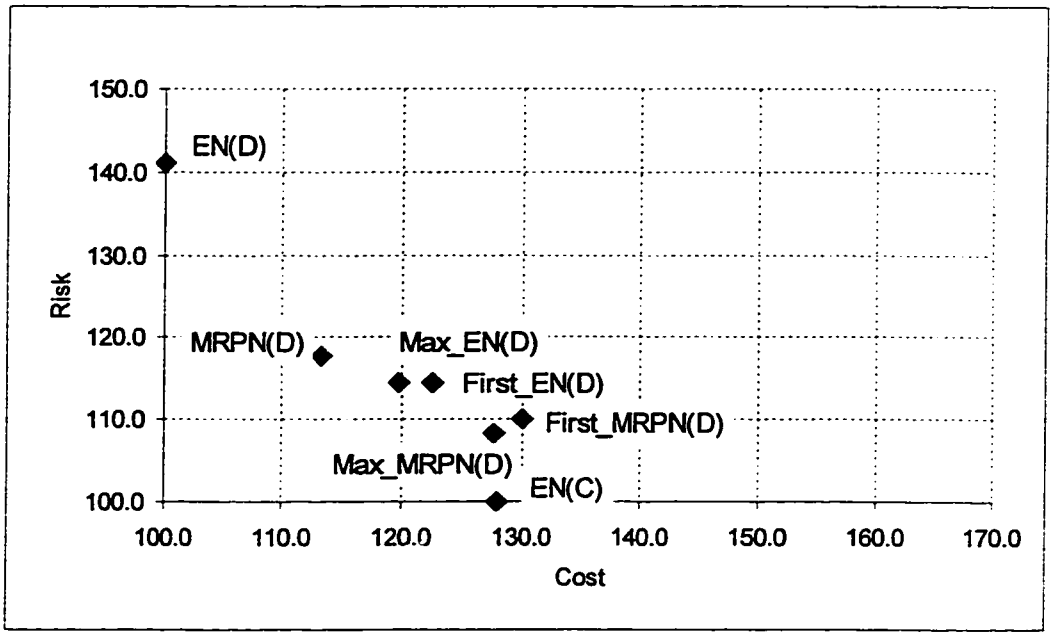

Figure 30 Cost-risk tradeoff for problems with 10x3 OD pairs on the 64-node network

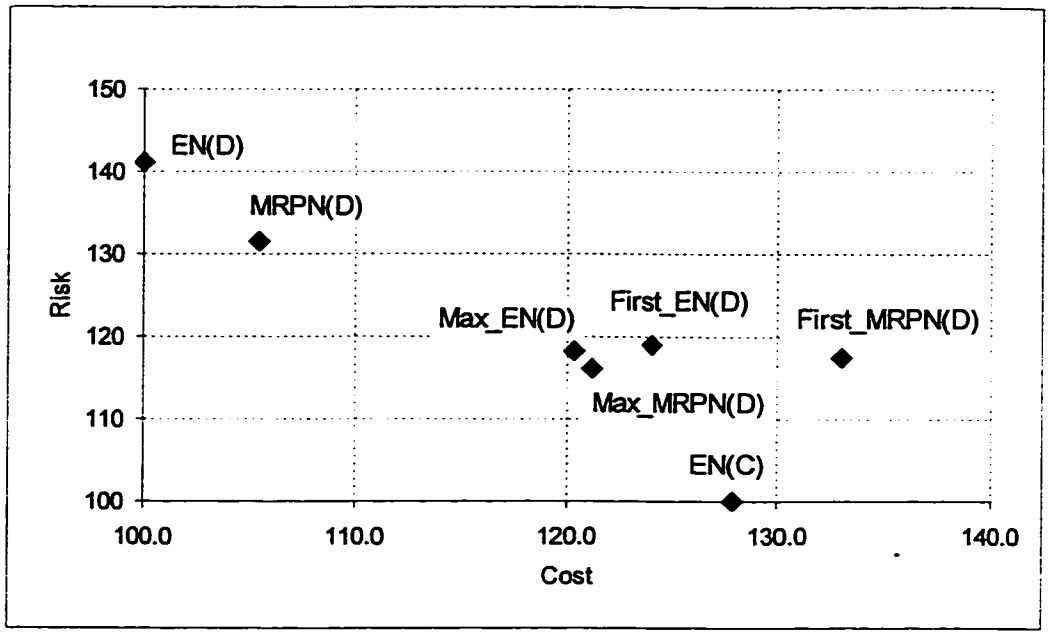

Figure 31 Cost-risk tradeoff for problems with 15x6 OD pairs on the 64-node network

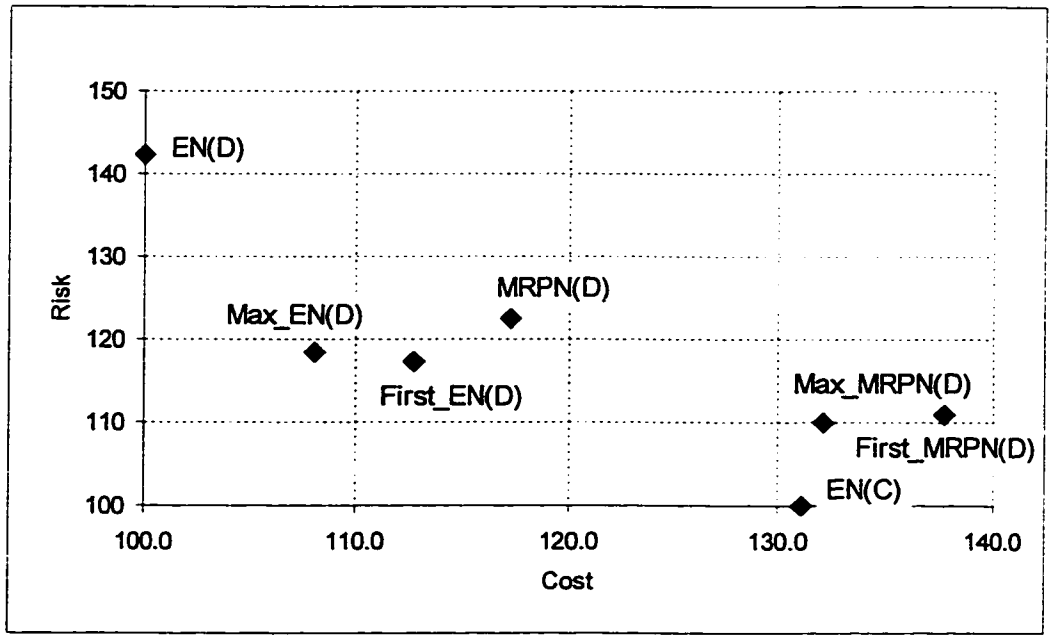

Figure 32 Cost-risk tradeoff for problems with 10x3 OD pairs on the 144-node network

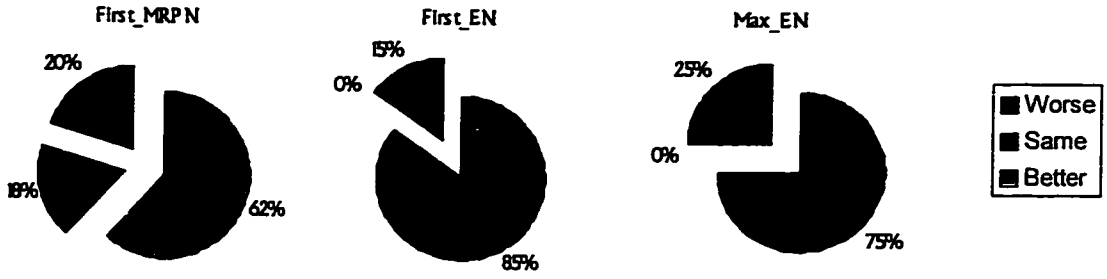

Figure 33 Comparison of procedures with Max_MRPN from a total risk perspective

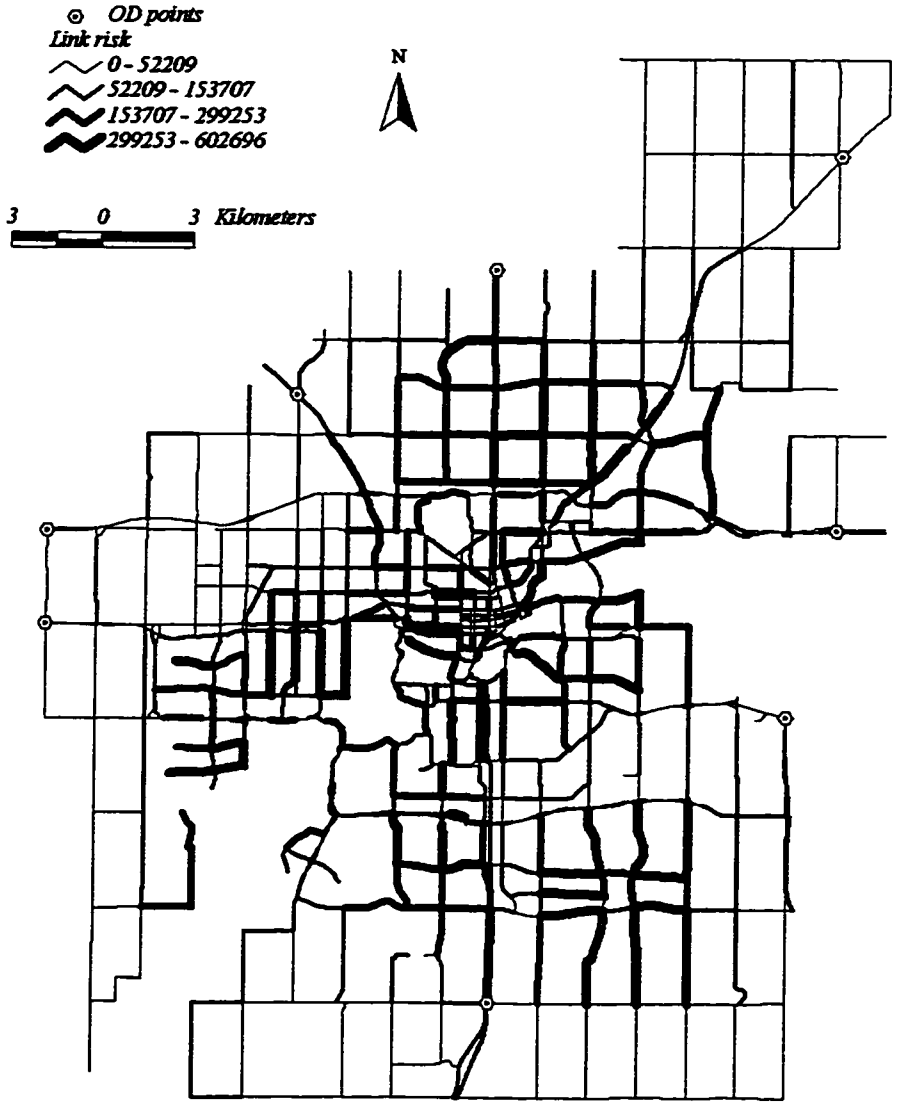

Figure 34 Edmonton arterial network and realistic OD points

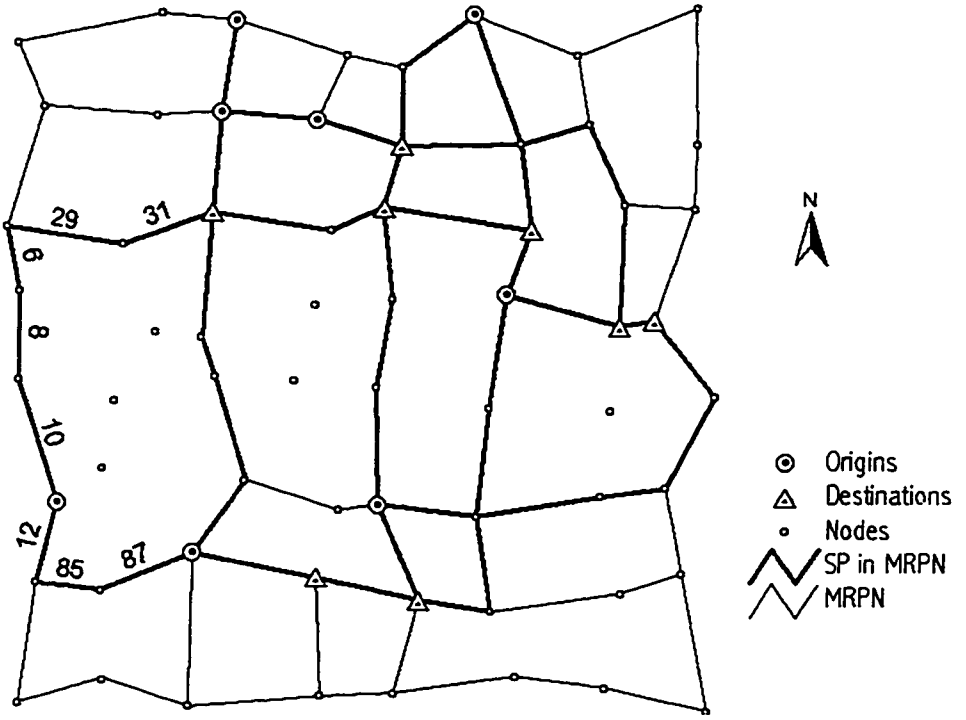

Figure 35 Network structure reconstruction

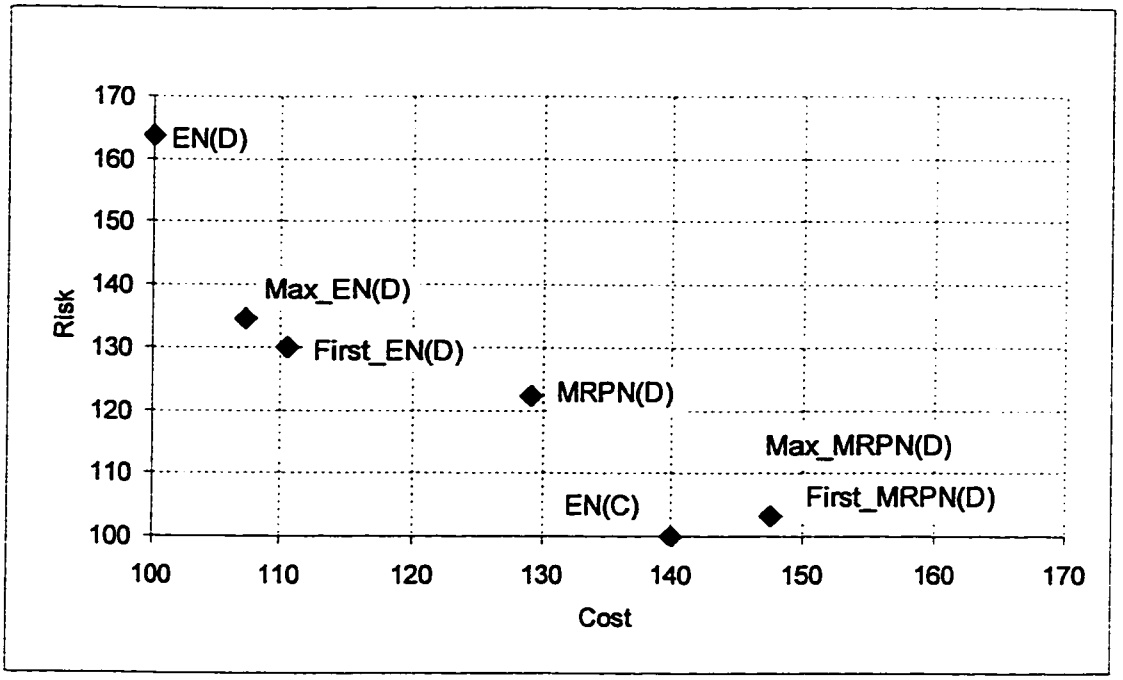

Figure 36 Cost-risk tradeoff for the realistic problem in the Edmonton network

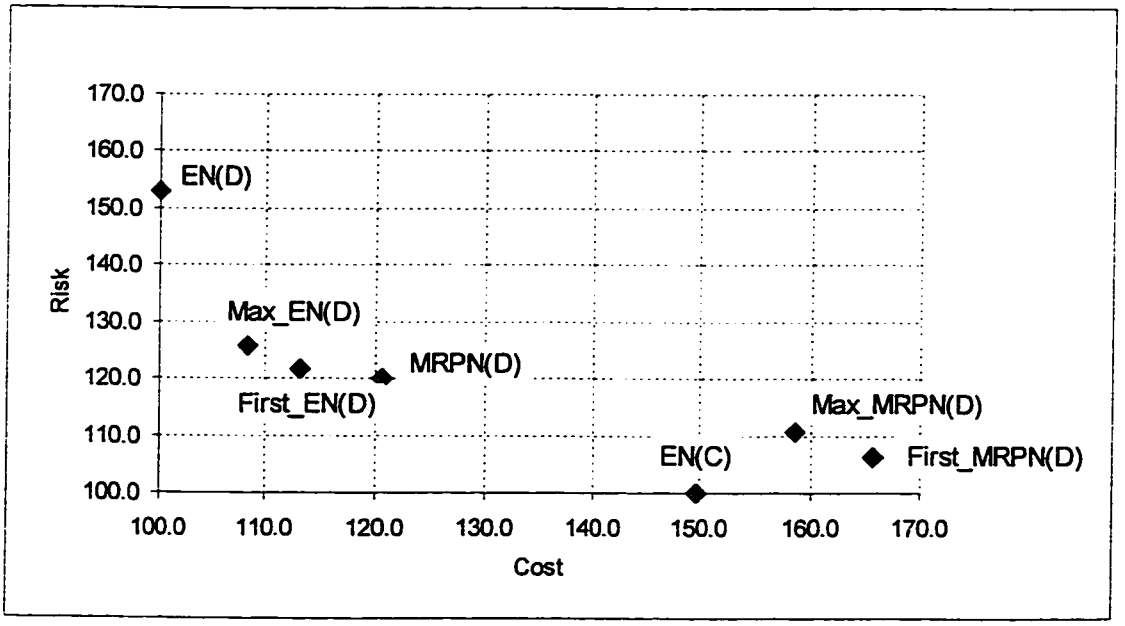

Figure 37 Cost-risk tradeoff for the random problem in the Edmonton network

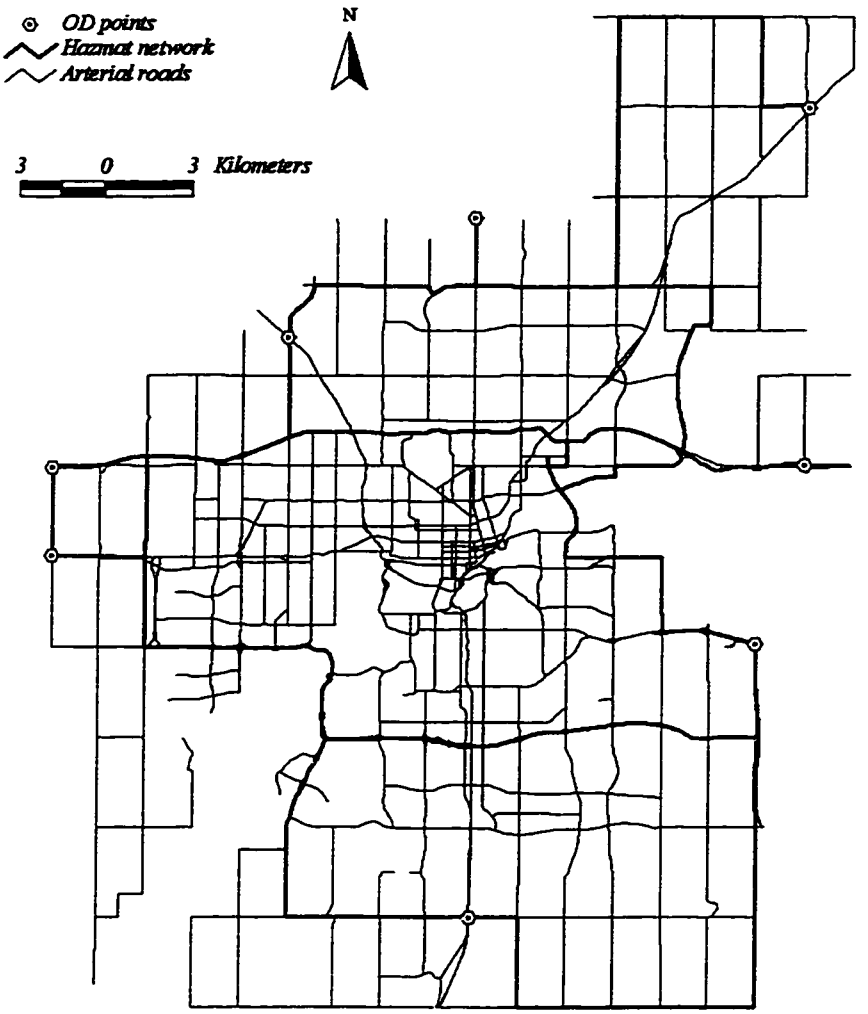

Figure 38 The solution network for the realistic problem

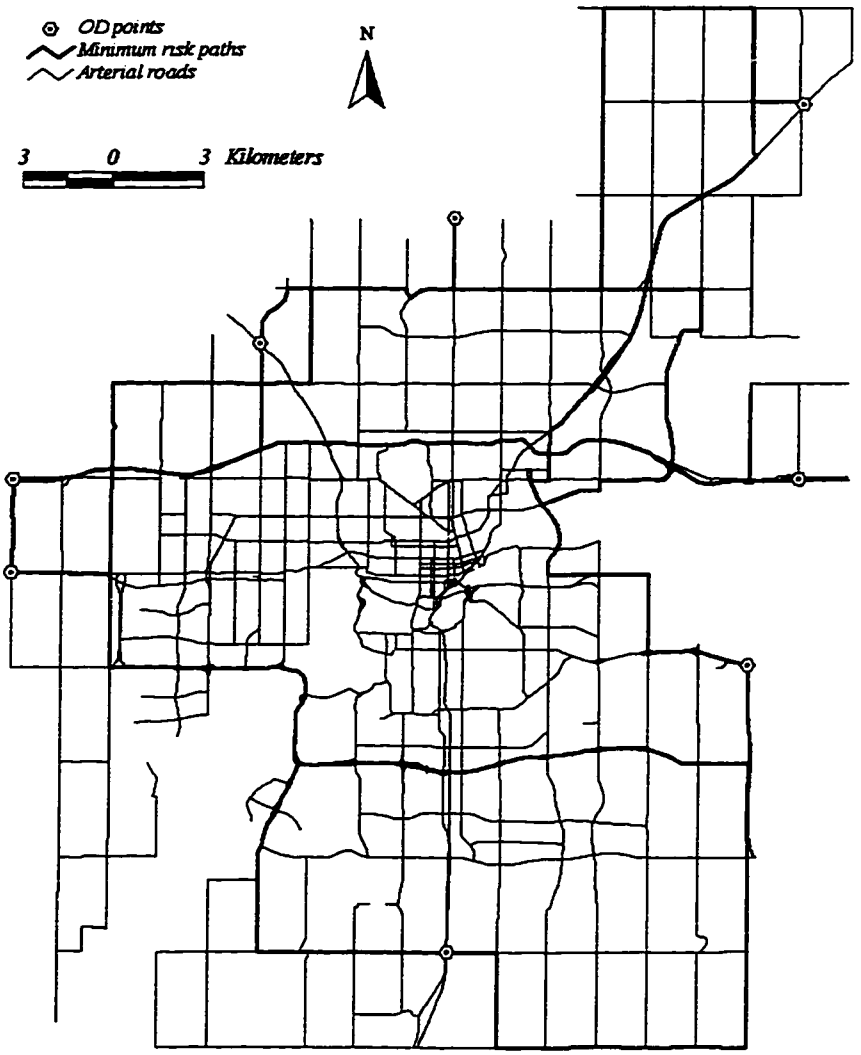

Figure 39 Minimal risk paths from all origins to all destinations

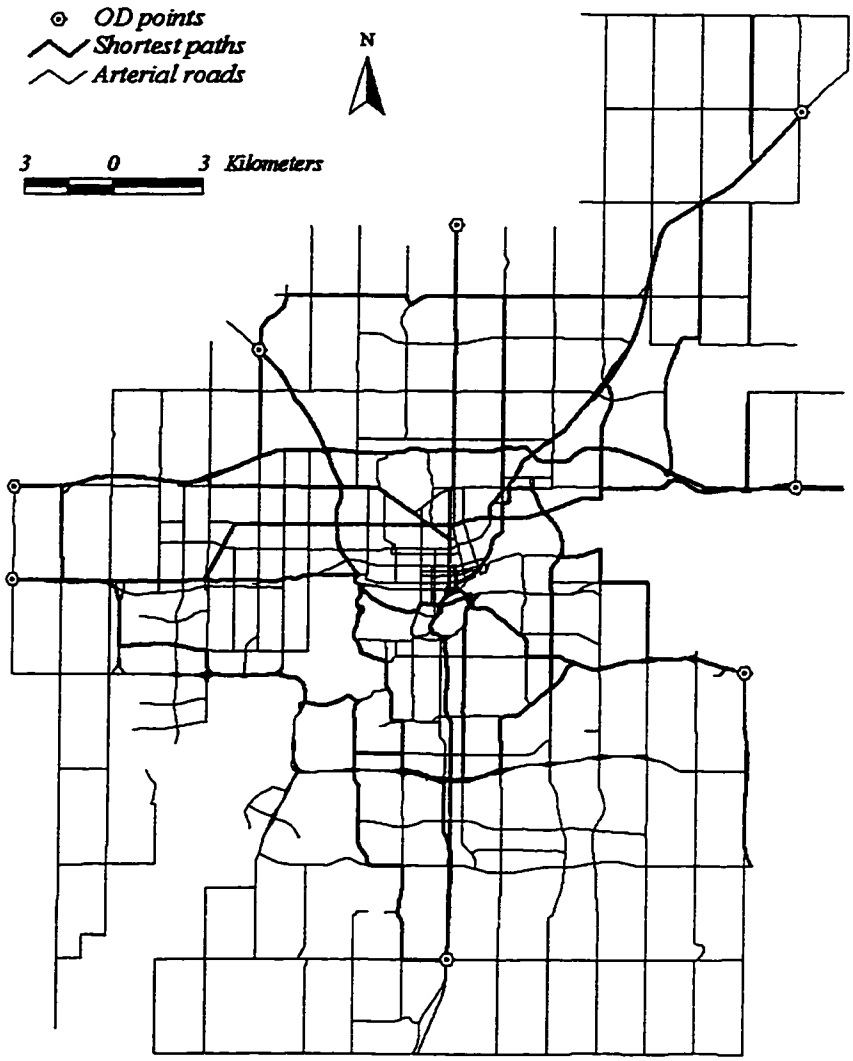

Figure 40 Shortest paths from all origins to all destinations

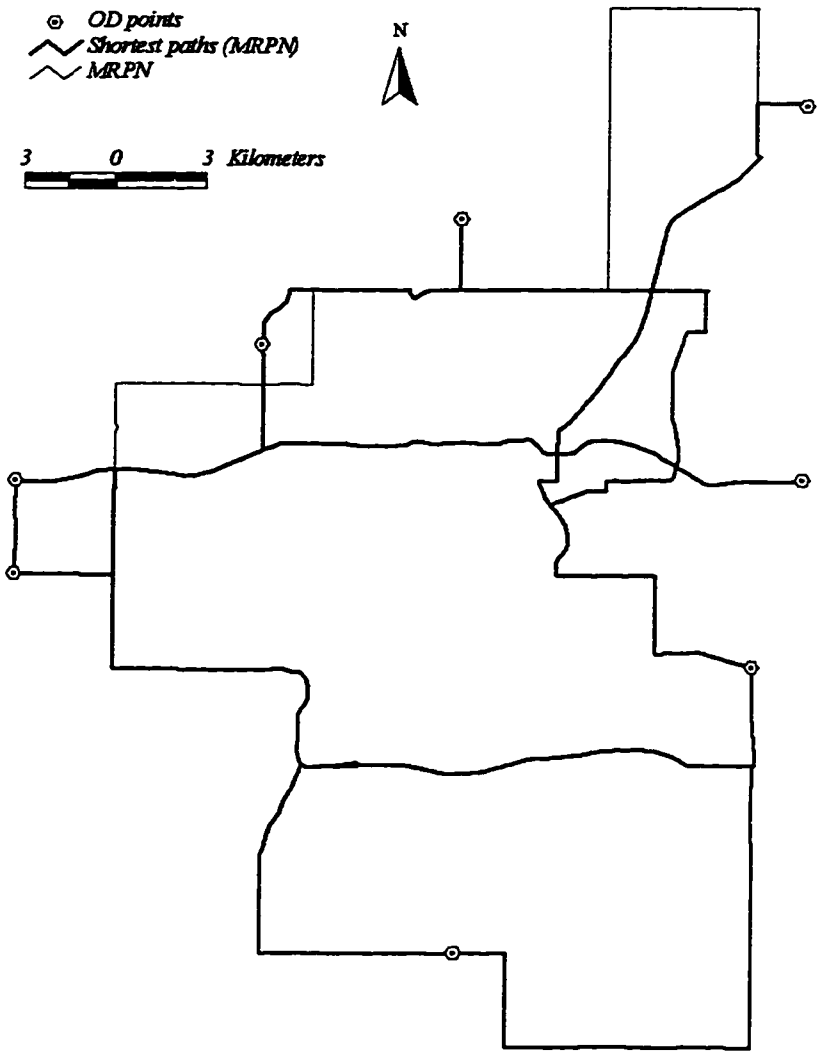

Figure 41 Shortest paths in MRPN

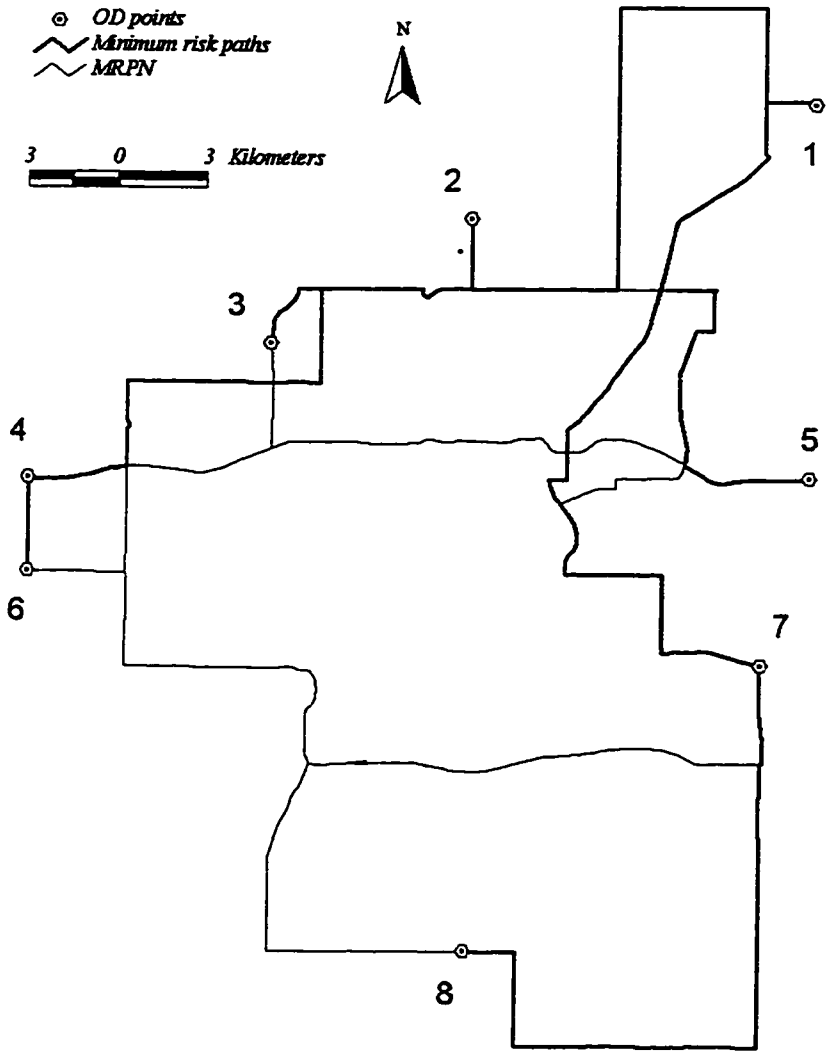

Figure 42 Minimal risk paths from node 1 to all other nodes

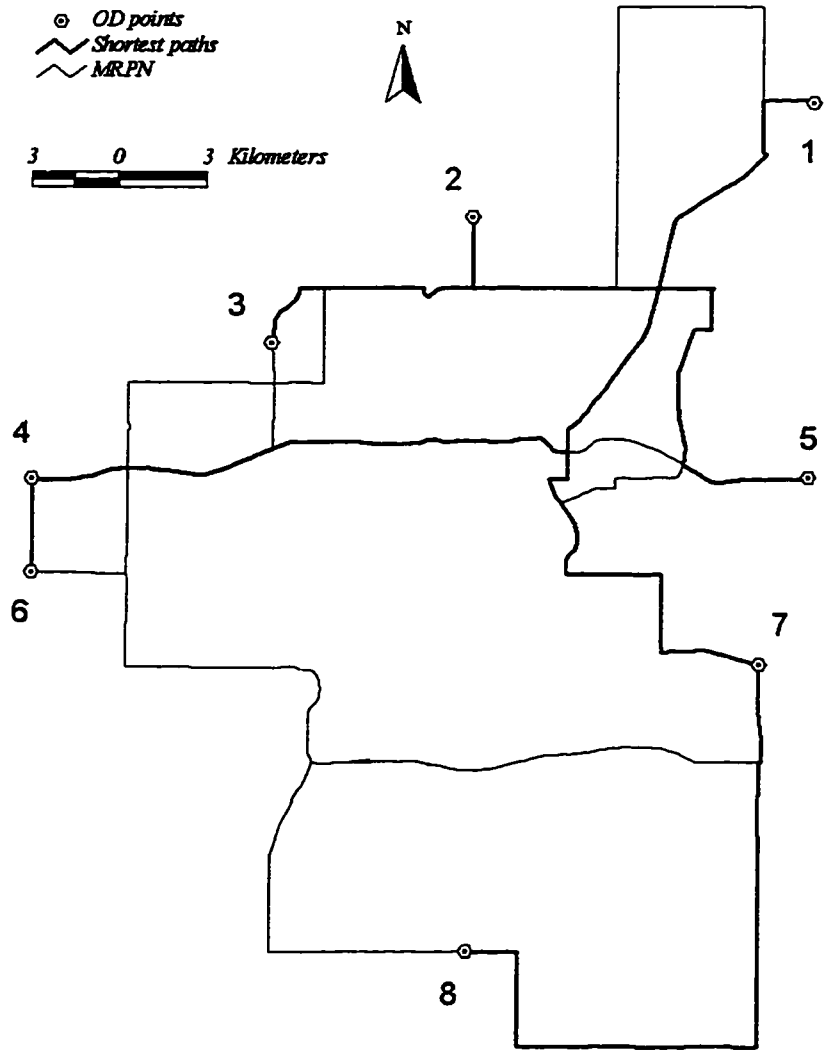

Figure 43 Shortest paths from node 1 to all other nodes

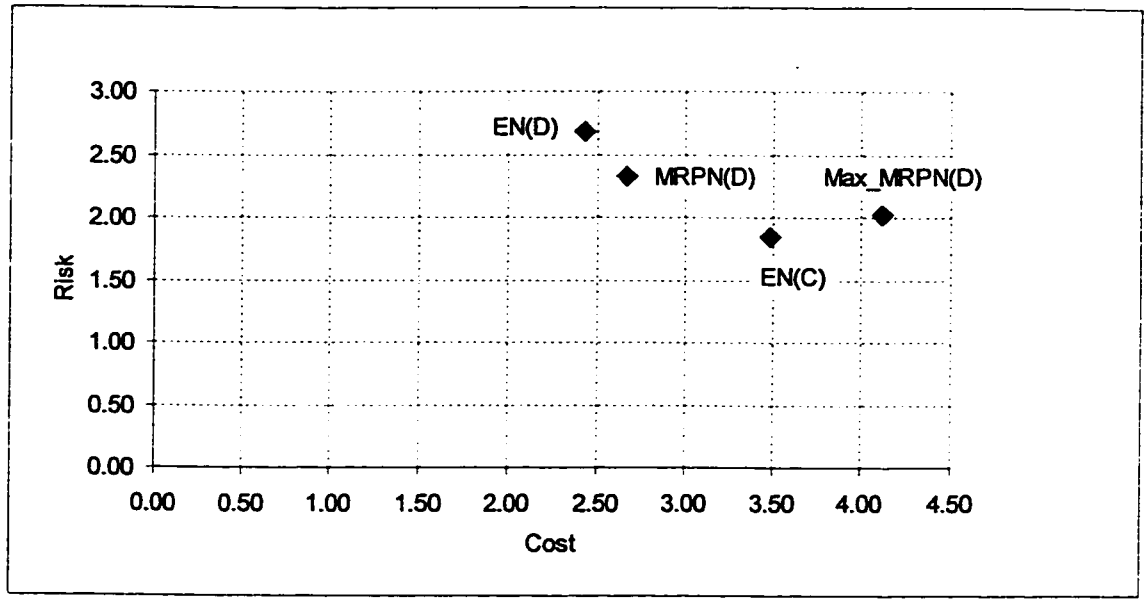

Figure 44 Cost-risk tradeoff for Path 3

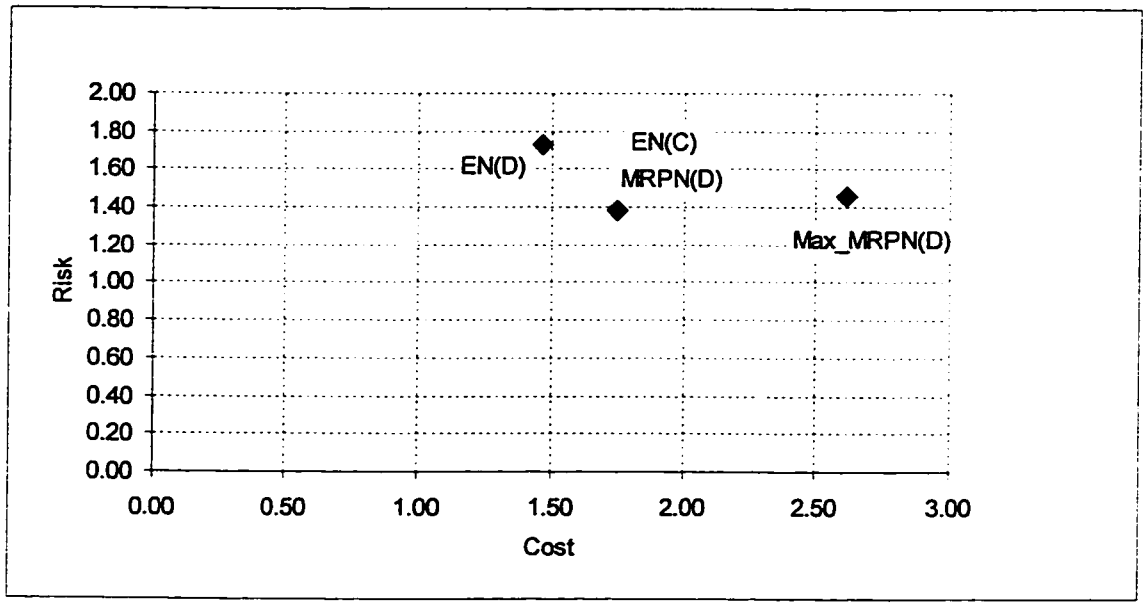

Figure 45 Cost-risk tradeoff for Path 4

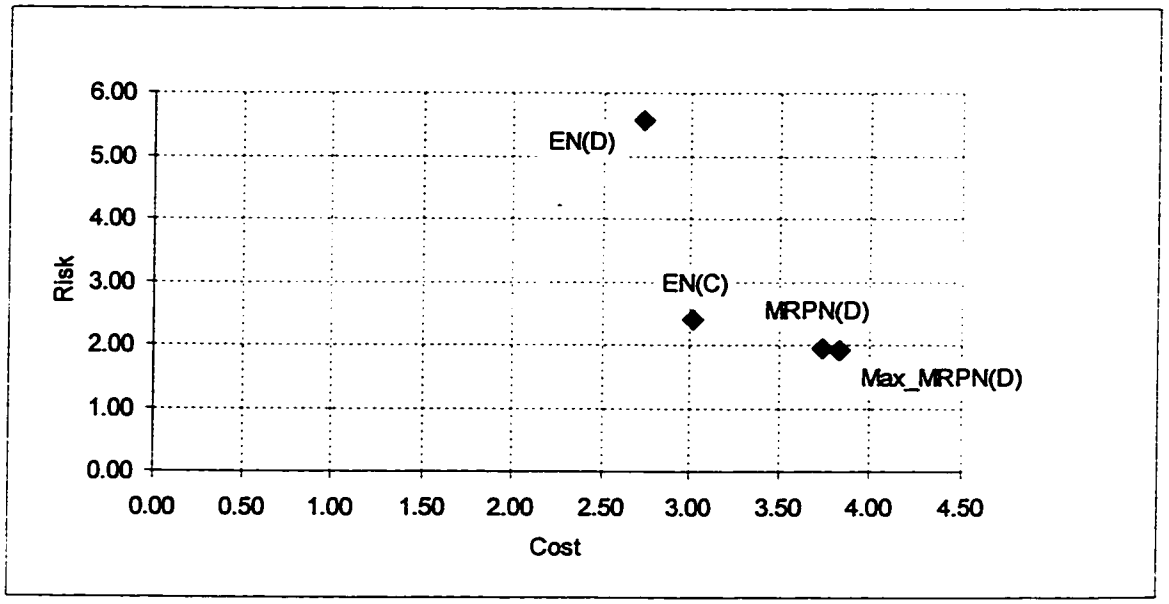

Figure 46 Cost-risk tradeoff for Paths 5

Chapter 5

INSPECTION STATION LOCATION

5.1 Introduction

Hazmat transportation is a highly regulated industry in Canada and the United States. Both countries have strict regulations on virtually all aspects of Hazmat handling including packaging, marking and documentation. Compliance with regulations during transit is particularly important because the population exposure can be very large in the case of an accident. However, it is not rare for shippers to violate the regulations either by intention or by ignorance. Between 1992, the year the Transportation of Dangerous Goods Act (TDGA) was proclaimed in Canada, and 1997, there have been 145 convictions federally (Transport Canada 1997). Unfortunately, many of the non-compliant drivers were only caught when they were involved in an accident. Trained inspectors and sometimes the RCMP are responsible for carrying out random inspections on highways. Due to a lack of trained personnel and resources, they are not able to identify the majority of the non-compliant trucks before accidents happen. Earlier research (Cox 1984) also indicates that insufficient staffing in the United States is a problem in enforcing Hazmat routing regulations.

One way to ease this problem is by locating inspection stations more effectively using location models. Traditional location models (Daskin 1995) deal with facilities that serve demands originating at fixed points or areas in space. The demands that inspection stations serve are moving traffic flows that cannot be approximated as fixed demand points or areas. Facilities that serve traffic are not uncommon. In addition to inspection stations, roadside billboards, gas stations and fast food restaurants are examples of facilities that serve the passing traffic flow. Location scientists have recognized two types of traffic flow and developed flow-intercepting facility location models for them. The first type of traffic is ordinary traffic that does not pose extra risk to the society other than regular traffic risks. Facilities serving this type of traffic aim to expose themselves to as much traffic as possible without worrying about where the flow is intercepted. Examples of these kinds of facilities

include fast food restaurants, gas stations and billboards. The location model for this type of facility is called the Flow Capturing Location Model (FCLM). The second type of traffic poses extra risk to the people on or near the road. Examples of this type of traffic include cars driven by drunk drivers and improperly loaded or maintained Hazmat trucks. It is to the benefit of society to detect and remove this type of traffic as early in their trip as possible. The model for locating this type of facility is called the Inspection Station Location Model (ISLM). ISLM was proposed quite recently (Hodgson *et al.* 1996). No algorithm has been successfully implemented to solve this problem yet.

The aim of this chapter is to find a good algorithm for ISLM. A tabu search (TS) algorithm and a vertex interchange algorithm were implemented and compared with a greedy algorithm used in previous studies. The algorithms were tested using realistic risks from a real world network. The remainder of the chapter is organized as follows. Section 2 describes the flow-intercepting models. Section 3 describes the algorithms. The computational results on an arbitrary network are presented in Section 4. Section 5 presents experimental results on a real-world network with realistic link risks. The conclusion follows in Section 6.

5.2 Flow-Based Location Models

Two flow-intercepting models, the flow-capturing location model (FCLM) and the inspection station location model (ISLM), have been developed so far. A simply heuristic algorithm can solve FCLM problems near optimally (Hodgson 1990). The objective of this chapter is to find a robust algorithm for the ISLM. Because of the inherent relationship between FCLM and ISLM, both models are introduced here.

5.2.1 Flow-capturing location model (FCLM)

FCLM was first proposed by Hodgson (1990) and Berman *et al.* (1992, 1995). It can be formulated as an integer programming (IP) model:

Maximize:

$$Z = \sum_{q \in Q} f_q y_q \tag{5.1}$$

Subject to:

$$\sum_{k \in N_q} x_k \geq y_q \quad \text{for all } q \in Q, \tag{5.2}$$

$$\sum_{k \in K} x_k = p \tag{5.3}$$

where:

q indicates a particular path

Q is the set of all paths

f_q is the flow along path q

y_q is a binary variable, = 1 if f_q is captured, = 0 if not

k indicates a potential facility location

K is the set of all potential facility locations

x_k is a binary variable, = 1 if there is a facility at k, = 0 otherwise

N_q is the set of nodes capable of capturing f_q (i.e., the set of nodes on path q)

p is the number of facilities to be located

The objective is to capture as much flow as possible. Constraint (5.2) states that the flow on q can be captured only if there is at least one facility on path q. Constraint (5.3) limits the number of facilities to p. Possible applications of this model are in the location of billboards and gas stations. Since the model was formulated, Hodgson *et al.* (1995) applied this model to a real-world network. Hodgson and Rosing (1992) studied the dual criterion trade-off between satisfying demands from points and flows if the facilities aim to serve both. The original FCLM only counts the benefit of exposure once for each flow. Hodgson and

Berman (1997) extended this model to incorporate the benefit of multiple exposures to locate billboards.

5.2.2 Inspection station location model (ISLM)

It is not appropriate to use FCLM to locate inspection stations because its objective is to maximize the flow intercepted without considering where the flows are intercepted. In the case of Hazmat truck inspection, it is more desirable to inspect and remove dangerous trucks as early in their trip as possible so that the risk imposed on the society is minimized. Hodgson *et al.* (1996) refer to the objective of ISLM as the "preventive approach" and refer to the objective of FCLM as the "punitive approach". Consider the demonstration problem in the diagram to the right. A dangerous truck will travel from A to B. The risk resulting from this truck travelling on AB is 10 units. In FCLM, the objective is to catch the driver during the trip. Thus, an inspector at A, B or any point in-between will achieve the same result - catch the driver (and issue a ticket). Whereas in ISLM, the objective is to stop the dangerous truck as early as possible to maximize the protection. Thus, A is the optimal solution where the protection achieved is 10 units. Stopping the truck at B does not do any good in terms of protecting the network for this shipment. C only protects the link segment CB. Since ISLM tries to maximize the protection to the network, it is more applicable for inspecting hazardous material transport than FCLM. ISLM is formulated as a mixed integer problem:

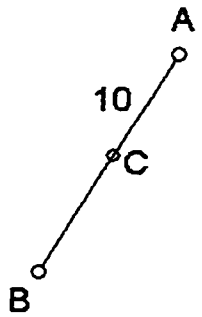

Maximize:

$$Z = \sum_{q=1}^{n_q} \sum_{i \in N_q} P_{qi} X_{qi} \tag{5.4}$$

Subject to:

$$\sum_{i \in N_q} X_{qi} \leq 1 \text{ for all } q \tag{5.5}$$

$$Y_i - X_{qi} \geq 0 \quad \text{for all } q \text{ and } i \in N_q \tag{5.6}$$

$$\sum_{i=1}^{n} Y_i = p \tag{5.7}$$

where

q indicates a particular path

n_q is the number of paths

i is the node number

P_{qi} is the protection available to path q at node i

$X_{qi} = 1$ if path q is protected by a station at node i, =0 if not

$Y_i = 1$ if there is an inspection station at i, =0 if not

N_q is the set of nodes capable of capturing f_q (i.e., the set of nodes on path q)

p is the number of facilities to be located

n is the number of nodes

The objective of the model is to maximize the total amount of protection. Constraint set (5.5) ensures the protection from only one inspection station is counted even if several inspection stations intercept it. Maximization forces it to be the one with the largest P_{qi}. Constraint set (5.6) ensures that a node can not provide protection to a path unless an inspection station is located at the node. Constraint (5.7) specifies that p facilities will be located.

5.3 Solution Procedures

The Flow Capturing Location Model and the Inspection Station Location Model have been shown to be NP-hard (Hodgson *et al.* 1996). Therefore, we need to develop heuristic algorithms for them. Like the p-median problem, FCLM and ISLM are combinatorial

problems with n-choose-p solutions, where n is the number of candidate locations and p is the number of facilities to be located. Hodgson used a greedy add procedure to solve FCLM and found that greedy algorithm works quite well for this model. When he applied the same algorithm to ISLM problems, however, the algorithm performed poorly. It suffers from the fact that facilities located in the early stages of the algorithm remain in place over the entire solution sequence even if their protection is rendered redundant by facilities added in the later stages. In this study, I implement a tabu search (TS) algorithm and a node interchange algorithm to solve the ISLM problem and compare the results with those from the greedy algorithm. I also looked into a refined greedy algorithm prescribed for a capacitated flow capturing location problem (Mirchandani *et al.* 1995).

5.3.1 Greedy algorithm

The greedy algorithm adds a facility at each step at the node that provides the greatest incremental protection to the network. It works in the following steps:

Step 1. Calculate the protection available at each node for a given set of Hazmat flows in the network.

Step 2. Add a facility at the node that provides the maximum protection. If the number of facilities added equals to p, end. Otherwise, go to step 3.

Step 3. Calculate the remaining protection available at each node, go to Step 2.

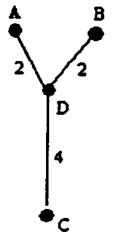

This algorithm works quite well for FCLM problems, but it has some obvious flaws when applied to ISLM problems. One reason for its failure is that once a facility is located, it cannot be relocated even if the later facilities take over the protection it was providing. It can be illustrated using the small problem shown in the graph to the right. The demonstration problem has two flows of 10 and 11 units from sources A and B respectively to a sink C. Link lengths are displayed next to each link in the graph. The protection available at each node is the product of the down-stream length and the amount of flow. The junction D is the best single facility location (Table 20), protecting flows from both sources down to the

sink. Neither upper branch is protected, however. To protect the network fully, we need to add two more facilities, one at A and one at B. After these two facilities are added, the facility at D becomes completely redundant. Interested readers are referred to a realistically sized example in Hodgson *et al.* (1996).

	First Facility	Second Facility	Third Facility
A	60	20	20
B	66	22	0
D	84	0	0
C	0	0	0
Protection	84	22	20

Table 20 Protection available at each node and risk removed by each facility

5.3.2 Refined greedy algorithm

The refined greedy algorithm was proposed by Mirchandani *et al.* (1995) for the FCLM problem. In this algorithm, every time a new facility is added, all the facilities that are on downstream direction of the flows that go through the new facility are relocated. This mechanism is designed to reduce the overlapping protection from later facilities. I tested this algorithm on my networks and found the algorithm falls into an infinite loop easily. One reason for these infinite loops can be illustrated using a simple example. Suppose there are two flows *ab* (from node *A* to node *B*, 10 units) and *ba* (from *B* to *A*, 5 units) traversing the same link *AB*, and we need to locate two facilities. AB is bi-directional and everything (such as accident probability) is the same for both directions. At the first step, the refined greedy algorithm will locate a facility at *A* because there are more flows originating from *A*. At the second step, a new facility is added at *B*. Because *A* is in the downstream direction of flow *ba* that is intercepted by *B*, the facility at *A* is removed. The algorithm then goes on to find a new location for this facility and end up with location *A*. After the facility is located at *A* again, the facility at *B* is removed because it is in the downstream direction of *ab*. Obviously, we are in an infinite loop. This is a simplistic example and a mechanism to jump out of the loop is easy to design. For larger problems, many links will carry reverse

flows and a mechanism that can avoid all possible pitfalls is not so obvious. Furthermore, a simple interchange phase will achieve what the refined greedy tries to achieve – the earlier facilities are given an opportunity to relocate. Therefore, I do not explore the refined greedy heuristic further.

5.3.3 Interchange algorithms

Two versions of an interchange algorithm are implemented. The first version starts from the solution of the greedy algorithm and the second version starts from a random solution. These two versions are called "Greedy + Interchange" and "Random Start Interchange" respectively. The interchange algorithms work as follows:

Step 1. Calculate the total amount of protection Z_0 from the initial solution. The p facilities in the initial solution are either selected randomly from all the potential points (n) or are selected with the greedy algorithm.

Step 2. Replace one of the p locations with one of the $n - p$ unselected locations and calculate Z_i. Try all possible swaps and record the swap that resulted in the most improvement $Z_i^* = \max (Z_i - Z_0)$.

Step 3. If $Z_i^* = 0$, stop. Otherwise accept the swap that result in Z_i^* and go to *Step 2.*

Interchange algorithms are often trapped in local optima and fail to find optimal solutions. One way to increase the probability that the final solution is the optimal solution rather than a local optimum is to start the interchange algorithm several times using different starting solutions. Modern heuristics use more intelligent ways to expand the portion of the search space that is explored to avoid being trapped in local optima. Tabu search (TS) is one of the modern heuristic procedures that have been applied to solve many combinatorial problems successfully (Glover and Laguna 1993).

5.3.4 Tabu search (TS) algorithm

The TS algorithm was first proposed by Glover (1977, 1989 and 1990a). In essence, TS works on three primary themes (Glover 1990b): 1) the use of flexible memory structures

designed to exploit evaluation criteria and historical search information more thoroughly than with a rigid memory structure (such as in branch-and-bound) or memoryless systems (such as in simple interchange algorithms); 2) an associated mechanism of control – for employing the memory structures – based on the interplay between conditions that constrain and free the search process (embodied in tabu restrictions and aspiration criteria); and 3) the incorporation of memory functions of different time spans, from short term to long term, to implement strategies for intensifying and diversifying the search. (Intensification strategies reinforce move combinations and solution features historically found to be good, while diversification strategies drive the search into new regions.)

The typical TS procedure works as follows. It starts from a random solution. It repeatedly examines all neighbors of the current solution, then moves to the best neighbor even if the move causes the objective function to deteriorate. This move (or the reverse move) is forbidden (becomes a tabu) for the next θ (tabu tenure) iterations unless using it will produce the best solution so far (aspiration and aspiration criteria). After a certain number of iterations, the best solution is recorded and the process is started over again. Instead of starting from a random solution this time, the initial solution is either composed of elite elements that most frequently improve the objective function value when appearing in the solution (intensification), or the elements that least frequently appear in the solution (diversification). The above procedure is for illustrating the concepts of TS only. When applied to specific problems, TS algorithms must be carefully tailored to the problem at hand (Benati and Laporte 1994).

Here is my implementation of tabu search algorithm for ISLM:

- Move and neighbor solutions – interchange of an unselected candidate location and a selected location is called a move. The solution resulting from a move is a neighboring solution of a particular solution.

- Tabu and tabu tenure – Once a move is made, these two nodes cannot be swapped again for the next θ iterations unless the new move meets the aspiration criteria. θ is a uniform random number in the range of [tmin, tmax], where tmin and tmax are the minimum and maximum tabu tenures respectively. The reason for using a random

number rather than a fixed one for tabu tenure is that it can avoid cycling. Practical experience indicates that random tabu tenure is more robust than using a fixed number (Glover and Laguna 1993, Benati and Laporte 1994). There are no generally applicable best ranges for tabu tenure; however, [7, 14] works well for many problems (Glover and Laguna 1993). Therefore, this range was used in this study.

- Aspiration - A forbidden move (tabu) can be overridden if it meets the aspiration rule. The aspiration criterion used here is that the move can improve the best result so far.

- Intensification and diversification – The algorithm keeps track of the number of times a location appears in a solution throughout the iterations. For diversification, I use the p nodes that appear least frequently in the previous iterations for the initial solution in the next start. Intensification is not employed for this problem.

The algorithm can be stated as follows:

Step 1. Set the number of starts s:=1, the number of iterations t:=1. Generate an initial solution randomly. Calculate Z_0 and set $Z_{BEST} = Z_0$. Set all values in the frequency list to 0. No swap is tabu.

Step 2. Consider all neighbor solutions X_i obtained by moving a facility from a node selected to a node not selected.

Step 3. Compute Z_i for each X_i and sort Z_i in descending order.

Step 4. If the move that results in the largest Z_i is not tabu or if it meets the aspiration criterion, select this move, reduce the tabu tag for all members in the tabu list by one, declare the swap of these two nodes as tabu for the next θ iterations where θ is selected randomly in the range of [7, 14], update the frequency list (increasing the frequency tag for nodes that appear in the solution by one), if and go to Step 5. Otherwise, select the best non-tabu neighbor solution and update the prequency list. If all possible moves are listed as tabu, lift the tabu status of the move that has the smallest tabu tag and repeat Step 4.

Step 5. Set t := t + 1. If t is equal to a preset upper limit, go to Step 6. Otherwise go to Step 2.

Step 6. Set s := s + 1. If s is equal to a preset upper limit, stop. Otherwise, set t := 1, redefine a new starting solution as the set of p locations that were included least frequently in all of the previous solution sets in Step 4 of the algorithm, clear the tabu list. Go to Step 2.

5.4 Computational Experiments

The algorithms described in the previous section were tested on a fifty-five-node network from Kroll (1988) that was used by Hodgson *et al.* (1996) for testing the greedy algorithm for the same model. Instead of assuming link risk to be proportional to the link length, I randomly generate link risks (Figure 47). The width of links is proportional to link risks in Figure 47. For a given network, the size of ISLM problems depends on the number of source-sink paths, the number of nodes these paths pass and the number of inspection stations. In creating test problems, I specified a single path—the shortest path—for each source and sink pair. The algorithms were tested on three problem sizes: 10-source and 10-sink (10x10) problems, 20x20 problems and 30x30 problems. The source and sink points were generated randomly. The amount of flow from each source to each sink was one unit. Therefore, the total number of paths in each problem setting was 100, 400 and 900 respectively. For each problem size, I generated 20 problems, each problem was solved for p=1,..., s, where p is the number of inspection stations and s is the number of sources. Therefore, I ran the algorithms 1200 times in total (Table 21).

Size	Number of Problems	P	Number of Instances
10x10	20	1..10	200
20x20	20	1..20	400
30x30	20	1..30	600
Total number of instances:			1200

Table 21 Number of test problems

The best way to evaluate a heuristic algorithm's performance is to compare the objective function values with known optima. Because inspection station problems can be very large, solving problems of reasonable size exactly is very difficult. However, there is a special characteristic in inspection station location problems: the optimal solution for fully protecting the network is obvious. To provide full protection to the network, a facility must be located at every source, i.e., when $p = s$ (s is the number of sources), the optimal solution is to locate one facility at each source. This is a trivial case. However, it can be used as a criterion to evaluate heuristic algorithms. A good heuristic should be able to find the optimal solution for this trivial case, although algorithms that find the optimal solution for it are not necessarily good. Among the 1200 test problems, 60 ($p = s$) problems belong to this special case. Table 22 lists the number of times each algorithm failed to find the optimal solution in this case. The interchange algorithm and TS are able to find optimal solutions in all 60 problems. Greedy fails once for the twenty 10x10 problems. It fails 17 and 18 times out of 20 problems for the 20x20 and 30x30 problems respectively. Although the objective function values from the greedy algorithm are very close to the optimal solutions (Table 23), the percentage of risk not removed shows a trend of growth when problem size becomes larger. Since interchange algorithms are very fast and easy to program, there is no reason we should tolerate this drawback of the greedy heuristic.

	Num. of Instances	Greedy	Greedy+Int	Random Int	Tabu
10x10	20	1	0	0	0
20x20	20	17	0	0	0
30x30	20	18	0	0	0

Table 22 Number of times heuristic fails to find optimal solutions for $p = s$ facilities

The problems for p=1,...,5 were solved exactly using complete enumeration. For these small problems, tabu search finds the optimal solutions for all problems. Both random start interchange and tabu search perform much better than Greedy and Greedy + Interchange algorithms in terms of times each algorithm finds an optimal solution (Table 24). Again, the objective function values from all algorithms are quite good (Table 25).

	Greedy	Greedy+Int	Random Int	Tabu
10x10	0.3	0	0	0
20x20	0.6	0	0	0
30x30	0.8	0	0	0

Table 23 Percentage of risk not removed by s facilities

Size	Total Num. of Problems	Greedy	Greedy+Int	Random Int	Tabu
10x10	100	8	0	0	0
20x20	100	11	10	2	0
30x30	100	24	10	1	0

Table 24 Number of times optimal solution not found for p=1..5

For reasonably large problems, optimal solutions are difficult to find. Since we are trying to develop a better heuristic than that already known, we can compare the heuristics among themselves. Figure 48 to Figure 50 plot the difference in mean percentage protection between Greedy and the other algorithms for each problem setting. Percentage protection is the ratio between the risk removed and the total amount of risk resulting from the shipments. The solution values are listed in tables in Appendix 1. These figures show that TS not only outperforms the greedy algorithm, it outperforms the interchange algorithms as well. When the problems become larger, the advantage of TS becomes more obvious.

Figure 51 to Figure 53 show the maximum difference in percentage protection between Greedy and other algorithms for each problem setting. The maximum difference between TS and the interchange algorithms is under 1.5 in most cases. The maximum difference between TS and greedy algorithm seems to be insensitive to the number of flow paths (although it differs with the number of inspection stations), and in all 1200 cases, it is less than 3.5. Random start interchange (with 3 starts) generally performs better than Greedy + Interchange. In some cases, however, Greedy + Interchange finds a better solution. Because both greedy and interchange algorithms are very fast, I suggest that the greedy

solution be used as one of the start solutions if a multiple start interchange algorithm is to be used in a decision support system.

Facilities		Greedy	Greedy+Int	Random Int	Tabu
10x10	1	"	"	"	"
	2	0.06%	"	"	"
	3	0.04%	"	"	"
	4	0.05%	"	"	"
	5	0.04%	"	"	"
20x20	1	"	"	"	"
	2	"	"	"	"
	3	0.37%	0.37%	"	"
	4	0.44%	0.36%	"	"
	5	0.30%	0.13%	0.42%	"
30x30	1	"	"	"	"
	2	0.38%	"	"	"
	3	0.59%	0.07%	"	"
	4	0.84%	0.42%	0.05%	"
	5	1.36%	0.54%	"	"

Table 25 Average percentage of risk not removed by p=1..5 facilities
(" means 0%)

5.5 Applying the Algorithms in a Real-World Network

The algorithms were applied to the real world network of Edmonton. The Edmonton arterial network has 736 nodes and 1,238 links. The risk value for each link was calculated in Chapter 3. Forty points were generated randomly, 20 were used for origins and the other 20 for destinations. The shortest paths were computed from each origin to each destination as flow paths. The amount of flow between each source-sink pair was one unit. The problem was solved for p=1, ..., 20. The results are listed in Table 26 and plotted in Figure 54. Figure 55 shows the difference in percentage protection between the greedy algorithm and other algorithms.

The computational results show that when the number of facilities increases, the greedy algorithm starts to show its weaknesses. First, it fails to find the optimal solution for the full protection ($p = s$) case. Second, the difference in objective function values between TS and greedy becomes larger as the value of p increases. The interchange algorithms perform much better than the greedy algorithm. Both interchange algorithms produce results that are inferior to TS in four instances. The difference in objective function values between the interchange algorithms and TS are quite small except for one case where the difference is 1.26. As in the experiments in the previous section, both tabu search and interchange algorithms find the optimal solution for the full protection case.

	Percent of Risk Removed (%)				Improvement over Greedy		
P	Greedy	Greedy+Int	Random Int	TS	Greedy+Int	Random Int	TS
1	23.69	23.69	23.69	23.69	0.00	0.00	0.00
2	33.11	33.11	33.11	33.11	0.00	0.00	0.00
3	42.47	42.47	42.47	42.47	0.00	0.00	0.00
4	48.64	48.64	48.64	48.64	0.00	0.00	0.00
5	54.51	54.51	54.51	54.51	0.00	0.00	0.00
6	59.53	59.53	59.53	59.53	0.00	0.00	0.00
7	64.05	64.05	64.05	64.05	0.00	0.00	0.00
8	68.44	68.44	68.44	68.44	0.00	0.00	0.00
9	72.67	72.67	72.67	72.67	0.00	0.00	0.00
10	76.74	76.74	76.74	76.74	0.00	0.00	0.00
11	80.22	80.82	80.82	80.82	0.60	0.60	0.60
12	83.68	84.28	84.50	84.50	0.60	0.82	0.82
13	86.49	87.97	86.71	87.97	1.48	0.22	1.48
14	88.95	90.52	89.85	90.52	1.57	0.90	1.57
15	90.97	92.55	92.40	92.55	1.57	1.42	1.57
16	92.73	94.45	94.42	94.45	1.71	1.69	1.71
17	94.19	95.90	96.35	96.35	1.71	2.16	2.16
18	95.48	97.19	97.64	97.64	1.71	2.16	2.16
19	96.69	98.40	98.84	98.84	1.71	2.16	2.16
20	97.87	100.00	100.00	100.00	2.13	2.13	2.13

Table 26 Solutions for problems in Edmonton network

5.6 Conclusions

A problem facing regulating agencies is to monitor the movement of Hazmat flow and enforce regulations regarding Hazmat transportation. Because resources for carrying out this task are limited, locating inspection stations optimally will maximize the benefit from limited resources. In this chapter, I implemented a tabu search algorithm and node interchange algorithms to solve the inspection station location problems. The tabu search algorithm was able to find better solutions than the greedy and interchange algorithms in both arbitrary and real-world networks. Both the interchange and tabu search algorithms overcome a major drawback in the greedy algorithm where facilities cannot be replaced after they are located.

Because ISLM locates facilities that catch traffic flow that is ubiquitous in this mobilized society, the application potential of ISLM is significant. When more and more applications are developed, some customized versions of the model will be developed to suit specific applications. In the context of Hazmat truck inspection, it is worth considering a game theory approach for locating inspection stations. The current model assumes that both flows and inspection stations are fixed. In real-world situations, the drivers will try to avoid the stations if they know where they are located. Therefore, there is a game-playing component in the Hazmat truck inspection problem: the facilities should be mobile and responsive to the behavior of drivers, which in turn is responsive to (what they know about) the location of inspection stations.

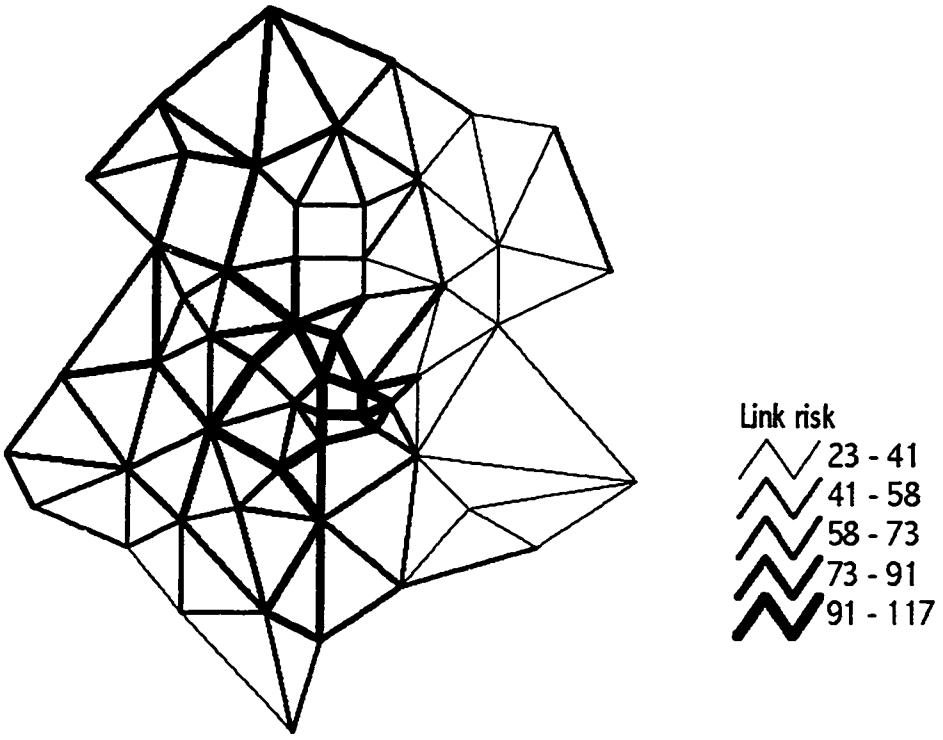

Figure 47 The fifty-five-node network

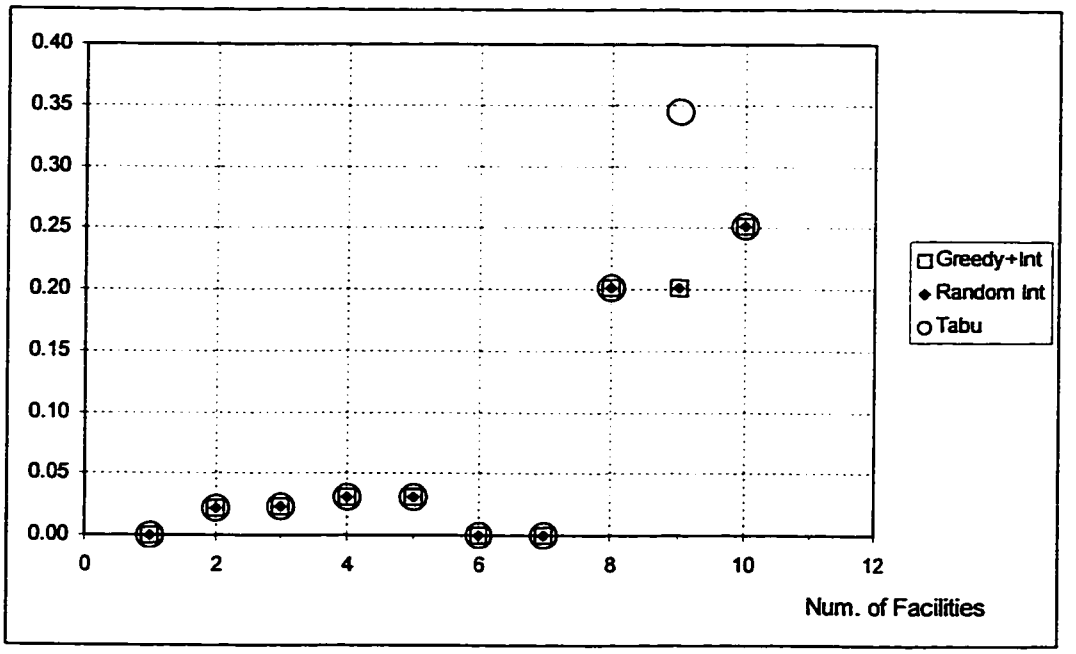

Figure 48 Performance of interchange and tabu search algorithms in comparison with greedy algorithm for 10x10 source-sink problems (mean values)

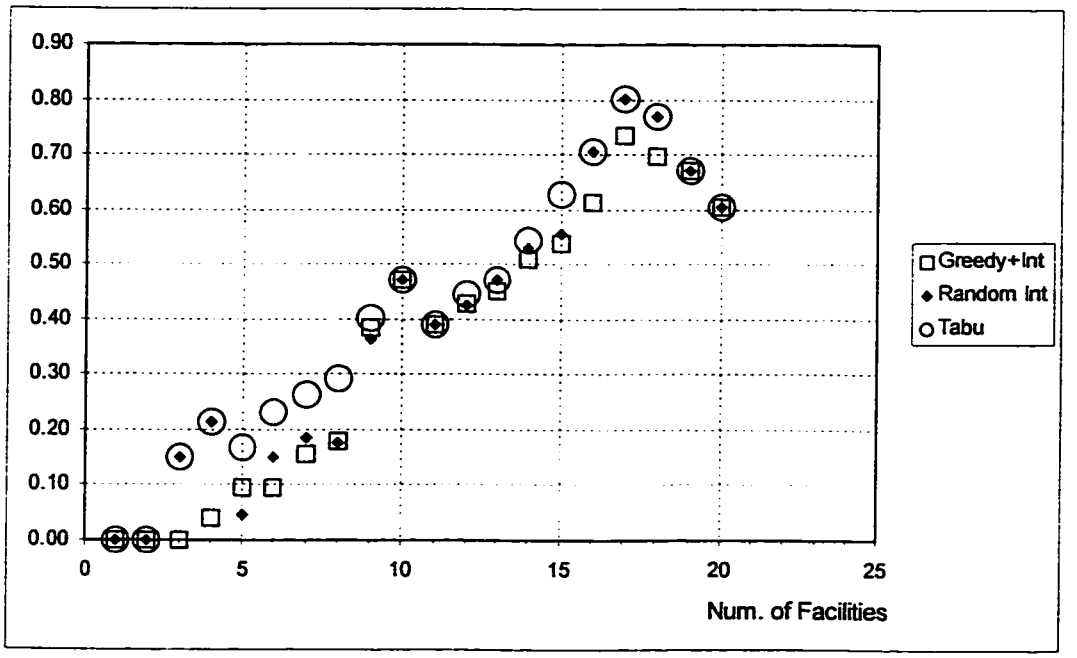

Figure 49 Performance of interchange and tabu search algorithms in comparison with greedy algorithm for 20x20 source-sink problems (mean values)

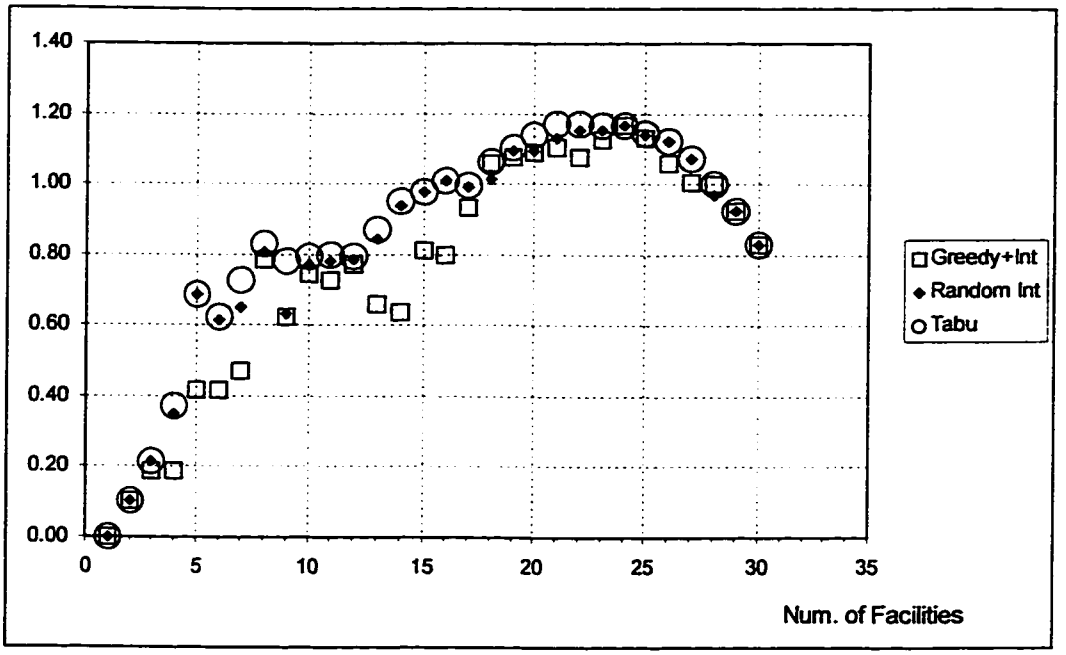

Figure 50 Performance of interchange and tabu search algorithms in comparison with greedy algorithm for 30x30 source-sink problems (mean values)

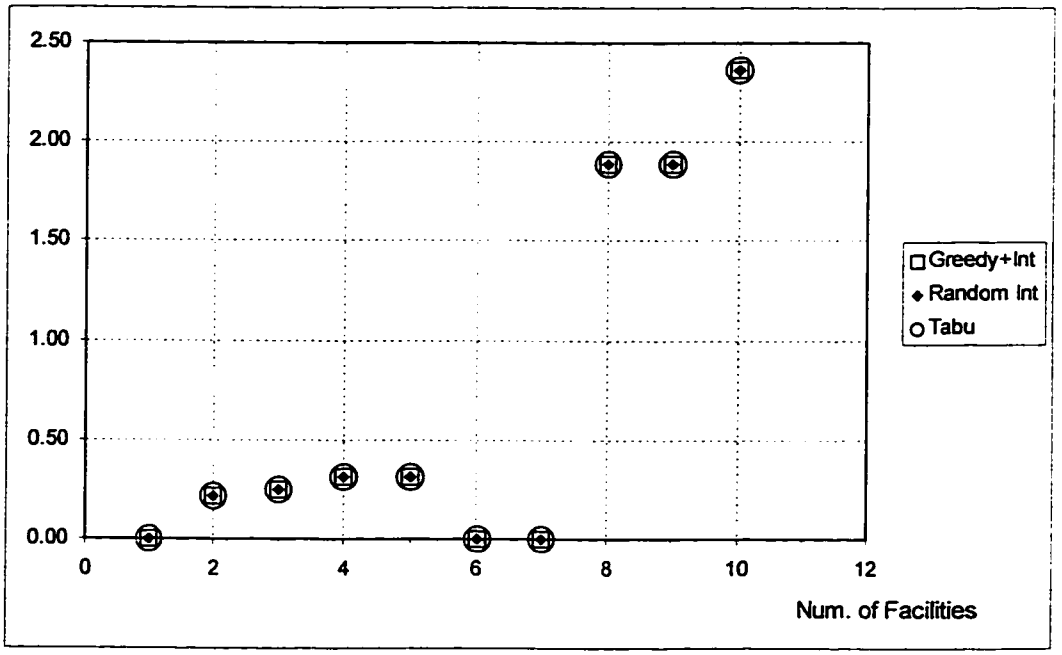

Figure 51 Maximum difference of percentage protection as compared to the greedy algorithm for 10x10 source-sink problems

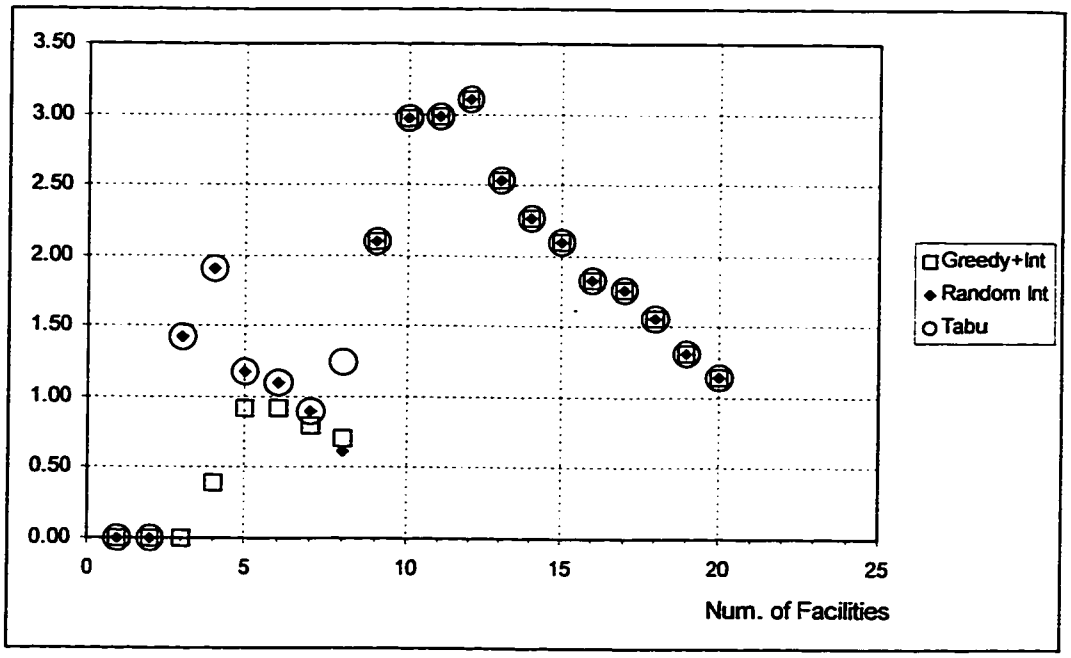

Figure 52 Maximum difference of percentage protection as compared to the greedy algorithm for 20x20 source-sink problems

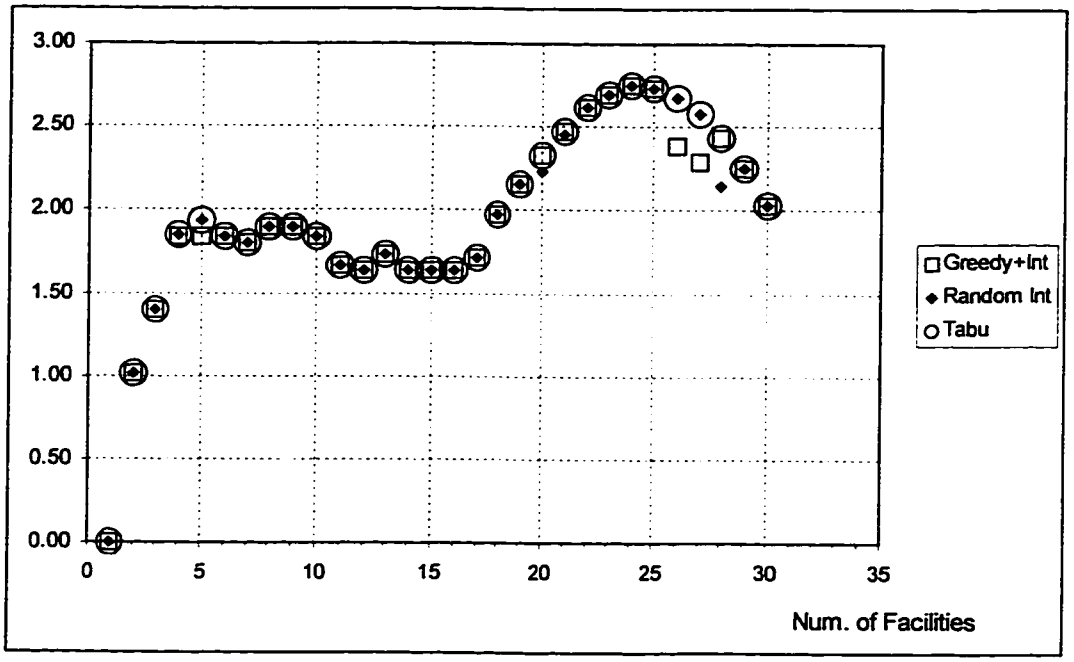

Figure 53 Maximum difference of percentage protection as compared to the greedy algorithm for 30x30 source-sink problems

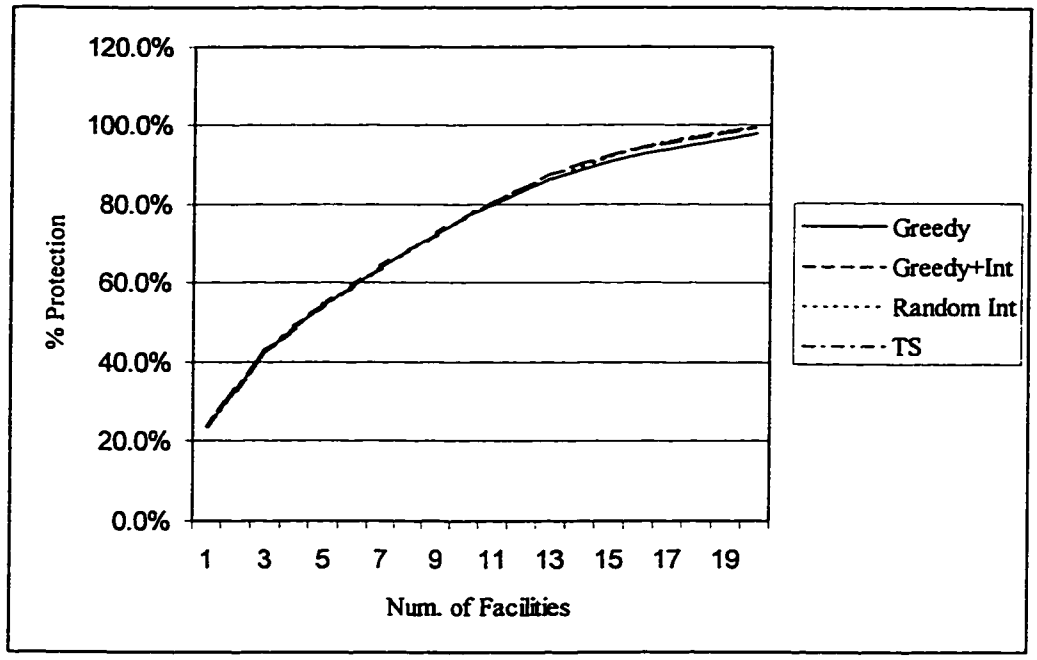

Figure 54 Cost effective curve for 20x20 problem on Edmonton network

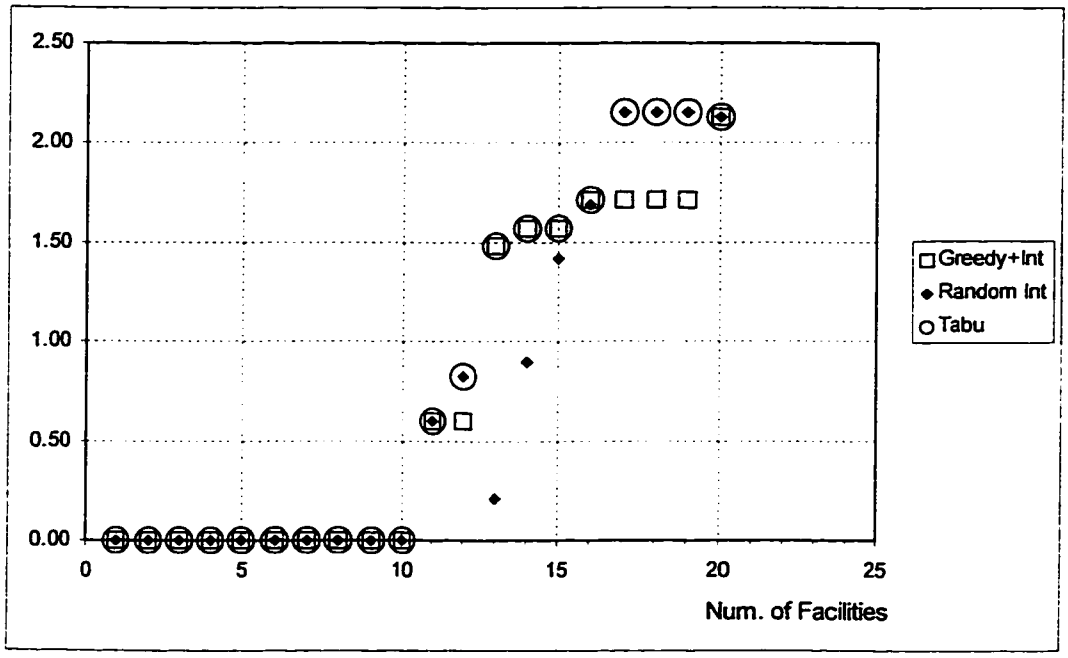

Figure 55 Differences in percentage protection between greedy and other algorithms

Chapter 6

SUMMARY AND CONCLUSIONS

Because of amount of hazardous materials shipped on transportation networks and their potential negative effects, the public is very sensitive to the risk associated with Hazmat shipments. Decisions related to Hazmat transportation involve multiple stakeholders, each having a different set of objectives. This has two implications: 1) from the analysis point of view, there is often no "best" solution for all objectives; and 2) consensus is often very difficult to build among different stakeholders. Spatial decision support systems (SDSS) that incorporate quantitative analysis methods and relevant data can facilitate the decision process and help making informed decisions. This research explored methods for developing SDSS based on GIS. It also solved some methodological problems related to Hazmat transport management. It has included four major components:

1) An evaluation of GIS tools for Hazmat transport decision support;

2) A new approach for incorporating dispersion models in network risk analysis;

3) A procedure for designing municipal Hazmat networks;

4) A new algorithm for the inspection station location model.

6.1 GIS Tools for Hazmat Transport Decision Support

GIS have experienced explosive growth in the last two decades. Numerous companies, public agencies and virtually all levels of governments are using GIS to manage and analyze their spatial data. For example, ESRI (1998), one of the major GIS software developers, reports that 200,000 copies of ArcView GIS have been sold worldwide. Since the transportation industry has been one of the largest user groups of GIS, transportation departments or companies should take advantage of their existing GIS system (expertise, software, hardware and database) for Hazmat transport decision support.

The benefit of GIS to Hazmat transport decisions includes spatial data management, enhanced risk assessment, built-in spatial analysis tools and the capability to incorporate special analytical functions.

Spatial data management is the basic yet the most important function of GIS. GIS allows spatial data to be included in Hazmat transportation analysis like never before. It organizes data into layers of information within a unified geographic framework, each layer can be used individually or together. When new data layers are added into analysis, it expands the perspective of the decision making process. Different data layers can be analyzed together to deepen insights into problems. GIS provides versatile methods for modeling spatial data. Vector data format is very useful for describing the topology of spatial objects, such as describing the network structure. Raster format is very useful for describing continuous objects, such as the distribution of pollutants. Vector and raster were used together to analyze the risk distribution and to help solving the Hazmat transportation problems in this study.

GIS can facilitate risk assessment in both the traditional and advanced risk analysis frameworks. In the traditional framework where risk is modeled as the product of the probability of accidents and the number of people living within a certain distance from the link, the buffer and intersect operations allow risk analysis accurately, efficiently and at a finer spatial scale. For risk analysis that considers wind conditions, the raster data model allows us to calculate the concentration levels at different locations, to combine the concentration (impact level) results with population data, and finally to calculate the risks for network links.

Routing algorithms have become available in many GIS software packages. With the help of customization tools of GIS, Hazmat routing capabilities that are comparable to these from expensive specialized SDSS can be developed easily. Hazmat decision analysis often needs some specialized functions that are not available in mainstream GIS software. Therefore, for GIS to be truly used as SDSS, specialized functions must be developed and linked to GIS. Developing special functions and interfaces for commercial GIS software has become a task for people with modest programming experience. Three methods for enhancing the analytical capabilities of GIS were discussed, with a focus on developing add-

ins and linking GIS with a professional solver. My experiments show that with a small amount of customization, GIS can be as helpful as specialized Hazmat decision support systems that are often very expensive. This is good news for every organization that has a GIS system. It is especially important for small organizations that have limited resources and are sometimes disadvantaged in decision processes. By utilizing their existing GIS, small organizations can analyze Hazmat transport decisions just as large organizations do.

GIS is an ideal framework for developing Hazmat transport decision support systems. The strengths of a GIS-based SDSS include strong spatial data management tools, improved risk analysis, excellent graphics processing capabilities, and flexibility in expanding the analytical capabilities.

6.2 Incorporating Dispersion Models in Network Risk Analysis

Risk analysis is a fundamental part of Hazmat transport studies. Traditional methods for evaluating risk are simplistic, ignoring the spatial distribution of impact resulting from Hazmat releases. For air-borne pollutants, they ignore the effect of wind conditions on the distribution of contaminants. Although some researchers have applied dispersion models that consider wind conditions to analyze risks from point-based sources, none has reported the ability to apply the models in network risk analysis without making very limiting assumptions.

This research developed a raster GIS-based approach to incorporate dispersion models in risk analysis. This approach transforms the impact area into a grid and the network into chains of grid cells. Each network cell is treated as a point source, and each impact grid cell is treated as a receptor cell. For each source cell, concentration level at the receptor cell can be calculated using the dispersion model efficiently. Concentration level is then combined with the population data to predict the potential consequences at the receptor cell. The total expected consequence at each receptor cell resulting from the entire network is the summation of the consequences at that cell from all source cells. This method is efficient and simple to implement.

More realistic risk analysis methods can improve Hazmat transport decisions that rely on risk predictions. The capability of incorporating wind conditions into risk analysis makes us

a step closer to real-time Hazmat transport decision-making. It opens the door to some very interesting new research topics. One such example is the cost-benefit analysis of seasonal Hazmat networks. In most places, prevailing wind speed and direction change seasonally. Thus, if a significant portion of Hazmat transported is air-borne, Hazmat networks should be seasonal from the dispersion perspective. On the other hand, seasonal Hazmat networks can incur extra costs for road signs and maintenance for extra roads. More importantly, driving safety may be compromised because the drivers need to drive on different roads in different seasons. Therefore, a cost-benefit analysis is necessary before decisions regarding seasonal routes are made. Without the capability to incorporate dispersion models, it is out of the question to think about designing seasonal routes.

Being able to calculate the concentration surface resulting from transportation activities on the network advances risk analysis methodology. However, the potential benefits of using the raster GIS approach go beyond that. First, because the values of raster cells can be modified individually, it is possible to combine the consequence grid with other data layers. For example, if some areas are more ecologically sensitive than other areas, we can create an ecological sensitivity layer and combine it with the consequence layer to produce a modified consequence layer. Second, dispersion models are based on some limiting assumptions. Some assumptions may be relaxed with the help of surface modeling capabilities of raster GIS. For the Gaussian plume model, such assumptions include homogeneity of wind conditions and topography. Raster GIS can store and analyze the change of winds and topography over space accurately. Assuming homogeneity of these two factors may not be necessary in a raster GIS framework. Relaxing such assumptions will dramatically improve the realism of dispersion models. This is very exciting topic for future studies.

6.3 Hazmat Network Design

Most North American cities designate roads for Hazmat trucks to reduce the risk resulting from Hazmat traffic. Hazmat routes need to be updated regularly due to changing road networks, demographics and shipping demands. Therefore, there is great application potential for analytical methods of optimal Hazmat network design. I approached this problem as a two-tiered risk minimization problem. Two factors were considered that will

affect the total risk: the network design decisions of authorities, and the routing decisions made by shippers who use the network. A game-like procedure is developed that takes the decision of shippers into consideration. This is an improvement over the current methods used by practitioners including the method suggested by the United States Federal Highway Administration (FHWA).

This research tested four versions of a network design procedure. The version favored by our experimental tests consists of two stages: in the first stage, the union of minimum risk paths is selected from the entire network; in the second stage, a greedy link removal algorithm is used to further reduce the network (and the total risk). Our results showed that the total risk in solution networks was significantly smaller than that in the entire network resulting from the same shipping demands. The greedy link removal algorithm, a process added to the existing network design methods used by practitioners, contributes significantly to the total risk reduction. Therefore, Hazmat networks designed with existing methods can be improved significantly. We suggest an improvement stage such as ours be added to the network design process. On the average, the greedy link removal algorithm was able to reduce the total risk to a level close to the ideal minimum risk values. However, for some problems, the risk value is significantly greater than the ideal value. A better algorithm than the greedy algorithm may be able to produce better results. This is an interesting topic for further studies.

6.4 A Tabu Search Algorithm for the Inspection Station Location Problem

The inspection station location model (ISLM) can be used to locate facilities inspecting Hazmat trucks travelling on networks. ISLM locates inspection stations to intercept traffic flow as early in their trip as possible so that the risk resulting from dangerous trucks is minimized. Despite the application potential of ISLM, no algorithm has been applied to solve this problem successfully yet. In this study I implemented a node interchange algorithm and a tabu search algorithm for this problem.

Both the interchange algorithm and the tabu search algorithm performed much better than the greedy algorithm for the test problems. They overcome a major drawback of the greedy algorithm: facilities cannot be relocated even if the protection they provide is taken over by other facilities. They were able to find the optimal solutions for all the test problems in the

full protection case. Tabu search performed better than the interchange algorithm. It was able to find the optimal solutions for all the small problems for which we knew the optimal solutions.

The application potential of ISLM is great. An application similar to Hazmat truck inspection is to locate check stops to catch and stop drunk drivers. Another potential application is to select the locations for displaying road-warning messages. When traffic jams happen in the network, drivers who are driving toward the jam sites should be warned as early as possible so that they can change their travel paths. When there are many traffic jams in different locations, it is not desirable to display all jam locations on every road-warning sign. It is best to display the warning of a particular jam at a selected set of locations that intercept the traffic flows that contains the maximum number of drivers who are travelling toward the jam site.

Hazardous materials transport is a very fertile research field. When dealing with every problem during this research, I found many more open topics. At the end of each chapter, I listed some future study topics related to that particular chapter. In addition to these research topics, I hope to see that the findings and methodological developments from this study are implemented in a real spatial decision support system. I believe that these tools, if implemented in a low-cost, easy-to-use decision support system, will contribute to the safe transportation of hazardous materials.

REFERENCES

1. ALK Associates (1996), PC*HAZROUTE User's Guide, Princeton, New Jersey, USA
2. Ang, J B, *et al.* (1989) "Development of a Systems Risk Methodology for Single and Multimodal Transportation Systems," Final Report, Office of University Research, US DOT, Washington, D.C.
3. Angle, R P and S K Sakiyama (1991) "Plume Dispersion in Alberta," Alberta Environment.
4. Barber, E and L Hilderbrand (1980) "Guidelines for Applying Criteria to Designate Routes for Transporting Hazardous Materials," Report No. FHWA-IP-80-15
5. Benati, S and G Laporte (1994) "Tabu Search Algorithms for the $(r|X_p)$-Medianoid and $(r|p)$-Centroid Problems," *Location Science*, **2**, 193-204
6. Berman, O, M J Hodgson and D Krass (1995) "Flow-Interception Problems," in Z Drezner (ed.) *Facility Location, A Survey of Applications and Motheds*, Springer-Verlag New York, Inc.
7. Berman, O, R C Larson and N Fouska (1992) "Optimal Location of Discretionary Service Facilities," *Transportation Science*, **26**, 201-11
8. Boffey, B and J Karkazis (1995) "Location, Routing and the Environment" in Z Drezner (ed.) *Facility Location, A Survey of Applications and Motheds*, Springer-Verlag New York, Inc.
9. Bosque J and Moreno A (1990) "Facility Location Analysis and Planning: a GIS Approach," *Proceedings EGIS 1990*, 87-94
10. Brooke *et al.* (1988), GAMS: A User's Guide, GAMS Development Corporation, Washington DC
11. Burrough, P A (1986), Principals of Geographic Information Systems for Land Resources Assessment, Oxford University Press, Oxford
12. Caliper (1997), TransCAD GIS User's Manual, Caliper Corporation, Newton, Massachusetts

13. Chakraborty, J and M P Armstrong (1995) "Using Geographic Plume Analysis to Assess Community Vulnerability to Hazardous Accidents," *Computers, Environment, and Urban Systems,* **19**, 1-17

14. Cox, G R (1984) "Routing and Scheduling of Hazardous Materials Shipments: Algorithmic Approaches to Managing Spent Nuclear Fuel Transport," Ph.D. dissertation, Cornell University

15. Cox, G R and M A Turnquist (1986) "Schedualing Truck Shippments of Hazardous Materials in the Presence of Curfews," *Transportation Research Record,* **1063,** 21-26

16. Current, J R, C S ReVelle and J L Cohon, 1985 "The maximum covering/shortest path problem: a multi-objective network design and routing formulation", *European Journal of Operations Research* **21**, 189-99

17. Daskin, M (1995) *Network and Discrete Location: Models, Algorithms, and Applications,* John Wiley and Sons, Inc.

18. Densham, P (1991) "Spatial Decision Support Systems" in Maguire, D J, M F Goodchild and D W Rhind, (eds.), *Geographical Information Systems: Principles and Applications,* Longman Scientific and Technical, pp. 403-12

19. Densham, P (1996) "Visual Interactive Locational Analysis" in Longley, P and M Batty (eds.), Spatial Analysis: *Modelling in a GIS Environment,* GeoInformation International, pp. 185-205

20. DOC (1994), "Truck Inventory and Use Survey," Bureau of the Census, Washington, D.C.

21. Dijkstra, E (1959) "A Note on Two Problems in Connection with Graphs," *Numerische Mathematik,* **1**, 101-18

22. Dionne R and M Florian (1979) "Exact and Approximate Algorithms for Optimal Network Design," *Networks,* **9**, 37-59

23. Eastman J R (1992) "IDRISI User's Guide Version 4.0," Worcester MA, Graduate School of Geography, Clark University

24. Erkut, E and V Verter (1994) "A Framework for Hazardous Materials Transport Risk Assessment," Research Papers in Management Science, Department of Finance and Management Science, Faculty of Business, University of Alberta

25. Erkut, E and V Verter (1995a) "Hazardous Materials Logistics," in Z Drezner (ed.) *Facility Location, A Survey of Applications and Motheds*, Springer-Verlag New York, Inc.

26. ESRI (1997) "Sears Wins Prestigious RITA Award for Its Logistics GIS," ESRI Press Release, October 3, 1997 (http://www.esri.com)

27. ESRI (1998) "GIS Solutions from ESRI", ESRI (http://www.esri.com/software)

28. Gifford, F A (1975) "Atmospheric dispersion models for environmental pollution applications," Chapter 2, Lectures on Air Pollution and Environmental Impact Analysis, American Meterological Society, Boston, 35-38.

29. Glickman, T S (1988), "Rerouting Railroad Shipments of Hazardous Materials to Avoid Populated Areas," *Accident Anal. Prevent.* **15**, 329-335

30. Glickman, T S and P K Raj (1993), "A Comparison of Theoretical and Actual Consequences in Two Fatal Ammonia Incidents," in F Saccomanno and K Cassidy (eds.), *Transportation of Dangerous Goods: Assessing the Risks, Institute for Risk Research*, University of Waterloo, Ontario, Canada

31. Glover, F (1977) "Heuristic for Integer Programming Using Surrogate Constraints," *Decision Sciences*, **8**, 156-166.

32. Glover, F (1989) "Tabu Search, Part I," *ORSA Journal on Computing*, **1**, 190-206.

33. Glover, F (1990a) "Tabu Search, Part II," *ORSA Journal on Computing*, **2**, 4-32.

34. Glover, F (1990b) "Tabu Search: A Tutorial," *Interfaces*, **20**, 74-94.

35. Glover, F and M Laguna (1993) "Tabu Search," in C. Reeves (Ed.), *Modern Heuristic Techniques for Combinatorial Problems*, Oxford: Blackwell

36. Goodchild, M *et al.* (1992) "Integration of GIS and Spatial Data Analysis: Problems and Possibilities," *International Journal of Geographic Information Systems*, Vol. **6**, No. 5, 407-423

37. Goodchild, M (1993) "The State of GIS for Environmental Problem Solving" in Goodchild, M, B Parks and L Steyaert (eds.) *Environmental Modelling with GIS*, Oxford University Press, New York, 8-15

38. Goodchild, M, B Buttenfield and J Wood (1994) "Introduction to Visualizing Data Validity" in H M Hearnshaw and D Unwin (eds.) *Visualization in Geographical Information Systems*, John Wiley and Sons

39. Gopalan R, K Kolluri, R Batta and M Karwan (1990) "Modeling Equity of Risk in the Transportation of Hazardous Materials," *Operational Research,* **38,** 961-73

40. Grange, G M (1980) "Report of the Mississauga Railway Accident Inquiry," Ministry of Supply and Services, Ottawa, Ontario, Canada

41. Hillsman, E L and P R Coleman (1989) "Integrating Demographic, Atmospheric, and Dose Information to Estimate Effects from Accidental Release of Chemical Agents," *The Environmental Professional,* **11,** 354-366

42. Hillier, F S and G J Lieberman (1990) *Introduction to Operations Research, Fifth Edition,* McGraw-Hill Publishing Company

43. Hodgson, M J (1990) "A Flow-Capturing Location-Allocation Model," *Geographical Analysis,* **22,** 268-79

44. Hodgson, M J and K E Rosing (1992) "A Network Location-Allocation Model Trading Off Flow Capturing and p-Median Objectives," *Annals of Operations Research,* **40,** 247-60

45. Hodgson, M J, K E Rosing and A L G Storrier (1995) "Applying the Flow Capturing Location-Allocation Model to Realistic Network Traffic Problems: The Case of Edmonton, Canada," Tinbergen Institute Series, Erasmus University, Rotterdam

46. Hodgson, M J, K E Rosing and J Zhang (1996) "Locating Vehicle Inspection Stations to Protect a Transportation Network," *Geographic Analysis,* **28,** 299-314

47. Hodgson, M J and Berman O (1997) "A Billboard Location Model," *Geographical & Environmental Modelling,* **1,** 25-45

48. Icancie, F (1984) "Hazardous Materials Routing Study," Final Report prepared by Portland Office of Energy Management, Portland, Oregon

49. Keen, P G W (1981) "Value Analysis: Justifying Decision Support Systems," *MIS Quarterly,* **5,** 1-15

50. Kessler, D (1986) "Establishing Hazardous Materials Truck Routes for Shipments Through the Dallas-Fort Worth Area," In: *Recent Advances in Hazardous Materials Transportation Research: An International Exchange,* pp. 79-87, Transportation Research Board, Washington, D.C.

51. List, G F, *et al.* (1991) "Modelling and Analysis for Hazardous Materials Transportation: Risk Analysis, Routing/Scheduling and Facility Location," *Transportation Science,* **25,** 100-114

52. McMaster, R B (1990) "Modelling Community Vulnerability to Hazardous Materials using Geographic Information Systems," in Donna, J P and D F Marble (eds.) *Introductory Readings in Geographic Information Systems,* Taylor & Francis

53. Magnanti, T L and R T Wong (1984) "Network Design and Transportation Planning Models and Algorithms," *Transportation Science,* **18,** 1-55

54. Maguire, D J and J Dangermond (1991) "The Functionality of GIS" in Maguire, D J, M F Goodchild and D W Rhind, (eds.), *Geographical Information Systems: Principles and Applications,* Longman Scientific and Technical, pp. 403-12

55. Maguire, D J (1991) "An Overview and Definitions of GIS" in Maguire, D J, M F Goodchild and D W Rhind, (eds.), *Geographical Information Systems: Principles and Applications,* Longman Scientific and Technical, pp. 9-20

56. Mirchandani, P, R Rebello and A Agnetis (1995) "The Inspection Station Location Problem in Hazardous Material Transportation: Some Heuristics and Bounds," *Infor,* **33,** 100-113

57. National Transportation Safety Board (1971) "Risk Concepts in Dangerous Goods Transportation Regulations," report NTSB-STS-71-1, US DOT, Washington, D.C.

58. Openshaw, S (1996) "Developing GIS-Relevant Zone-Based Spatial Analysis Methods" in Longley, P and M Batty (eds.), Spatial Analysis: *Modelling in a GIS Environment,* GeoInformation International, pp. 55-73

59. Pasquill, F. (1962) "Atmospheric Diffusion," D. Van Nostrand Co., Ltd., London

60. Patel, M. H. and Alan J. Horowitz (1994) "Optimal Routing of Hazardous Materials Considering Risk of Spill," *Transportation Research A,* **28,** 119-132

61. Pijawka, D, S Foote and A Soesilo (1985), "Risk Assessment of Transporting Hazardous Material: Route Analysis and Hazard Management," *Transportation Research Record,* **1020,** 1-6

62. ReVelle, C, J Cohon and D Shobrys (1991) "Simultaneous Siting and Routing in the Disposal of Hazardous Wastes," *Transportation Science,* **25,** 138-45

63. Robbins J (1981) "Routing Hazardous Materials Shipments" Ph.D. dissertation, Indiana University

64. Rowe, W D (1983) "Risk Assessment Process for Hazardous Materials Transportation," National Co-operative Highway Research Program Report 103

65. RT-Soft (1996), Av-Route User's Guide, RT-Soft Inc.

66. Saccamanno, F and A Chan (1985) "Economic Evaluation of Routing Strategies for Hazardous Road Shipments," *Transportation Research Record*, **1020,** 12-18

67. Shobrys D (1981) "A Model for the Selection of Shipping Routes and Storage Locations for a Hazardous Substance" Ph.D. dissertation, John Hopkins University

68. Slade, D H (1968) "Meterology and Atomic Energy 1968," TID-24190. US At. Energy Comm., Oak Ridge, Tennessee

69. Stern, A, *et al.* (1976) "Fundamentals of Air Pollution,"Academic Press, New York

70. Sprague, R H and E D Carlson (1982) *Building Effective Decision Support Systems,* Prentice-Hall, Englewood Cliffs

71. Statistics Canada, CANSIM Database, 1998

72. Statistics Canada, 1996 Census Data

73. Stewart A M (1990), The development of a Risk Based Procedure for Evaluating Transport of Dangerous Goods Policies, master's thesis, Department of Civil Engineering, Queen's University, Kingston, Ontario, Canada

74. Tomlin, C D (1990) Geographic Information Systems and Cartographic Modelling, Englewood Cliffs, NJ, Prentice-Hall

75. Transport Canada (1997a), *Dangerous Goods Newsletter*, Vol. **17**, No. 1

76. Transport Canada (1997b), *Dangerous Goods Newsletter*, Vol. **17**, No. 3

77. Turner, D B (1970) "Workbook of Atmospheric Dispersion Estimates," Office of Air Programs Publications No. AP-26, US EPA, Research Triangle park, North Carolina

78. Venkatram, A (1988) "Topics in Applied Dispersion Modeling," in Venkatram, A and J C Wyngaard (eds.), *Lectures on Air Pollution Modeling,* American Meteorology Society, Boston

79. Verter, V and E Erkut (1995) "Hazardous Materials Logistics: an Annotated Bibliography," in A Haurie and C Carraro (eds.) *Operations Research and Environmental Management,* Kluwer Publishing Company

80. Willer D (1990) "A Spatial Decision Support System for Bank Location: A Case Study," NCGIA Technical Report 90-9, NCGIA, Santa Barbara, California

81. Wood, M and K Brodlie (1994) "ViSC and GIS: Some Fundamental Considerations" in Hearnshaw, H M and D J Unwin (eds.) *Visualization in Geographic Information Systems,* John Willy & Sons, Chichest, England

82. Zhan, F B and C E Noon (1998) "Shortest Path Algorithms: An Evaluation Using Real Road Networks," Transportation Science, **31,** 1-16

83. Zografos, K G and C F Davis (1989) "Multiobjective Programming Approach for Routing Hazardous Materials," *Transportation Engineering Journal,* ASCE **115,** 661-73

APPENDIX 1

These tables are for Chapter 5.

Number of Facilities	% Protection Provided			
	Greedy	Greedy+Int	Random Int	Tabu
1	23.0	23.0	23.0	23.0
2	39.7	39.7	39.7	39.7
3	52.7	52.7	52.7	52.7
4	63.2	63.2	63.2	63.2
5	72.1	72.1	72.1	72.1
6	80.3	80.3	80.3	80.3
7	87.2	87.2	87.2	87.2
8	92.5	92.7	92.7	92.7
9	96.7	96.9	96.9	97.1
10	99.7	100.0	100.0	100.0

Table 27 Percentage of protection achieved for 10x10 source-sink problems in Kroll network

Number of Facilities	% Protection Provided			
	Greedy	Greedy+Int	Random Int	Tabu
1	18.2	18.2	18.2	18.2
2	30.7	30.7	30.7	30.7
3	40.7	40.7	40.9	40.9
4	48.6	48.7	48.8	48.8
5	55.4	55.5	55.4	55.6
6	61.3	61.4	61.4	61.5
7	66.4	66.6	66.6	66.7
8	71.0	71.2	71.2	71.3
9	75.0	75.4	75.4	75.4
10	78.8	79.2	79.2	79.2
11	82.3	82.7	82.7	82.7
12	85.3	85.7	85.7	85.7
13	88.0	88.4	88.4	88.4
14	90.4	90.9	90.9	90.9
15	92.5	93.0	93.1	93.1
16	94.3	94.9	95.0	95.0
17	95.9	96.6	96.7	96.7
18	97.2	97.9	98.0	98.0
19	98.4	99.1	99.1	99.1
20	99.4	100.0	100.0	100.0

Table 28 Percentage of protection achieved for 20x20 source-sink problems in Kroll network

Number of Facilities	% Protection Provided			
	Greedy	Greedy+Int	Random Int	Tabu
1	16.2	16.2	16.2	16.2
2	27.4	27.5	27.5	27.5
3	36.4	36.6	36.6	36.6
4	43.7	43.9	44.1	44.1
5	49.8	50.2	50.5	50.5
6	55.0	55.5	55.7	55.7
7	59.6	60.0	60.2	60.3
8	63.5	64.3	64.3	64.3
9	67.0	67.6	67.6	67.8
10	70.1	70.9	70.9	70.9
11	72.9	73.6	73.7	73.7
12	75.4	76.2	76.2	76.2
13	77.7	78.4	78.6	78.6
14	79.9	80.6	80.9	80.9
15	82.0	82.8	82.9	82.9
16	83.9	84.7	84.9	84.9
17	85.7	86.6	86.7	86.7
18	87.3	88.3	88.3	88.3
19	88.8	89.8	89.8	89.9
20	90.1	91.2	91.2	91.3
21	91.4	92.5	92.5	92.6
22	92.6	93.6	93.7	93.7
23	93.6	94.8	94.8	94.8
24	94.6	95.8	95.8	95.8
25	95.6	96.7	96.7	96.7
26	96.4	97.5	97.5	97.5
27	97.2	98.2	98.3	98.3
28	97.9	98.9	98.9	98.9
29	98.6	99.5	99.5	99.5
30	99.2	100.0	100.0	100.0

Table 29 Percentage of protection achieved for 30x30 source-sink problems in Kroll network

APPENDIX 2

TRANS.GMS (GAMS input file for the transportation problem)

```
$OFFSYMXREF OFFSYMLIST

SETS

    I    / EDMONTON, CALGARY /
    J    / SWAN, LLOYD /

PARAMETERS

    A(I)
        / EDMONTON   12
          CALGARY 18 /

    B(J)
        / SWAN  16
          LLOYD    14 / ;

TABLE D(I,J)

                SWAN        LLOYD
    EDMONTON    216         246
    CALGARY     504         518 ;

SCALAR  F   /1/ ;

PARAMETER C(I,J) ;

    C(I,J) = F * D(I,J);

VARIABLES
    X(I,J)
    Z ;

POSITIVE VARIABLE X ;

EQUATIONS
    COST
    SUPPLY(I)
    DEMAND(J) ;

COST .. Z =E= SUM((I,J), C(I,J)*X(I,J)) ;

SUPPLY(I) .. SUM(J, X(I,J)) =L= A(I) ;

DEMAND(J) .. SUM(I, X(I,J)) =G= B(J) ;

MODEL TRANSPORT /ALL/ ;

SOLVE TRANSPORT USING LP MINIMIZING Z ;

DISPLAY X.L, X.M ;
```

TRANS.LST (GAMS output file for the transportation problem)

```
GAMS 2.25.087  386/486 DOS                          08/22/98 22:40:52
PAGE     1
G e n e r a l   A l g e b r a i c   M o d e l i n g   S y s t e m
C o m p i l a t i o n


  2
  3  SETS
  4
  5       I    / EDMONTON, CALGARY /
  6       J    / SWAN, LLOYD /
  7
  8  PARAMETERS
  9
 10       A(I)
 11           / EDMONTON   12
 12             CALGARY 18 /
 13
 14       B(J)
 15           / SWAN  16
 16             LLOYD    14 / ;
 17
 18  TABLE D(I,J)
 19
 20                     SWAN         LLOYD
 21       EDMONTON      216          246
 22       CALGARY       504          518 ;
 23
 24  SCALAR  F   /1/ ;
 25
 26  PARAMETER C(I,J) ;
 27
 28       C(I,J) = F * D(I,J);
 29
 30  VARIABLES
 31       X(I,J)
 32       Z ;
 33
 34  POSITIVE VARIABLE X ;
 35
 36  EQUATIONS
 37       COST
 38       SUPPLY(I)
 39       DEMAND(J) ;
 40
 41  COST .. Z =E= SUM((I,J), C(I,J)*X(I,J)) ;
 42
 43  SUPPLY(I) .. SUM(J, X(I,J)) =L= A(I) ;
 44
 45  DEMAND(J) .. SUM(I, X(I,J)) =G= B(J) ;
 46
 47  MODEL TRANSPORT /ALL/ ;
 48
 49  SOLVE TRANSPORT USING LP MINIMIZING Z ;
 50
```

```
51  DISPLAY X.L, X.M ;
52
53
54
```

```
  55
```

COMPILATION TIME   =   0.050 SECONDS   VERID MW2-25-087

---- COST =E=

COST.. - 216*X(EDMONTON,SWAN) - 246*X(EDMONTON,LLOYD) -
504*X(CALGARY,SWAN)

      - 518*X(CALGARY,LLOYD) + Z =E= 0 ; (LHS = 0)

---- SUPPLY =L=

SUPPLY(EDMONTON).. X(EDMONTON,SWAN) + X(EDMONTON,LLOYD) =L= 12 ;
(LHS = 0)

SUPPLY(CALGARY).. X(CALGARY,SWAN) + X(CALGARY,LLOYD) =L= 18 ; (LHS =
0)

---- DEMAND =G=

DEMAND(SWAN).. X(EDMONTON,SWAN) + X(CALGARY,SWAN) =G= 16 ; (LHS = 0
***)

DEMAND(LLOYD).. X(EDMONTON,LLOYD) + X(CALGARY,LLOYD) =G= 14 ; (LHS =
0 ***)

---- X

X(EDMONTON,SWAN)
                (.LO, .L, .UP = 0, 0, +INF)
     -216   COST
        1   SUPPLY(EDMONTON)
        1   DEMAND(SWAN)

X(EDMONTON,LLOYD)
                (.LO, .L, .UP = 0, 0, +INF)
     -246   COST
        1   SUPPLY(EDMONTON)
        1   DEMAND(LLOYD)

X(CALGARY,SWAN)
                (.LO, .L, .UP = 0, 0, +INF)
     -504   COST
        1   SUPPLY(CALGARY)
        1   DEMAND(SWAN)

REMAINING ENTRY SKIPPED

---- Z

Z
                (.LO, .L, .UP = -INF, 0, +INF)
        1   COST

MODEL STATISTICS

BLOCKS OF EQUATIONS	3	SINGLE EQUATIONS	5
BLOCKS OF VARIABLES	2	SINGLE VARIABLES	5
NON ZERO ELEMENTS	13		

GENERATION TIME = 0.060 SECONDS

EXECUTION TIME = 0.060 SECONDS VERID MW2-25-087

G e n e r a l A l g e b r a i c M o d e l i n g S y s t e m
Solution Report SOLVE TRANSPORT USING LP FROM LINE 49

S O L V E S U M M A R Y

MODEL	TRANSPORT	OBJECTIVE	Z
TYPE	LP	DIRECTION	MINIMIZE
SOLVER	BDMLP	FROM LINE	49

**** SOLVER STATUS 1 NORMAL COMPLETION
**** MODEL STATUS 1 OPTIMAL
**** OBJECTIVE VALUE 11860.0000

RESOURCE USAGE, LIMIT	0.000	1000.000
ITERATION COUNT, LIMIT	5	1000

GAMS/BDMLP 1.1 Feb 10, 1995 003.048.026-032.000 386/486 DOS-W

A. Brooke, A. Drud, and A. Meeraus,
Analytic Support Unit,
Development Research Department,
World Bank,
Washington, D.C. 20433, U.S.A.

Work space allocated -- 0.03 Mb

EXIT -- OPTIMAL SOLUTION FOUND.

	LOWER	LEVEL	UPPER	MARGINAL
---- EQU COST	.	.	.	1.000

---- EQU SUPPLY

	LOWER	LEVEL	UPPER	MARGINAL
EDMONTON	-INF	12.000	12.000	-288.000
CALGARY	-INF	18.000	18.000	.

---- EQU DEMAND

	LOWER	LEVEL	UPPER	MARGINAL
SWAN	16.000	16.000	+INF	504.000
LLOYD	14.000	14.000	+INF	518.000

---- VAR X

	LOWER	LEVEL	UPPER	MARGINAL

EDMONTON.SWAN	.	12.000	+INF	.
EDMONTON.LLOYD	.	.	+INF	16.000

G e n e r a l A l g e b r a i c M o d e l i n g S y s t e m
Solution Report SOLVE TRANSPORT USING LP FROM LINE 49

VAR X

	LOWER	LEVEL	UPPER	MARGINAL
CALGARY .SWAN	.	4.000	+INF	.
CALGARY .LLOYD	.	14.000	+INF	.

	LOWER	LEVEL	UPPER	MARGINAL
---- VAR Z	-INF	11860.000	+INF	.

**** REPORT SUMMARY : 0 NONOPT
0 INFEASIBLE
0 UNBOUNDED

```
----     51 VARIABLE  X.L

                SWAN       LLOYD

EDMONTON      12.000
CALGARY        4.000      14.000


----     51 VARIABLE  X.M

               LLOYD

EDMONTON      16.000


EXECUTION TIME       =        0.050 SECONDS        VERID MW2-25-087


USER: Dr. Erhan Erkut                                 G960404:1609As-
MW2
      University of Alberta, Faculty of Business

**** FILE SUMMARY

INPUT      C:\GAMS\TRANS1.GMS
OUTPUT     C:\GAMS\TRANS1.LST
```

IMAGE EVALUATION
TEST TARGET (QA-3)

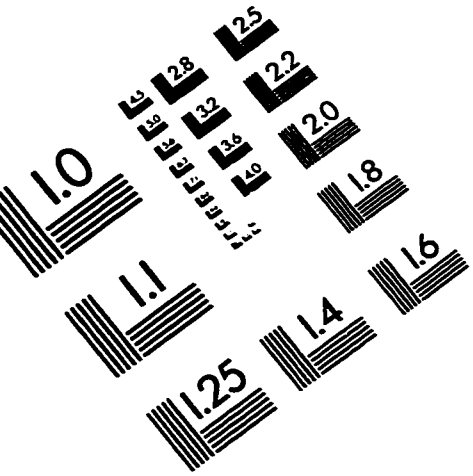

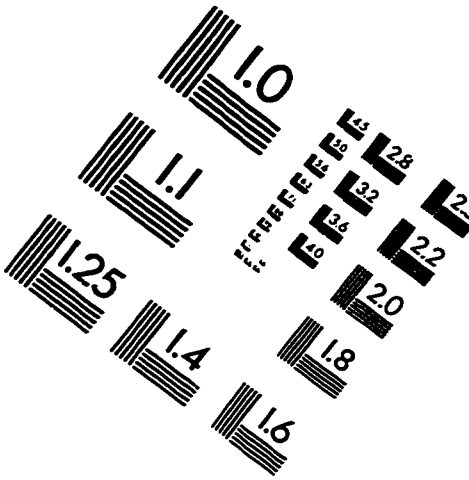

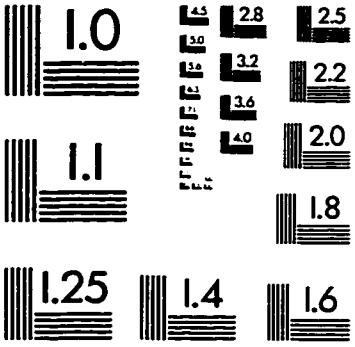

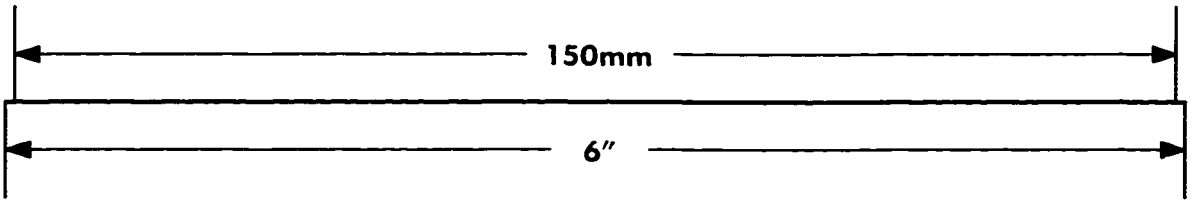

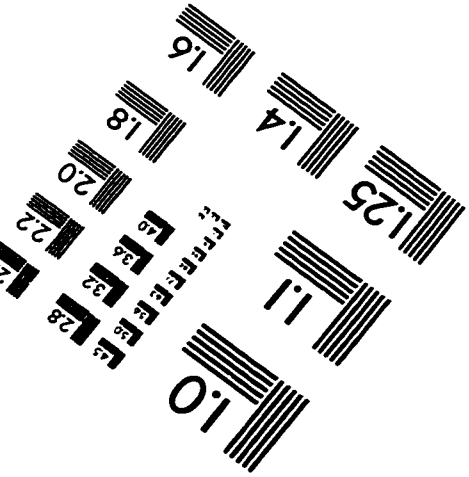

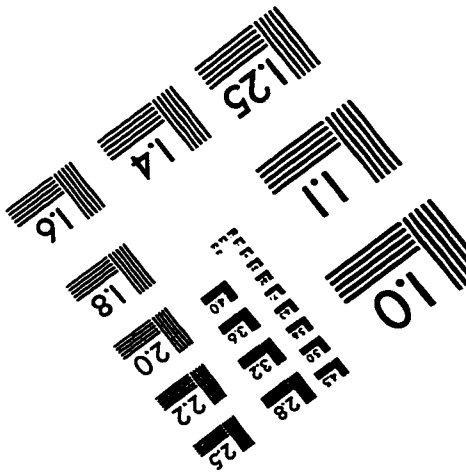

APPLIED IMAGE, Inc
1653 East Main Street
Rochester, NY 14609 USA
Phone: 716/482-0300
Fax: 716/288-5989